

University of Nebraska - Lincoln

DigitalCommons@University of Nebraska - Lincoln

Nebraska Department of Transportation
Research Reports

Nebraska LTAP

12-2019

Precast Concrete Deck-to-Girder Connection using UHPC

George Morcous

University of Nebraska-Lincoln, gmorcous2@unl.edu

Mostafa Abo El-Khier

University of Nebraska - Lincoln, maboel-khier2@huskers.unl.edu

Follow this and additional works at: <https://digitalcommons.unl.edu/ndor>



Part of the [Transportation Engineering Commons](#)

Morcous, George and Abo El-Khier, Mostafa, "Precast Concrete Deck-to-Girder Connection using UHPC" (2019). *Nebraska Department of Transportation Research Reports*. 247.

<https://digitalcommons.unl.edu/ndor/247>

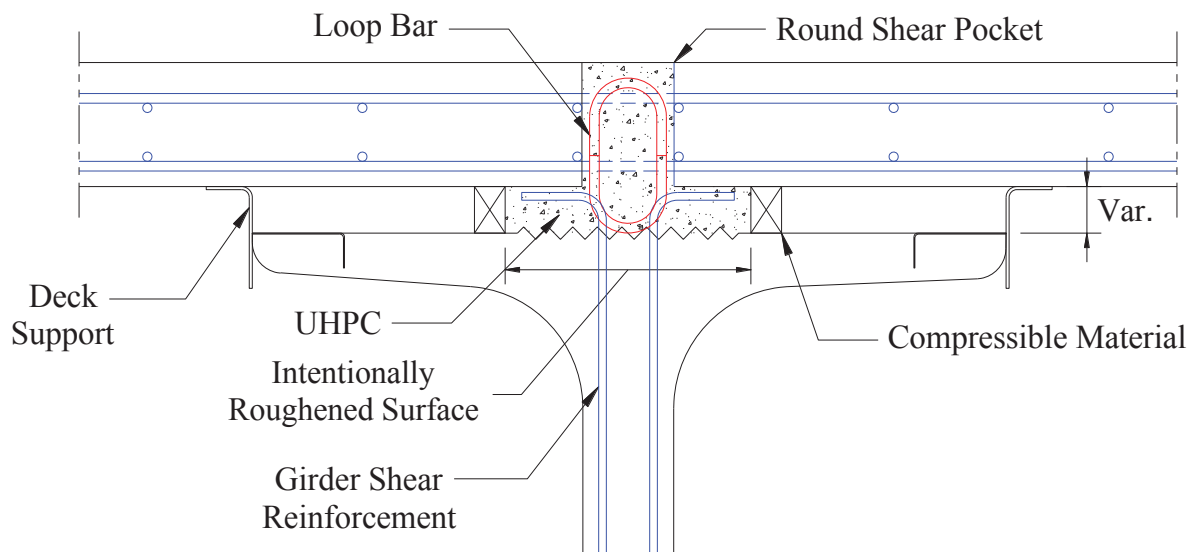
This Article is brought to you for free and open access by the Nebraska LTAP at DigitalCommons@University of Nebraska - Lincoln. It has been accepted for inclusion in Nebraska Department of Transportation Research Reports by an authorized administrator of DigitalCommons@University of Nebraska - Lincoln.

Precast Concrete Deck-to-Girder Connection using UHPC

Nebraska Department of Transportation (NDOT)

Project No. M085

Final Report



December 2019

Precast Concrete Deck-to-Girder Connection using UHPC

A Report on Research Sponsored by

Nebraska Department of Transportation (NDOT)

Principle Investigator

George Morcous, Ph.D., P.E.

Durham School of Architectural Engineering and Construction (DSAEC), College of
Engineering, University of Nebraska-Lincoln (UNL)

Research Assistant

Mostafa Abo El-Khier, Ph.D. Candidate

Durham School of Architectural Engineering and Construction (DSAEC), College of
Engineering, University of Nebraska-Lincoln (UNL)

December 2019

TECHNICAL REPORT DOCUMENTATION PAGE

1. Report No. M085	2. Government Accession No.	3. Recipient's Catalog No.	
4. Title and Subtitle Precast Concrete Deck-to-Girder Connection using UHPC		5. Report Date December 30, 2019	
		6. Performing Organization Code	
7. Author(s) Mostafa Abo El-Khier and George Morcous		8. Performing Organization Report No. No.	
9. Performing Organization Name and Address Durham School of Architecture Engineering and Construction University of Nebraska-Lincoln Omaha, Nebraska 68182-0178		10. Work Unit No.	
		11. Contract SPR-1(19) (M085)	
12. Sponsoring Agency Name and Address Nebraska Department of Transportation Research Section 1400 Hwy 2 Lincoln, NE 68502		13. Type of Report and Period Covered Final Report July 2018-December 2019	
		14. Sponsoring Agency Code	
15. Supplementary Notes			
16. Abstract <p>The implementation of ultra-high-performance concrete (UHPC) in bridge construction has been growing rapidly in the last two decades due to its excellent mechanical properties, workability, and durability. This report presents a new UHPC connection between precast concrete deck panels and bridge girders that eliminates changes to the design and production of girder shear connectors commonly used in conventional cast-in-place concrete deck construction. In conventional construction, girder shear reinforcement or studs are extended into the cast-in-place concrete deck to transfer interface shear and create composite section. In the new connection, girder shear reinforcement or studs are kept underneath the deck panels, while UHPC is used instead to fill the haunch and shear pockets and transfer interface shear between deck panels and girders. Using UHPC and eliminating changes to standard shear connectors make precast concrete deck systems more economical and enhance their constructability.</p> <p>The report presents the experimental investigation conducted to evaluate the interface shear resistance of UHPC using direct shear, slant shear, L-shape push-off, and double shear tests. Also, three full-scale specimens of the new connection were constructed and tested to evaluate its structural performance and constructability. Based on the experimental investigation results, empirical equations were developed to predict the interface shear resistance of the new connection and develop design aids for different bridge types and configurations. Design procedures and construction recommendations were also developed based on the outcomes of the experimental investigation.</p>			
17. Key Words UHPC, Deck-to-Girder Connection, Interface Shear, Push-off Test, Bridge Design		18. Distribution Statement No restrictions. This document is available through the National Technical Information Service. 5285 Port Royal Road Springfield, VA 22161	
19. Security Classification (of this report) Unclassified	20. Security Classification (of this page) Unclassified	21. No. of Pages 95	22. Price

DISCLAIMER

The contents of this report reflect the views of the authors, who are responsible for the facts and the accuracy of the information presented herein. The contents do not necessarily reflect the official views or policies neither of the Nebraska Department of Transportations nor the University of Nebraska-Lincoln. This report does not constitute a standard, specification, or regulation. Trade or manufacturers' names, which may appear in this report, are cited only because they are considered essential to the objectives of the report.

The United States (U.S.) government and the State of Nebraska do not endorse products or manufacturers. This material is based upon work supported by the Federal Highway Administration under SPR-1(19) (M085). Any opinions, findings and conclusions or recommendations expressed in this publication are those of the author(s) and do not necessarily reflect the views of the Federal Highway Administration.”

ACKNOWLEDGEMENTS

Funding for this project was provided by the Nebraska Department of Transportation (NDOT) under project number SPR-P1(19) M085 – Precast Concrete Deck-to-Girder Connection using UHPC. The authors would like to express their gratitude for the support and guidance provided by the NDOT Technical Advisory Committee as well as graduate research assistants; Antony Kodsy and Ahmed Elkhoully, for their help during mixing UHPC and casting specimens. The authors gratefully acknowledge the material donation of LafargeHolcim in the US. Findings and conclusions of this project are of the authors and do not reflect the sponsor agencies and collaborators.

ABSTRACT

The implementation of ultra-high-performance concrete (UHPC) in bridge construction has been growing rapidly in the last two decades due to its excellent mechanical properties, workability, and durability. This report presents a new UHPC connection between precast concrete deck panels and bridge girders that eliminates changes to the design and production of girder shear connectors commonly used in conventional cast-in-place concrete deck construction. In conventional construction, girder shear reinforcement or studs are extended into the cast-in-place concrete deck to transfer interface shear and create composite section. In the new connection, girder shear reinforcement or studs are kept underneath the deck panels, while UHPC is used instead to fill the haunch and shear pockets and transfer interface shear between deck panels and girders. Using UHPC and eliminating changes to standard shear connectors make precast concrete deck systems economical and enhance their constructability.

The report presents the experimental investigation conducted to evaluate the interface shear resistance of UHPC using direct shear, slant shear, L-shape push-off, and double shear tests. Also, three full-scale specimens of the new connection were constructed and tested to evaluate its structural performance and constructability. Based on the experimental investigation results, empirical equations were developed to predict the interface shear resistance of the new connection and develop design aids for different bridge types and configurations. Design procedures and construction recommendations were also developed based on the outcomes of the experimental investigation.

Table of Contents

ABSTRACT	i
Table of Contents	ii
List of Figures	iv
List of Tables	vii
CHAPTER 1. INTRODUCTION	1
1.1. Background.....	1
1.2. Problem Statement.....	2
1.3. Research Objectives.....	3
1.4. Report Outline.....	3
CHAPTER 2. LITERATURE REVIEW	5
2.1. Introduction.....	5
2.2. Deck-To-Girder Bridge Connection Using UHPC.....	5
2.3. Interface Shear Resistance of UHPC.....	7
2.3.1. Interface Shear Resistance of Monolithic UHPC.....	8
2.3.2. Interface Shear Resistance between Hardened Conventional Concrete and Fresh UHPC (CC-UHPC).....	12
2.4. Existing Provisions for Interface Shear Resistance.....	24
CHAPTER 3. PROPOSED DECK-TO-GIRDER CONNECTION	27
3.1. Introduction.....	27
3.2. Initial Design.....	27
3.3. Proposed Deck-to-Girder Connection Using UHPC.....	30
3.4. Construction Sequence of New Connection.....	34
3.5. Study Methodology.....	38
CHAPTER 4. EXPERIMENTAL INVESTIGATION	40
4.1. Introduction.....	40
4.2. Material Properties.....	40
4.3. Evaluate Interface Shear Resistance of Monolithic UHPC.....	40
4.3.1. Direct Shear Test.....	41
4.3.2. L-Shape Push-off Test.....	43
4.3.3. Double Shear Test.....	46
4.4. Evaluate Interface Shear Resistance of CC-UHPC.....	52

4.4.1. Slant Shear Test	52
4.4.2. L-Shape Push-off Test.....	57
4.5. Full-Scale Push-off Test.....	63
CHAPTER 5. DESIGN PROCEDURES AND DESIGN AIDS.....	72
5.1. Introduction	72
5.2. Design Procedure	72
5.3. Design Aids.....	75
CHAPTER 6. SUMMARY AND CONCLUSIONS.....	77
6.1. Summary	77
6.2. Conclusions	78
REFERENCES.....	79
APPENDIX A	81

List of Figures

<i>Figure 1.1: National Bridge Inventory by Deck Structure Type in 2016</i>	2
<i>Figure 1.2: Precast Concrete Deck-to-Girder Connection using threaded rods and HSS-formed shear pockets in the deck panels</i>	3
<i>Figure 2.1: Panel-to-Panel Connection over Steel Girder (Graybeal 2014)</i>	6
<i>Figure 2.2: Hidden UHPC Deck-to-Girder Connection in Steel Girder (a) and Concrete Girder (b) (Graybeal 2014)</i>	6
<i>Figure 2.3: New Haunch-to-Deck Connection Using UHPC through Shear Lug (a) and Rebar Dowels (b) (Haber et al. 2017)</i>	7
<i>Figure 2.4: Shear Friction Theory (Birkeland and Birkeland 1966)</i>	7
<i>Figure 2.5: Vertical Interface Shear Push-off specimen of Monolithic UHPC (Crane 2010)</i>	8
<i>Figure 2.6: Average Interface Shear Resistance of Monolithic UHPC with and without Interface reinforcement (Crane 2010)</i>	9
<i>Figure 2.7: Shear Testing on Inverted L-Shape UHPC Specimen (Maroliya 2012)</i>	9
<i>Figure 2.8: Effect of Fiber Content and Curing Methods on Direct Shear Strength of Monolithic UHPC without Interface reinforcement (Maroliya 2012)</i>	10
<i>Figure 2.9: Monolithic L-Shape UHPC Specimen Test Setup and Specimen Dimensions (Jang et al. 2017)</i>	10
<i>Figure 2.10: Small and Large Scale Push-off Test of Monolithic UHPC without Interface reinforcement (Haber et al. 2017)</i>	11
<i>Figure 2.11: Small and Large Scale Push-off Test of Monolithic UHPC without Interface reinforcement (Haber et al. 2017)</i>	11
<i>Figure 2.12: Portland-Cement Concrete Section Dimensions.</i>	12
<i>Figure 2.13: Slant Shear Test; (a) Mortar Different Roughened Surfaces and Trapezoidal Shear Key, (b) Test Setup (Harris et al. 2011)</i>	13
<i>Figure 2.14: Failure Modes; (a) Failure along Interface Plane, (b) Normal Concrete Failure (Harris et al. 2011)</i>	14
<i>Figure 2.15: Interface Shear Resistance of Cement Type III Mortar with Different Surface Textures (Harris et al. 2011)</i>	14
<i>Figure 2.16: (a) Mix Proportions of UHPFC and NC, (b) Surface Textures, and (c) Test Configuration (Tayeh et al. 2012)</i>	15
<i>Figure 2.17: Different Surface Texture Effect on Interface Shear Resistance of NC-UHPC (Tayeh et al. 2012)</i>	16
<i>Figure 2.18: Slant Shear Composite Specimen Dimensions (Muñoz 2012).</i>	17
<i>Figure 2.19: Different Surface Textures (Muñoz 2012)</i>	17
<i>Figure 2.20: Slant Shear Test Configuration (Muñoz 2012).</i>	18
<i>Figure 2.21: Effect of Interface Angle on Interface Shear Resistance at 8 Days of UHPC (Muñoz 2012).</i>	18
<i>Figure 2.22: Test Setup and Instrumentation of Large Prism Slant Shear Test (Aaleti and Sritharan 2017)</i>	20
<i>Figure 2.23: Samples of NC-UHPC Interfaces of Specimen with Different Failure Modes (Aaleti and Sritharan 2017)</i>	21

<i>Figure 2.24: Effect of Surface Texture Depth and NC Compressive Strength on Interface Shear Resistance of NC-UHPC (Aaleti and Sritharan 2017)</i>	22
<i>Figure 2.25: L-Shape Specimen Dimensions and Different Surface Treatment of NSC-UHPC (Jang et al. 2017)</i>	23
<i>Figure 2.26: L-Shape Test Results of NSC-UHPC Specimens (Jang et al. 2017)</i>	23
<i>Figure 2.27: Fluted Construction Joint with Indented Fibers (NF-P-18-710-UHPC 2016)</i>	25
<i>Figure 3.1: Initial Design Connection (Option I)</i>	28
<i>Figure 3.2: Initial Design Connection (Option II)</i>	28
<i>Figure 3.3: Initial Design Proposed Panel Trough</i>	28
<i>Figure 3.4: Alternatives for Panel Reinforcement and Pre-Tensioning</i>	29
<i>Figure 3.5: Proposed Precast Concrete Deck-To-Concrete Girder Connection</i>	30
<i>Figure 3.6: Proposed Precast Concrete Deck-To-Steel Girder Connection</i>	31
<i>Figure 3.7: Panel Reinforcement and Pre-Tensioning for Proposed Connection</i>	32
<i>Figure 3.8: Interface Shear Resisting Area; (a) at the Top of the Concrete Girder and (b) at the Soffit of the Deck Panels</i>	33
<i>Figure 3.9.1: Construction Sequence of the Proposed Precast Concrete Deck-to-Concrete Girder Connection Using UHPC</i>	35
<i>Figure 3.9.2: Construction Sequence of the Proposed Precast Concrete Deck-to-Concrete Girder Connection Using UHPC</i>	36
<i>Figure 3.9.3: Construction Sequence of the Proposed Precast Concrete Deck-to-Concrete Girder Connection Using UHPC</i>	37
<i>Figure 3.10: Study Methodology for Evaluating Proposed Connection</i>	39
<i>Figure 4.1: Direct Shear Test Setup</i>	41
<i>Figure 4.2: Double Shear Failure Mode of Direct Shear Test Specimen</i>	41
<i>Figure 4.3: The Obtained Direct Shear Test Results and Their Comparison to the Literature</i>	42
<i>Figure 4.4: Effect of Flowability on Direct Shear Test Results</i>	42
<i>Figure 4.5: L-Shape Push-off Specimen Preparation</i>	43
<i>Figure 4.6: L-Shape Push-off Specimen Details</i>	44
<i>Figure 4.7: L-Shape Push-off Test; (a) Test Setup, and (b) Failure Mode</i>	44
<i>Figure 4.8: Interface Shear Resistance versus Relative Displacements of Monolithic L-Shape Push-off Test; (a) Slip, and (b) Crack width</i>	45
<i>Figure 4.9: L-Shape Push-off Test Results of Monolithic UHPC and their Comparison to the Literature</i>	46
<i>Figure 4.10: Double Shear Test Specimen Details; (a) Section Elevation, and (b) Side View</i>	47
<i>Figure 4.11: Concrete Section of Double Shear Test Specimen</i>	48
<i>Figure 4.12: Concrete Section Preparation of Double Shear Test Specimen; (a) Removed Plastic Pipe, and (b) Applying Wax on Concrete Surfaces</i>	48
<i>Figure 4.13: Double Shear Specimen Forming</i>	49
<i>Figure 4.14: Double Shear Specimen Test Setup; (a) Front View, and (b) Side View</i>	49
<i>Figure 4.15: Double Shear Specimen Failure Mode; (a) Double Shear Failure, (b) No. 5 Bar Rupture</i> ..	50
<i>Figure 4.16: Interface Shear Resistance versus Measured Slip at Top and Bottom Interface Planes for Double Shear Specimen #1 (left) and #2 (right)</i>	50
<i>Figure 4.17: Interface Shear Resistance versus Average Measured Slip of Double Shear Test</i>	51

Figure 4.18: Interface Textures of Hardened Concrete Section; (a) Smooth, (b) Shallow Grooved, and (c) Deep Grooved.....	52
Figure 4.19: Slant Shear Test Specimen Dimensions and Test Setup.....	53
Figure 4.20: Slant Shear Specimen Failure Modes; a) Interface Failure, b) Interface Failure and CC Fracture, and c) CC Failure.....	53
Figure 4.21: Interface Shear Resistance of CC-UHPC at Different UHPC Compressive Strength for Different Surface Textures.....	54
Figure 4.22: Average Interface Shear Resistance of CC-UHPC with Different Surface Textures.....	56
Figure 4.23: Results of Slant Shear Test and their Comparison to the Literature.	57
Figure 4.24: L-Shape Push-off Specimen Details and Test Setup.	58
Figure 4.25: Interface Surface Roughening and Different Reinforcement across Interface; No Reinforcement (Left), 2#3 (Middle), and 2#4 (Right).....	58
Figure 4.26: L-Shape Push-off Test Setup.....	59
Figure 4.27: CC Failure Modes of L-Shape Specimens with different interface reinforcement ratios; (a) No Reinforcement, (b) 0.44%, and (c) 0.8%.....	60
Figure 4.28: Effect of Different Interface Reinforcement on Measured Slip between the Two L-Shape Sections; (a) No Reinforcement, (b) 0.44%, and (c) 0.8%.	61
Figure 4.29: Effect of Different Interface Reinforcement on Crack Width; (a) No Reinforcement, (b) 0.44%, and (c) 0.8%.	62
Figure 4.30: Average Interface Resistance of CC-UHPC Obtained from L-Shape Push-off Test and Their Comparison with Proposed Equations.	63
Figure 4.31: Full-Scale Push-Off Specimen Details.....	64
Figure 4.32: Shear Pockets Forming and Slab Reinforcement Details.....	65
Figure 4.33: CC Interface Shear Area Preparation.....	66
Figure 4.34: #5 Loop Bar Details and Installation.	66
Figure 4.35: UHPC Casting for UHPC#2 Specimen.	67
Figure 4.36: UHPC Filled Shear Pockets to Top Surface.....	67
Figure 4.37: Cross-Section of UHPC Cylinders Obtained from Each Full-Scale Push-Off Specimen; (a) UHPC#1, (b) UHPC#2. And (c) UHPC#3	68
Figure 4.38: Full-Scale Push-Off Specimen Test Setup.....	69
Figure 4.39: Load versus Relative Vertical Displacement of Full-Scale Push-off Specimens.	70
Figure 4.40: Load versus Measured Slip of Full-Scale Push-off Specimens.....	70
Figure 4.41: Full-Scale Specimen Failure Modes; (a)UHPC#1, (b)UHPC#2, and (c)UHPC#3.	71
Figure 5.1: Flowchart of General Design Procedures for Proposed System.....	72
Figure 5.2: Design Procedure flowchart of new connection.....	74
Figure 5.3: Design Chart for UHPC with Compressive Strength of 17 ksi.....	75
Figure 5.4: Design Chart for UHPC with Compressive Strength of 21.7 ksi.....	76
Figure 5.5: Demonstration of Using the Design Aid Chart.....	76

List of Tables

<i>Table 2.1: Slant Shear Composite Specimen Dimensions in Different Standards</i>	12
<i>Table 2.2: the macrotecture depths of prepared surfaces ((Muñoz 2012)</i>	17
<i>Table 2.3: Different Mix Proportions Used in Evaluating Local UHPC Properties, Ib/Yard³ (Rangaraju et al. 2013)</i>	19
<i>Table 2.4: Slant Shear Test Results and Failure Modes (Rangaraju et al. 2013)</i>	19
<i>Table 2.5: Summary of NC-UHPC Interface Test Matrix (Aaleti and Sritharan 2017)</i>	20
<i>Table 2.6: UHPC Cohesion and Friction Factors of UHPC for Different Surface Textures based on NF-P-18-710-UHPC 2016</i>	26
<i>Table 4.1: UNL UHPC Mix Proportions</i>	40
<i>Table 4.2: Interface Shear Resistance Analysis of Monolithic UHPC with Interface Reinforcement</i>	51
<i>Table 4.3: Interface Surface Texture Categories Based on the Literature of CC-UHPC Interface Resistance</i>	55
<i>Table 4.4: CC-UHPC Cohesion and Friction Coefficients of Different Interface Surface Textures</i>	56
<i>Table 4.5: L-Shape Push-off Specimens Details and Labels</i>	59
<i>Table 4.6: L-Shape Push-off Test Results and Compared to Proposed Equation</i>	60
<i>Table 4.9: Full-Scale Push-off Test Results</i>	70

Chapter 1. Introduction

1.1. Background

In 2009, FHWA launched Every Day Counts (EDC) program to speed up highway construction. Accelerated Bridge Construction (ABC) is bridge construction that uses innovative planning, design, materials, and construction methods in a safe and cost-effective manner to reduce the onsite construction time that occurs when building new bridges or replacing and rehabilitating existing bridges (FHWA, 2011). FHWA works with states to identify and implement innovations for ABC, such as:

- Geosynthetic Reinforced Soil-Integrated Bridge System (GRS-IBS)
- Prefabricated Bridge Elements and Systems (PBES)
- Slide-in Bridge Construction (SIBC)
- Ultra-High-Performance Concrete (UHPC) for Connections

FHWA published national bridge inventory for bridges across US in 2016. One of the classifications is bridge deck structure type as shown Figure 1.1. Cast-in-place (CIP) concrete deck is the most common used bridge deck type which represents 59.3% of the total bridge deck systems. The CIP deck system requires a long duration for forming deck, placing reinforcement, casting and curing concrete which leads to long traffic lane closures and detouring. Also, the inconsistent quality is a major challenge facing CIP concrete which caused by several factors such as environmental conditions and placing, finishing, and curing of concrete. As a result, CIP concrete decks experience excessive early-age shrinkage cracking which decreases bridge durability and requires overlay. These disadvantages highly impact the construction time and project budget.

One of ABC innovations is the implementation of prefabricate bridge elements in construction. Recently, precast concrete deck panels have been successfully used in ABC projects in various forms and systems. Casting deck panels out-side the construction site in a high-quality controlled environment reduces the deck cracking and provides more durable elements. Then, the precast deck panels are mobilized to the construction site which reduce the construction time and traffic closure. These advantages make the precast concrete deck panels system more durable and cost-effective compared to CIP concrete deck system. The precast deck panels are connected to the supporting girders through longitudinal and transverse connections or/and shear pockets filled with flowable grouting material.

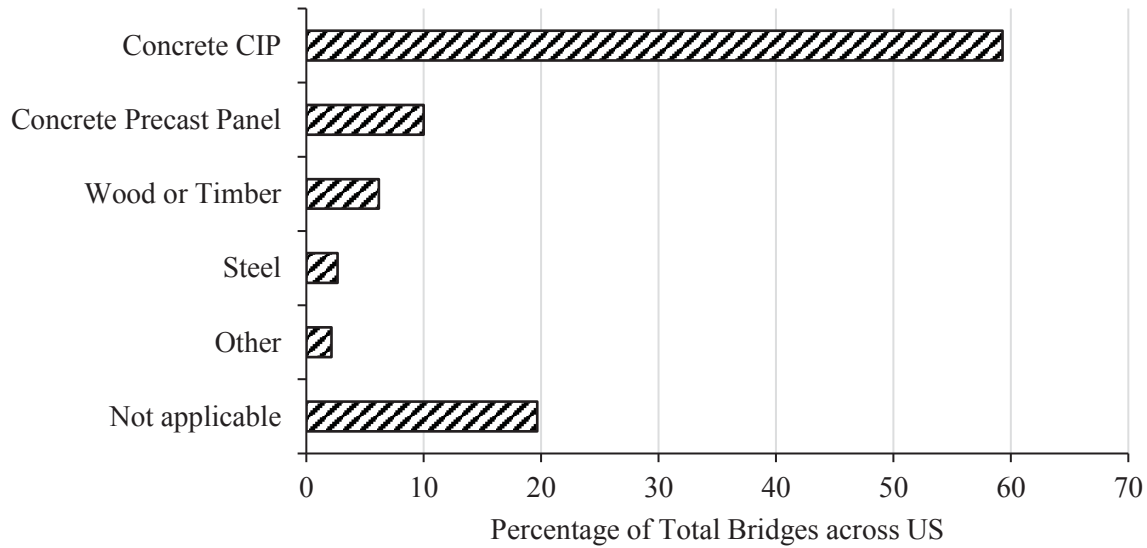


Figure 1.1: National Bridge Inventory by Deck Structure Type in 2016.

Another ABC innovation is using Ultra-High Performance Concrete (UHPC) in bridge connections. UHPC is a new generation of cementitious materials that has exceptional mechanical properties, durability, and workability. The low water-to-binder ratio, high binder content, use of supplemental cementitious material, high particle-packing density, and use of steel fibers significantly enhance the fresh and hardened UHPC properties compared to conventional concrete (CC). According to ASTM C1856-17, UHPC is characterized by a minimum specified compressive strength of 17 ksi, maximum aggregate size less than 1/4 in. and flow between 8-10 in. UHPC became commercially available in the U.S. through several proprietary sources around the year 2000. Since its introduction to the commercial market, the use of UHPC in various applications has been the focus of multiple research endeavors. The exceptional properties of UHPC makes it an ideal grouting material for field casting of connections that enhances the service life of bridges.

1.2. Problem Statement

The method used in Nebraska for connecting precast concrete deck panels and precast/prestressed concrete girders to create composite section is extending shear connectors from the girder into HSS-formed shear pockets in the deck panels, and then filling the pockets and haunch area using self-consolidating concrete (SCC) as shown in Figure 1.2. This method requires high level of quality control/quality assurance (QA/QC) in spacing the shear connectors during girder fabrication as well as shear pockets during panel fabrication to avoid any possible conflict between them during erection. It also requires the use of special shear connectors, such as threaded rods, and adjust their heights to achieve minimum embedment in the shear pockets to develop the design capacity, which complicates girder production and compromise its

economics. Therefore, there is a need for a simplified deck-to-girder connection that maintains girder design the same as it is for CIP concrete deck construction as well as allows adequate tolerances in the production and erection of the precast components.

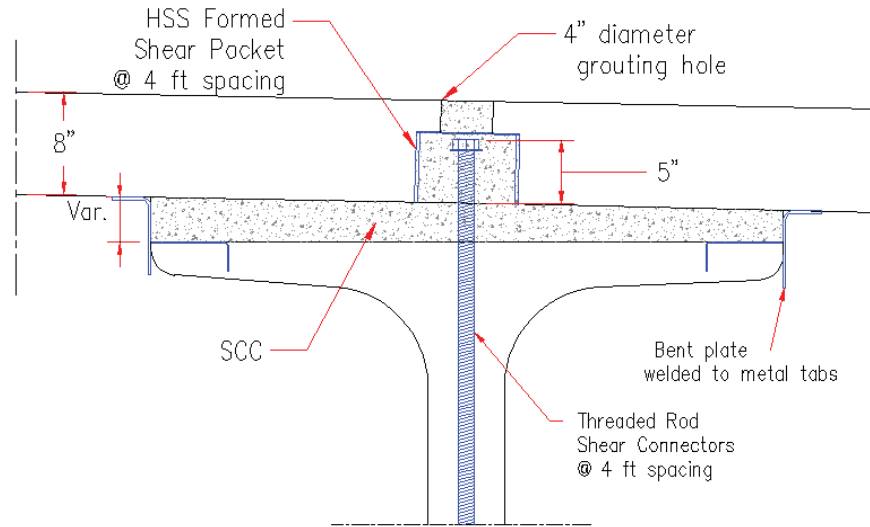


Figure 1.02: Precast Concrete Deck-to-Girder Connection using threaded rods and HSS-formed shear pockets in the deck panels.

1.3. Research Objectives

The general objective of this research is to promote the use of UHPC in the construction of precast deck-to-girder system bridges. The specific objectives are to:

1. Develop a new UHPC connection between precast concrete deck panels and bridge girders that eliminates any changes to girder design/production and any possible conflict between deck and girder reinforcement.
2. Investigate the interface shear resistance of monolithic UHPC and between fresh UHPC cast on hardened conventional concrete, which are needed for the design of the new connection.
3. Investigate the constructability and structural performance of the new connection in full-scale specimens.
4. Provide design procedure and construction recommendations.

1.4. Report Outline

This report consists of six chapters as follows.

Chapter 1 - Introduction

Chapter 2 - Literature Review: The literature review presents the existing deck-to-girder connections using UHPC and the interface shear resistance of UHPC. Two different interface shear planes are controlling the design of deck-to-girder bridge connections; interface shear plane in monolithic UHPC and between fresh UHPC and hardened conventional concrete (CC-UHPC). This chapter summarizes the different test methods conducted to evaluate the resistance of these two planes

Chapter 3 – Proposed Deck-To-Girder Connection: This chapter introduces a new UHPC connection between precast concrete deck panels and precast/prestressed concrete girders and show how it could be used with steel bridge girders. The new connection makes advantage of the excellent mechanical properties of UHPC as well as its exceptional workability and durability. Also, bridge construction sequence using the new connection is presented.

Chapter 4 – Experimental Investigation: This chapter illustrates the experimental investigation procedure, small-scale and full-scale testing, to evaluate the interface shear resistance of monolithic UHPC and of fresh UHPC cast on hardened conventional concrete (CC-UHPC). Direct shear, L-shape push-off, double shear tests were conducted to evaluate interface shear resistance of monolithic UHPC. The literature review conducted on interface shear resistance of CC-UHPC was summarized and analyzed to propose prediction equations. Then, slant shear test and L-shape push-off test were conducted to evaluate and validate these equations. The constructability and structural performance of the proposed connection was investigated through full-scale push-off tests.

Chapter 5 – Design Procedures and Design Aids: This chapter provides a design methodology for the proposed connection based on the prediction equations obtained from the experimental investigation. An example bridge from PCI Bridge Design Manual 2014 (PCI BDM Ex. 9.1a) is used to present the design procedure of the proposed connection. Design aids were also generated to simplify connection design.

Chapter 6 – Summary and Conclusions: This chapter presents a summary of the report and the main conclusions drawn from the experimental investigation and recommendations for using UHPC as a grouting material in the new deck-to-girder connection.

Chapter 2. Literature Review

2.1. Introduction

The literature review presents the existing deck-to-girder connections using UHPC and the test methods conducted to evaluate the interface shear resistance of UHPC. Two different interface shear cases are relevant to design of deck-to-girder bridge connections: interface shear of monolithic UHPC; and interface shear between fresh UHPC and hardened conventional concrete (CC-UHPC). Both cases are reviewed and predicted equations were developed based on previous research.

2.2. Deck-To-Girder Bridge Connection Using UHPC

This section summarizes the literature review conducted on UHPC used for deck-to-girder connections. Typically, this connection is made of shear connectors, such as bent rebars or threaded rods in concrete girders, and shear studs in steel girders, that are embedded into discrete shear pockets or continuous troughs in the precast concrete deck panels. Then, a flowable concrete or grout is used to fill these pockets or troughs to establish the connection. One of the disadvantages of these systems is that shear connectors are required to have minimum embedment into the shear pockets/troughs to develop the design capacity, which necessitates high level of QA/QC and complicates girder and panel production.

UHPC connections were developed to eliminate this problem and simplify production and erection procedure, which consequently improve construction speed and economy. A series of interstate highway bridges near Syracuse, NY were constructed using UHPC deck-to-girder connections developed by NYSDOT (Graybeal 2014). These connections consist of panel-to-panel longitudinal shear key with lap spliced transverse reinforcing rebars over the girder lines. Conventional shear studs ($\frac{3}{4}$ in. x $3\frac{1}{4}$ in.) are welded to the top flange of the steel I-girder as shown in Figure 2.1. The V-shaped shear keys have roughened/exposed aggregate finish to properly bond with the field-cast UHPC that connects the adjacent panels to each other and to the supporting girders. Dimensions of the longitudinal joint is typically 7 in. at the top and bottom of the deck slab and 10 in. at the middle of deck slab. Length and spacing of lap splices depend on bar size and type.

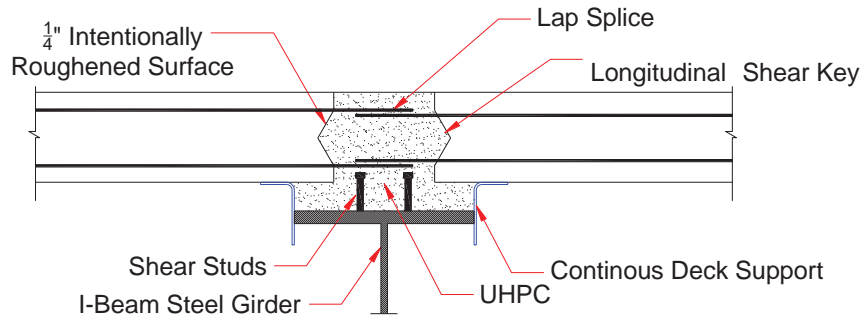


Figure 2.1: Panel-to-Panel Connection over Steel Girder (Graybeal 2014)

Another precast concrete deck-to-steel girder connection was recently developed and tested using UHPC (Graybeal 2014). In this connection, $\frac{3}{4}$ in. x $3\frac{1}{4}$ in. shear studs are installed on the girder top flange similar to cast-in-place (CIP) deck construction (i.e. similar spacing requirements). A 10.5 in. wide and 4.5 in. deep trough with exposed aggregate finish is formed in precast concrete deck slab with 2 in. grouting holes every 24 in. over each girder line as shown in Figure 2.2a. Shear studs are kept below the bottom mat of deck reinforcement without embedment in the deck panels to simplify panel and girder production and eliminate any conflicts during panel installation. An interstate highway bridge near Syracuse, NY was constructed using this connection concept with single field casting of UHPC through grouting holes for each girder line to hide the connection and eliminate the need for deck overlay. The same concept can be used with concrete girders by replacing the shear studs with conventional shear reinforcement (i.e. U bars) that are extended above the top flange and below the bottom mat of deck reinforcement (Graybeal 2014) as shown in Figure 2.2b. This connection has been tested but not implemented yet.

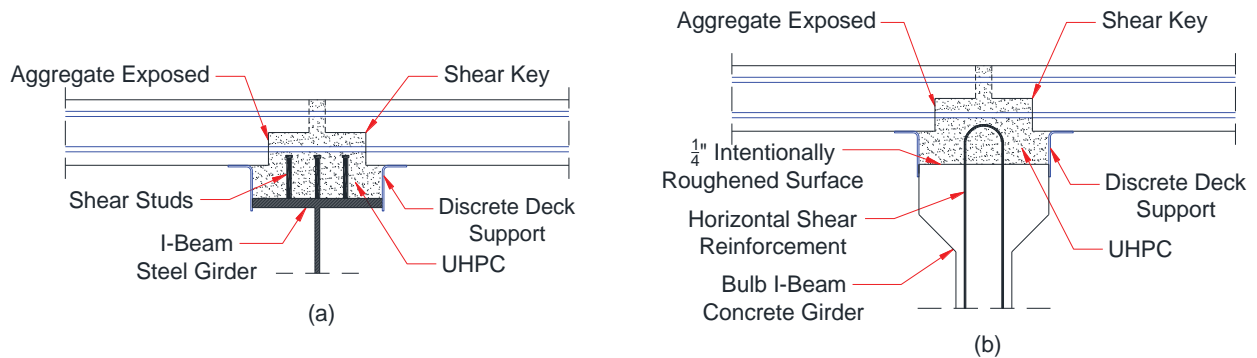


Figure 2.2: Hidden UHPC Deck-to-Girder Connection in Steel Girder (a) and Concrete Girder (b) (Graybeal 2014)

Recently, a study was conducted on implementing UHPC as a grout for deck-to-steel girder composite connection using two new concepts (Haber et al. 2017): a) using shear lugs through deck slab with different areas, and b) using vertical rebar dowels from the deck slab to connection without lugs as

shown in Figure 2.3. The second concept was investigated for different haunch thicknesses 5 in. and 3.5 in. and different distributions of shear studs. Push-off specimens were fabricated by having a symmetric layout with W10x60 steel beam at the middle connected to two 20 in. x 24 in. precast slabs through a grouted UHPC connection. The push-off test was performed by applying the shear force on the steel stub and evaluate the connection performance at the shear interface surface. The UHPC shear lugs have shown to be effective in transferring shear forces and the location and number of shear studs have an effect of the capacity of the connection. Adding rebar dowels to the connection increases the shear resistance, develops better anchorage, and achieve ductile failure behavior due to rebar dowel action.

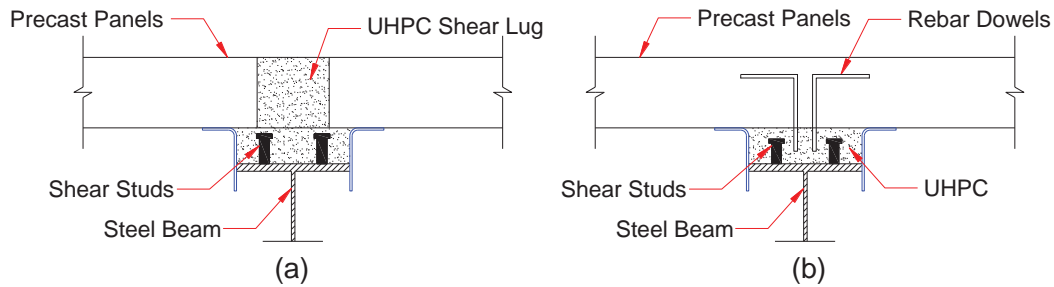


Figure 2.3: New Haunch-to-Deck Connection Using UHPC through Shear Lug (a) and Rebar Dowels (b) (Haber et al. 2017)

2.3. Interface Shear Resistance of UHPC

The interface shear resistance is the maximum shear stress that prevents the relative slide between two concrete components or layers. The interface shear behavior between two different concrete layers was first presented by Birkeland and Birkeland (1966) using cohesion and friction as the two mechanisms that control the interface shear resistance as shown in Figure 2.4. The interface shear resistance is needed to achieve the composite action between bridge girders and deck.

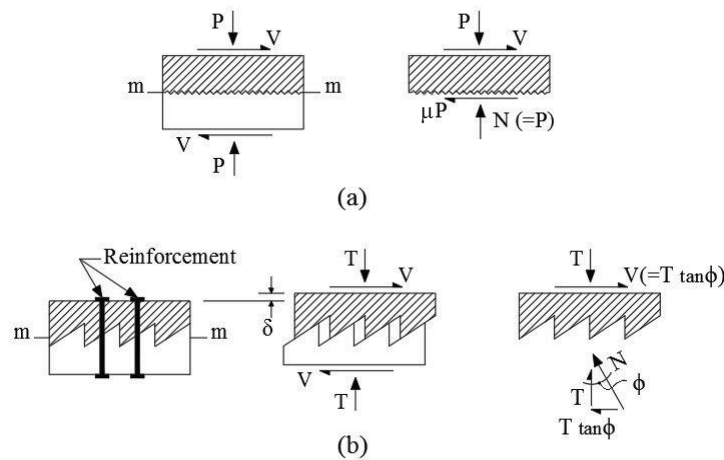


Figure 2.4: Shear Friction Theory (Birkeland and Birkeland 1966).

In the following subsections, the interface shear resistance of UHPC is presented for the two cases that are relevant to the design of deck-to-girder connections:

1. Interface shear resistance of monolithic UHPC
2. Interface shear resistance between hardened conventional concrete and fresh UHPC (CC-UHPC)

2.3.1. Interface Shear Resistance of Monolithic UHPC

Crane (2010) performed vertical interface shear push-off tests of monolithic UHPC specimens to determine whether ACI 318 (2008) and AASHTO LRFD (2007) equations of interface shear are applicable to monolithic UHPC. UHPC specimens with un-cracked and pre-cracked interfaces, and with reinforcement ratios of 0 and 0.5% were tested. Three identical push-off specimens were tested for each combination of interface type and reinforcement ratio as shown in Figure 2.5. Test results indicated that the ultimate interface shear resistance was significantly higher than that predicted for monolithic concrete in all cases. Regression analysis was performed to estimate UHPC cohesion and friction coefficients (c and μ). For un-cracked UHPC, $\mu = 4.5$, and $c = 2$ ksi were proposed, and for cracked monolithic UHPC, $\mu = 4.0$, and $c = 0.65$ ksi were proposed. These high values were attributed to the contribution of the steel fibers distributed across pre-existing cracks even when no mild shear reinforcement is used. Also as expected, the specimens with reinforced UHPC exhibited more ductile behavior than those with unreinforced UHPC. The average interface shear resistance of un-cracked monolithic UHPC increases by 48% with the increase of interface reinforcement ratio from 0 to 0.5% as shown in Figure 2.6.

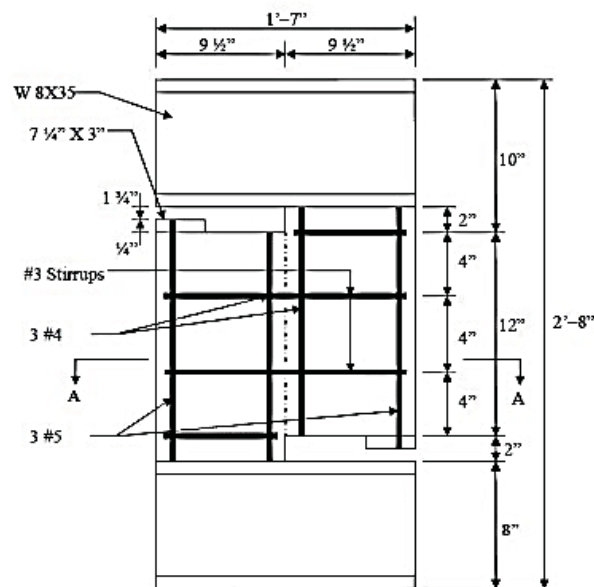


Figure 2.5: Vertical Interface Shear Push-off specimen of Monolithic UHPC (Crane 2010)

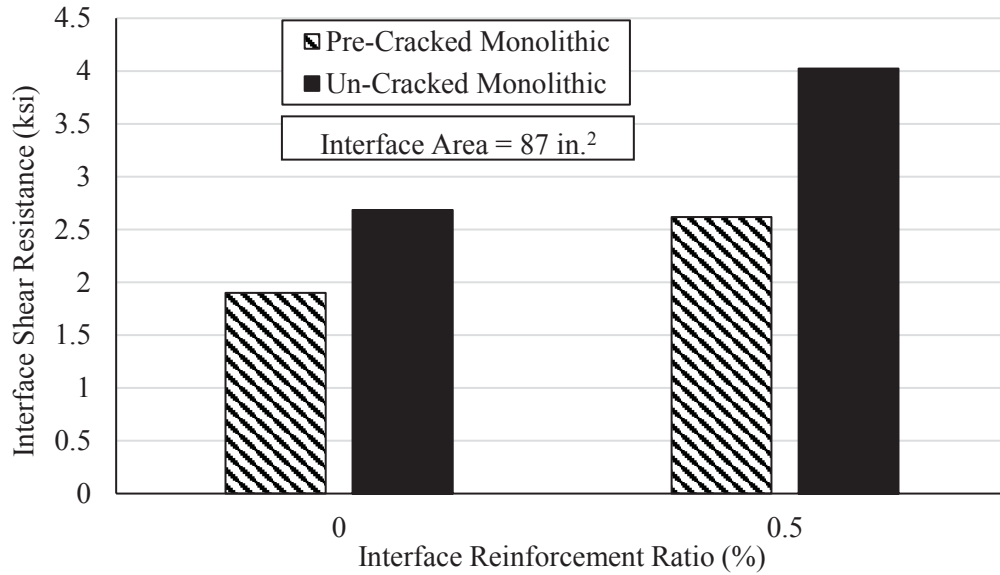


Figure 2.6: Average Interface Shear Resistance of Monolithic UHPC with and without Interface reinforcement (Crane 2010)

Maroliya (2012) investigated the behavior of reactive powder concrete (which is another term for UHPC) in direct interface shear. A series of direct shear specimens having inverted “L” shape in shear failure plane were tested using monolithic UHPC with different percentages of steel fibers as shown in Figure 2.7. Test results showed that plain UHPC samples failed in a brittle manner at the first-crack load, which happens to be the maximum load taken by the specimen. On the other hand, samples having 2.5% fibers indicated multiple visible cracks, while samples having 2% fibers resulted in a maximum load much higher than the first-crack load, which clearly reflects failure after the strain hardening of the material. These results helped concluding that UHPC exhibits a ductile failure mode depending on the percentage of fibers. Figure 2.8 shows the effect of different fiber content and curing methods on the direct shear strength of monolithic UHPC. Results also indicated an average value of direct shear strength for normal cured monolithic UHPC with 2% fiber volume fraction of about 2 ksi.

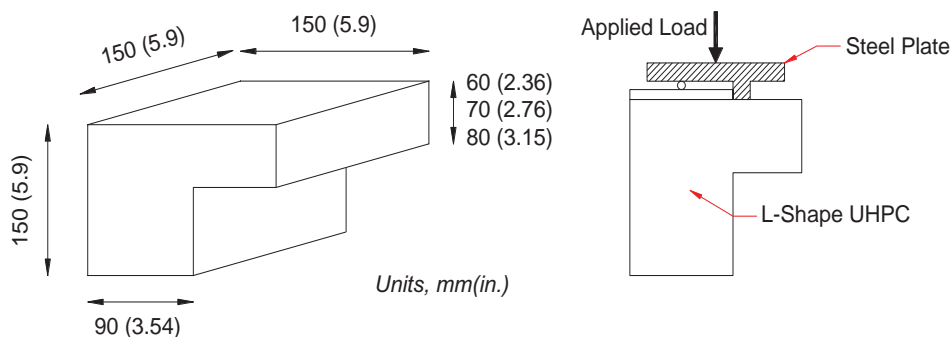


Figure 2.7: Shear Testing on Inverted L-Shape UHPC Specimen (Maroliya 2012)

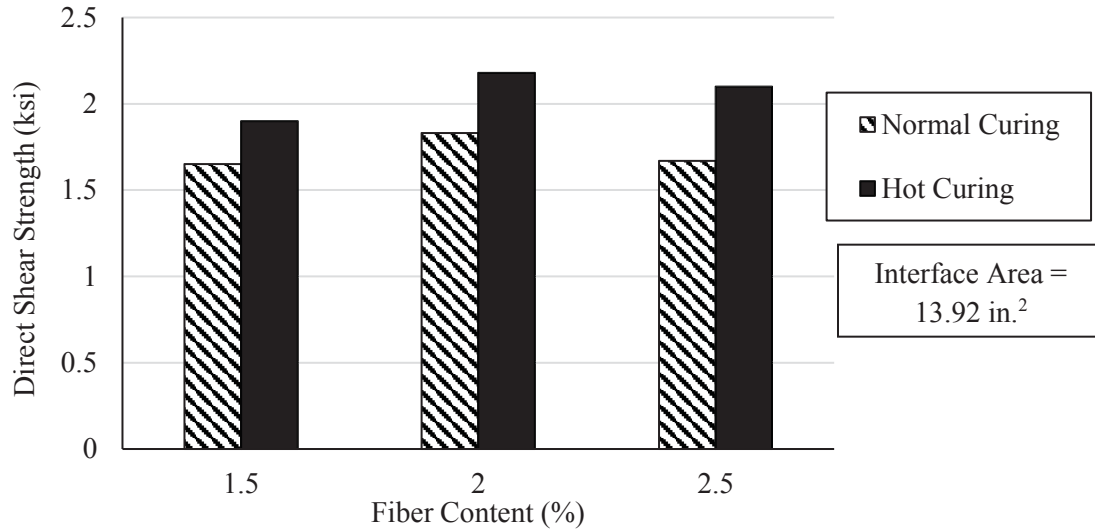


Figure 2.8: Effect of Fiber Content and Curing Methods on Direct Shear Strength of Monolithic UHPC without Interface reinforcement (Maroliya 2012)

Jang et al. (2017) conducted vertical shear test on L-shape specimen to evaluate the monolithic interface shear resistance of UHPC without interface reinforcement as shown in Figure 2.9. The UHPC matrix consists of water-to-binder ratio (w/b) of 0.14, type I/II Portland cement, Australian silica sand, and silica with a fiber content of 1.5% of volume. The UHPC achieved 29.08 ksi at 91 days. A vertical load was applied on the specimen with a rate of 0.024 in./min. till failure. Four LVDTs were used to capture the horizontal and relative vertical displacement in the L-shape specimen. The interface shear resistance of monolithic UHPC without interface reinforcement was 2.72 ksi with interface shear area of 46.50 in.².

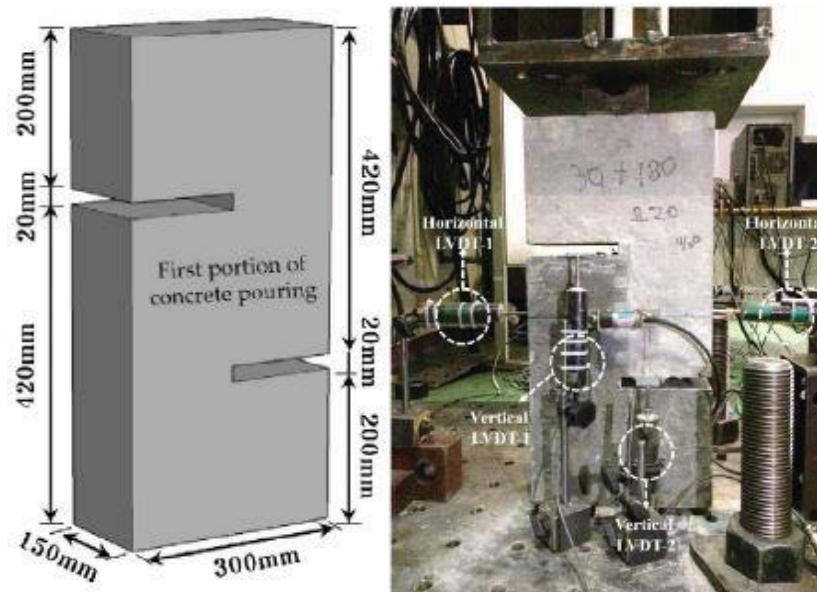


Figure 2.9: Monolithic L-Shape UHPC Specimen Test Setup and Specimen Dimensions (Jang et al. 2017)

Small and large scale push-off testing were performed to obtain the direct shear capacity of UHPC (Haber et al. 2017). Three small specimens composed of 6 in. long with 2 in. square cross section beams were tested by applying vertical load on the beam that was fixed by square supports from both ends. The UHPC were poured from one end for controlling the fiber orientation to be perpendicular to the applied loads. 14 in. by 24 in. two precast concrete slab with lug pockets were pre-fabricated and the lugs were filled with UHPC with a stub. A vertical load was applied on the UHPC stub to investigate the shear capacity of the proposed UHPC shear lugs. The direct shear testing for the small and large specimens are shown in Figure 2.10. The Specimens exhibit a double shear failure and the test results are summarized in Figure 2.11. A range of 4 ksi to 8 ksi UHPC direct shear capacity were achieved according to the tested specimens.

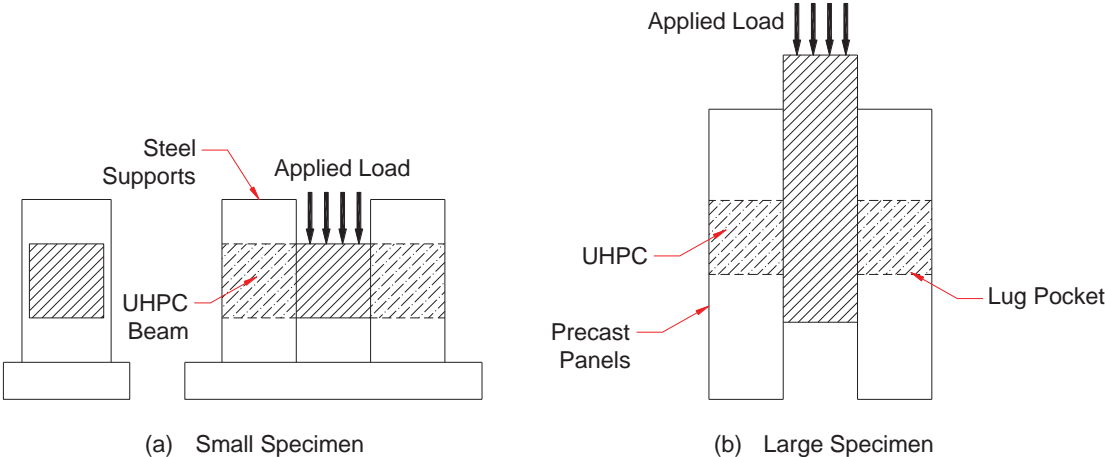


Figure 2.10: Small and Large Scale Push-off Test of Monolithic UHPC without Interface reinforcement (Haber et al. 2017)

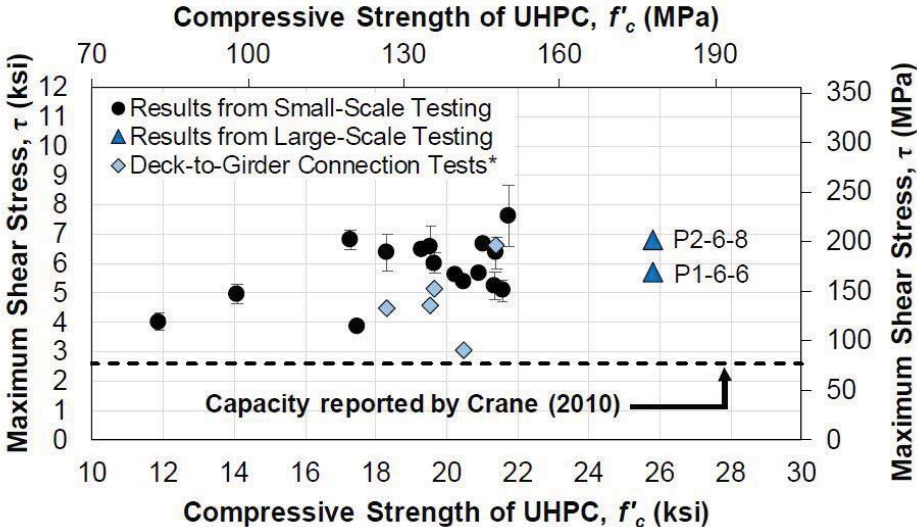


Figure 2.11: Small and Large Scale Push-off Test of Monolithic UHPC without Interface reinforcement (Haber et al. 2017)

2.3.2. Interface Shear Resistance between Hardened Conventional Concrete and Fresh UHPC (CC-UHPC)

Slant shear test and L-shape push-off tests are the most common testing techniques to evaluate the interface shear resistance between UHPC cast on hardened conventional concrete (CC-UHPC) with and without interface reinforcement. Slant shear test is conducted to evaluate the bond resistance over the interface plane between two materials. The type and dimensions of slant shear specimens and interface angle change according to the code as shown in Table 2.1. British and French standards use prism specimens while ASTM C882 uses cylindrical specimen. Interface plane angle with the horizontal axis is 60° in all codes.

Table 2.1: Slant Shear Composite Specimen Dimensions in Different Standards

Standard	Type of Specimen	Dimensions	Interface Plane Angle with Horizontal Axis
ASTM C882/C882M-13a	Cylinder	3x6 in.	60°
BS EN 12615:1999	Prism	3.9x3.9x15.7 in. or 1.6x1.6x6.3 in	60°
French standard NFP 18-872	Prism	3.9x3.9x11.8 in	60°

ASTM C882/C882M-13a is used mainly for determining the bond resistance of a layer of epoxy-resin-base material between either two hardened or between hardened and fresh Portland-cement concrete. The slant shear test is performed on 3 in. by 6 in. specimens with an interface plane angle of 60° with horizontal axis as shown in Figure 2.12. The specimen sections are prepared by placing Portland-cement mortar in the mold in two layers of approximately equal volume which was uniformly rodded 25 time per each layer. The compressive strength of the concrete section should have at least 4,500 psi at 28 days after being cured. Based on 60° angle inclined interface plane, the area of the elliptical interface plane is twice the area of the specimen base. The specimens shall be tested at $73 \pm 2^\circ\text{F}$ in compression after capping in accordance with test method C39/C39M. A minimum of three composite specimens are required for each test type.

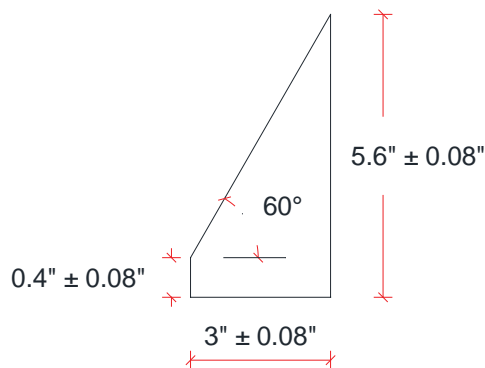


Figure 2.12: Portland-Cement Concrete Section Dimensions.

The interface shear resistance between a UHPC overlay and hardened normal concrete substrate with different textures was investigated in the literature by three different test procedures: slant shear test, flexural test, and split prism test (Harris et al. 2011). The slant shear test was performed according to ASTM C882/C882M to evaluate the interface shear resistance using 3×6 in. composite cylinders. A total of twenty-seven composite cylinders were fabricated and tested. The hardened section composed of Type III normal concrete mortar that had compressive strength of 5000 psi at 28 days with moist curing (f'_m). Three different surface textures were applied to the interface shear plane; smooth (no surface preparation), low roughened (average depth of 0.1 in.), and high roughened (0.20 in. transverse grooves) surfaces as shown in Figure 2.13(a). Wire brush treatment and handheld metal grinder were used to obtain the low and high roughened surfaces respectively. Also, trapezoidal shear key (fluted), with 0.50 in. depth and 0.63 in.² area, was prepared as a precast scenario for using UHPC as a protective overlay. The hardened concrete mortar sections were placed back inside the molds and filled with UHPC. The composite specimens were cured under ambient conditions for 10 days till the UHPC and normal concrete gained compressive strength of 15 ksi and 5 ksi, respectively. The composite specimens were loaded under compression until failure happened either on the interface plane or the concrete crashed as shown in Figure 2.13(b). The interface shear resistance was calculated by dividing the peak load by the interface surface area.



Figure 2.13: Slant Shear Test; (a) Mortar Different Roughened Surfaces and Trapezoidal Shear Key, (b) Test Setup (Harris et al. 2011)

The composite specimens with smooth interface exhibited failure along interface plane, however, the roughened interface specimens had a normal concrete compression failure as shown in Figure 2.14. The average interface shear resistance for smooth surface was 1.6 ksi and it increased with 28%, 56%, and 57% with applying low roughened, high roughened surfaces, and shear key, respectively, as shown in Figure 2.15.



Figure 2.14: Failure Modes; (a) Failure along Interface Plane, (b) Normal Concrete Failure (Harris et al. 2011)

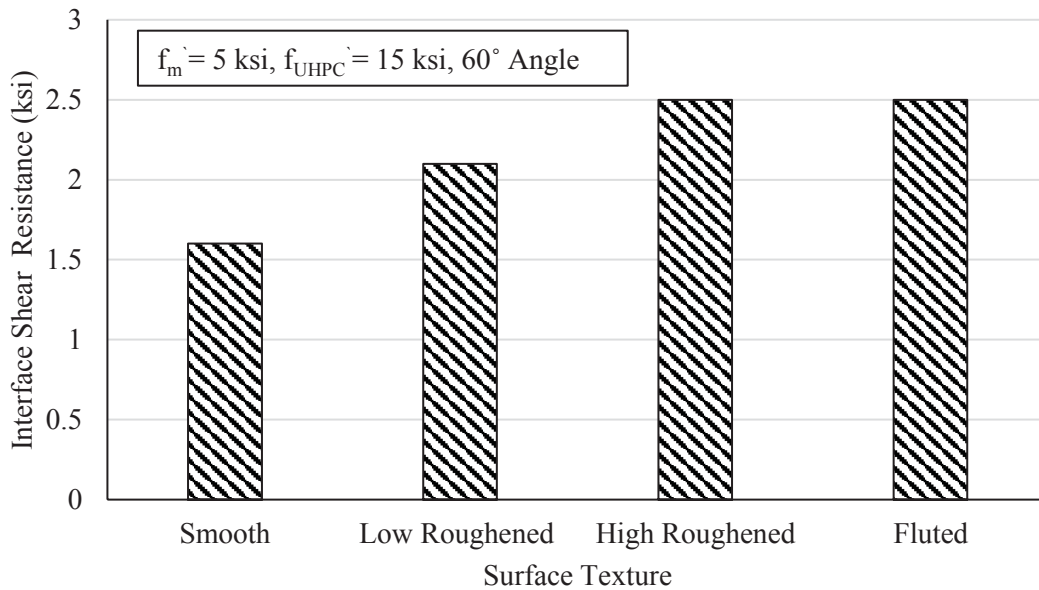


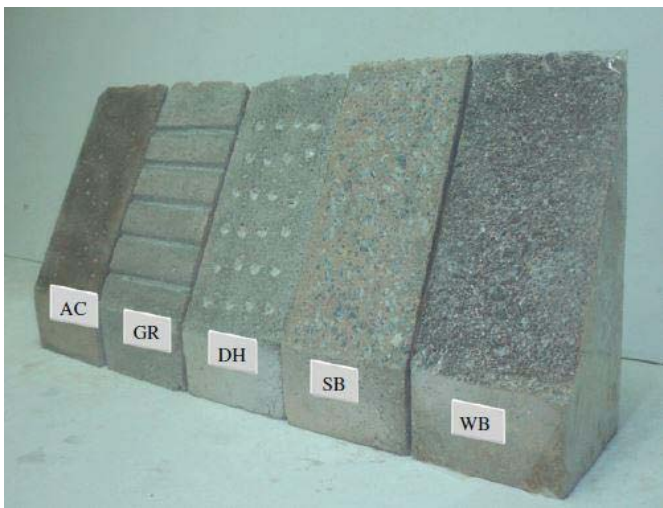
Figure 2.15: Interface Shear Resistance of Cement Type III Mortar with Different Surface Textures (Harris et al. 2011)

Tayeh et al. (2012) investigated the mechanical and permeability properties of interface between normal concrete (NC) substrate, which represents old concrete, and an overlay of ultra-high performance fiber concrete (UHPFC) as a repair material. The interface shear resistance and influence of different surface roughening were evaluated through performing slant shear test and splitting tensile test. The mix proportions of UHPFC and NC are shown in Figure 2.16(a). The slant shear composite specimens were fabricated using prism of 3.9x3.9x11.8 in. with interface angle with vertical of 30°. The interface plane was prepared with five different surface textures: as cut, sand blasted, wire brushed, drilled holes (0.4 in. diameter and 0.2 depth), and grooved (0.4 in. width and 0.2 in. depth) as shown in Figure 2.16(b). The compressive strength of NC and UHPFC at 28 days were 6.53 and 24.66 ksi, respectively. The test was conducted according to ASTM C288 and the test setup is shown in Figure 2.16(c).

Table 1
Mix proportions for NC substrate and UHPFC.

Concrete type (kg/m ³)	NC substrate	UHPFC
OPC (Type 1, 42.5R)	400	768
Coarse aggregate (max. 12.5 mm)	930	–
River sand (F.M. = 2.4)	873	–
Mining sand (<1180 μm)	–	1140
Silica fume (23.7 m ² /g)	–	192
Steel fiber ($L_f = 10$ mm, $d_f = 0.2$ mm)	–	157
Superplasticizer (PCE-based)	4	40
Water	200	144
Total	2407	2441
W/B	0.5	0.15
Cube strength, $f_{c,28d}$	45 MPa	170 MPa
Split cylinder tension strength, $f_{sp,28d}$	2.75 MPa	15.3 MPa

(a)



(b)



(c)

Figure 2.16: (a) Mix Proportions of UHPFC and NC, (b) Surface Textures, and (c) Test Configuration (Tayeh et al. 2012)

Four different failure modes were observed: pure interfacial failure, interfacial failure with minor NC cracking, interfacial failure with NC fracture, and substrata failure. The interface shear resistance was calculated by dividing the maximum applied load by the interface contact area. The sand-blasted texture specimens give the highest interface shear resistance of 2.58 ksi. The surface texture clearly influences the interface shear resistance, as compared to surface without preparation, the interface shear resistance increases with 105%, 60%, 47%, and 41% for sand blasted, grooved, wire brushed, and drilled holes surfaces as shown in Figure 2.17.

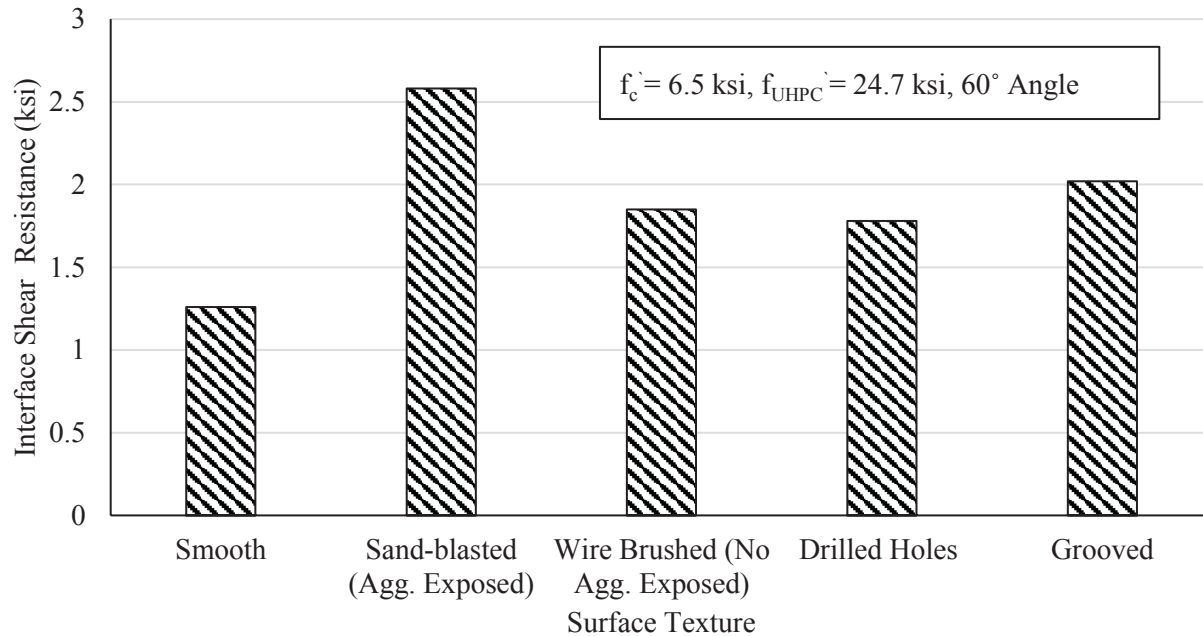


Figure 2.17: Different Surface Texture Effect on Interface Shear Resistance of NC-UHPC (Tayeh et al. 2012)

Muñoz (2012) conducted a study on using UHPC as a repair material by investigating the interface shear resistance between UHPC and normal strength concrete (NSC). The interface shear resistance was evaluated by three different test methods: slant shear test, splitting prism test, and pull-off test. The slant shear test was conducted to obtain the interface shear resistance of different surface preparation treatment and interface angles. The slant shear composite specimens were 3.5x3.5x14 in prism to allow casting concrete substrate contrasting ASTM C 882 that use mortar substrate as shown in Figure 2.18. This study focused on four different surface textures: brushed, sandblasted, grooved, and roughened (exposed aggregate), and two different interface angles with horizontal axis, 60° and 70°. The normal concrete sections were casted in wooden forms and cured in two stages: 24 hours in moist cure before demolding and, then, in a lime water tank for 28 days. The compressive strength of NSC mixes was 6.46 ksi, 6.61 ksi, and 8.11 ksi for grooved and brushed, roughened, and sandblasted surface texture specimens respectively. A steel brush and drill-bit, sandblasting equipment, wet saw, and concrete retarder were used to obtain the brushed, sandblasted, grooved, and roughened interface surface textures respectively. Two different methods were used to evaluate the roughening degree, the macrotexture depth test and the concrete surface preparation index given by International Concrete Repair Institute (ICRI) guide. Figure 2.19 and Table 2.2 shows the different surface textures and the degree of roughening measurement.

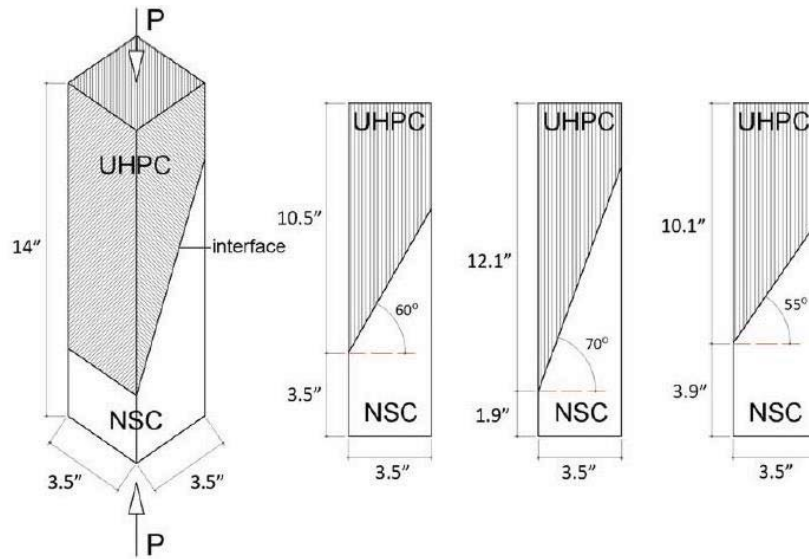


Figure 2.18: Slant Shear Composite Specimen Dimensions (Muñoz 2012).

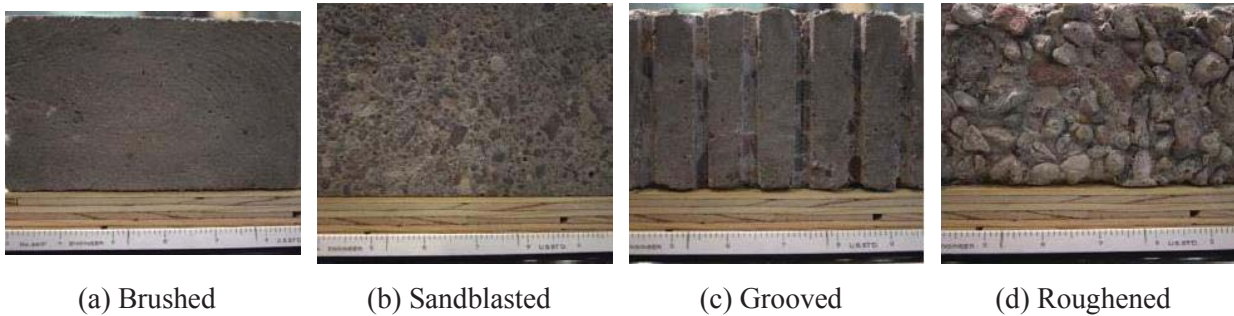


Figure 2.19: Different Surface Textures (Muñoz 2012).

Table 2.22: the macrotexture depths of prepared surfaces ((Muñoz 2012)

Surface	ICRI Profile	Macrotexture Depth (in)
Brushed	1,3	0.03
Sandblasted	4,5	0.03
Grooved	Not applicable	Not applicable
Roughed	Aggregate exposure >8,9	0.09

The composite specimens consisted of hardened NSC blocks with prepared interface surface texture after curing in a water tank and Ductal®JS1000 UHPC poured on the blocks. Four composite specimens were tested at 8 days for each texture. A load rate of 35 psi/second was used to apply load using compression machine till failure as shown in Figure 2.20. The tested specimens exhibited different failure modes. The slant shear specimens with 60° interface angle and 8 days of UHPC exhibited NSC failure. However, the 70° interface angle brushed surface specimens had interface failure, the other surface textures expressed NSC failure. Figure 2.21 shows the effect of interface angle on the interface shear resistance for different surface texture at 8 days of UHPC. The interface shear resistance was calculated by dividing the maximum applied load by the interface contact area. The interface shear resistance of sandblasted

specimens is the highest compared to the other surface texture specimens. The higher compressive strength of sandblasted NSC section might give a wrong conclusion as mention by the authors. Failure modes and interface shear resistance are affected by the change of the interface angles. The interface shear resistance at 8 days for all surface preparations exceeded the requirements specified by ACI 546.3R-06 at 7 days and satisfied the minimum bond requirements for 28 days.



Figure 2.20: Slant Shear Test Configuration (Muñoz 2012).

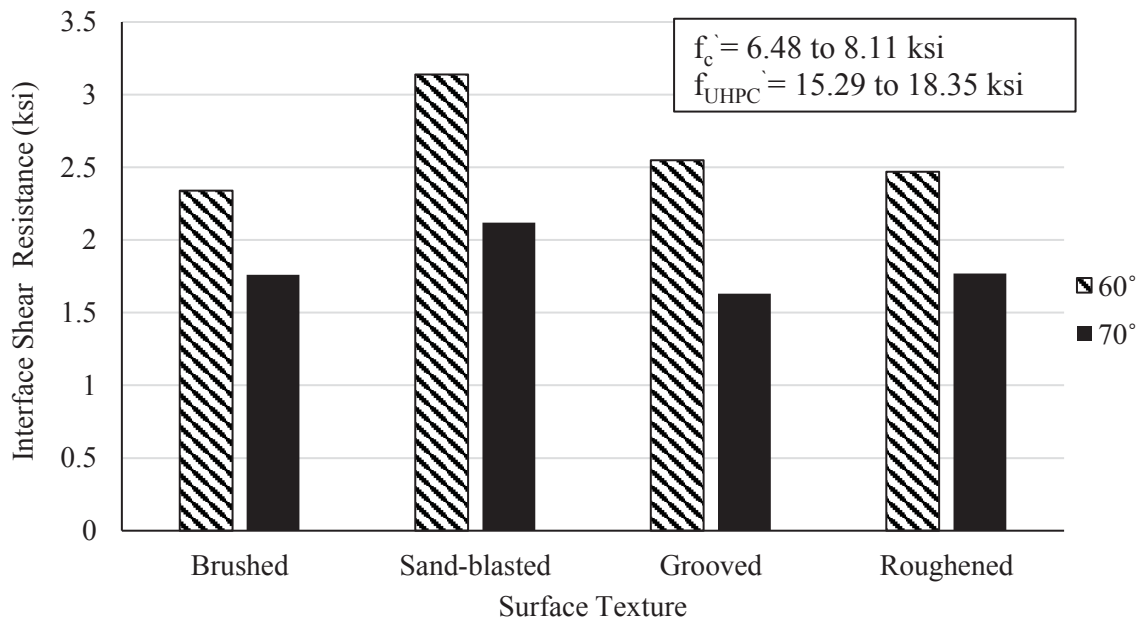


Figure 2.21: Effect of Interface Angle on Interface Shear Resistance at 8 Days of UHPC (Muñoz 2012).

Rangaraju et al. (2013) performed a study on developing local UHPC using available materials in South Carolina and evaluating its performance as shear key grout for bridge systems. Slant shear test was conducted to evaluate the interface shear resistance of the local UHPC as a part of determining the local

UHPC mix properties. The slant test was performed according to ASTM C882 with modifications, using normal concrete representing bridge deck instead of concrete mortar. The normal concrete was cast in 3x6 in. cylinders and moist-cured for a 28-day period. The range of normal concrete compressive strength was from 5.92 to 7.61 ksi. The interface surface was then treated by sand-blasting to obtain a roughened surface. Four different UHPC mixes were poured on the top of normal concrete section, demolded after 1 day, and moist-cured for 6 days. The composite specimens were tested at 7 and 28 days under compression rate according to ASTM C39. Most of the specimens failed in the normal concrete portion, one specimen exhibited interface failure. The maximum applied loads and failure modes are shown in Table 2.3.

Table 2.3: Different Mix Proportions Used in Evaluating Local UHPC Properties, Ib/Yard³ (Rangaraju et al. 2013)

UHPC ID	Cement	Sand	Silica fume (SF)	Water	SP, %	Steel microfiber**
UHPC 1	1601	2002	-	320	RQ	-
UHPC 2	1300	1949	260	312	RQ	-
UHPC 3	1273	1909	255	305	RQ	270
UHPC 4	1249	1873	250	300	RQ	270

*SP quantity is expressed in terms of percentage by weight of the total cementitious material (cement + silica fume)

**microfiber dosage is expressed in terms of percentage by volume of the non-microfiber mixture
RQ indicates required quantity to obtain a full flow of 150%

Table 2.4: Slant Shear Test Results and Failure Modes (Rangaraju et al. 2013)

UHPC ID	Maximum Applied Force					
	7-days			28-days		
	Average, kips	COV, %	Failure Location	Average, kips	COV, %	Failure Location
UHPC 1	28.3	2.0	Concrete	46.2	4.7	Concrete
UHPC 2	32.7	8.4	Concrete	56.2	5.2	Concrete & UHPC
UHPC 3	64.6	6.6	Interface & Concrete	58.5	9.6	Concrete
UHPC 4	62.7	11.2	Concrete	66.9	10.5	Concrete

The shear transfer behavior across the interface plane between UHPC and normal concrete (NC) was investigated analytically and experimentally by conducting slant shear test and flexural test (Aaleti and Sritharan 2017). The slant shear testing was performed to evaluate the effect of NC compressive strength, interface roughness, curing condition, and pouring sequence on the direct shear transfer behavior. Prismatic specimens consist of normal concrete with five different texture along the interface plane and UHPC were used for performing the slant shear test. The composite specimen dimensions were 4.5 in. × 6 in. in cross-section and 24 in. long and interface angle of 53.1° with the horizontal axis as shown in Figure 2.22.

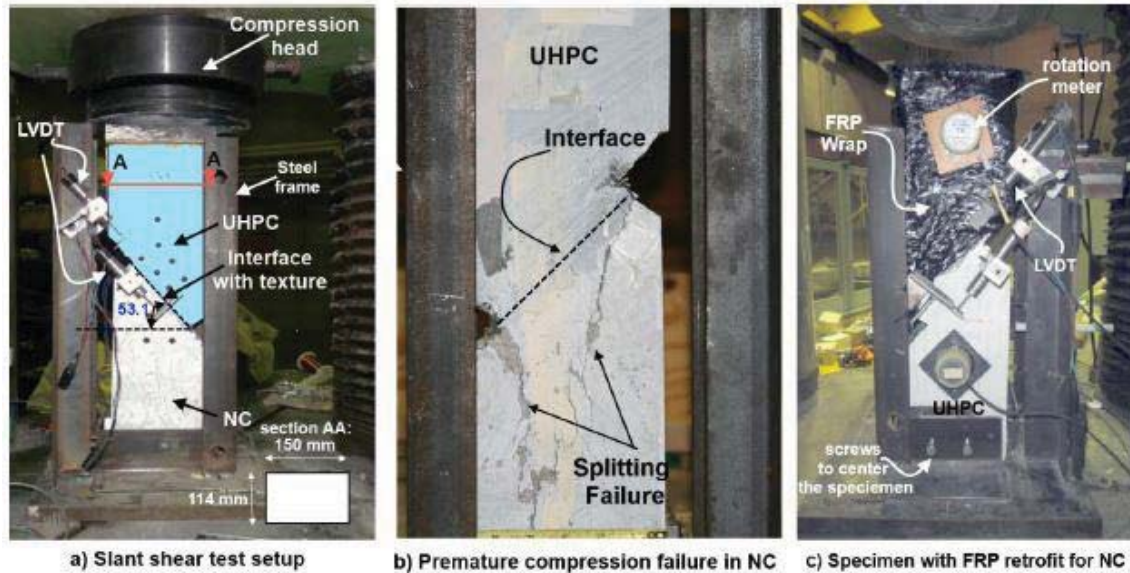


Figure 2.22: Test Setup and Instrumentation of Large Prism Slant Shear Test (Aaleti and Sritharan 2017)

A total of sixty specimens were fabricated with three normal concrete compressive strength, five different textures, and four different curing conditions as shown in Table 2.5. The surface textures were obtained by adding form liners to the interface shear plane. The five surface textures represented low roughness (< 0.06 in.), medium roughness (0.12 in.), and high roughness (0.2 in. to 0.25 in.). The NC sections of composite specimens were cast vertically, and their compressive strength were obtained at 28 days and at the time of slant shear specimen testing. Then, UHPC was used to cast the second section of composite specimens. The texture depth of composite section was measured before pouring the second half. Based on ASTM C882, a uniaxial compression load was applied at the end of the composite slant shear specimens using a universal testing machine as shown in Figure 2.22. Four linear variable differential transducers (LVDTs) were used to capture the slip at the interface shear plane. Two rotation meters were used to capture any rotation induced by possible eccentricity of loading.

Table 2.5: Summary of NC-UHPC Interface Test Matrix (Aaleti and Sritharan 2017)

Specimen Type	Texture (# of specimens)	Casting Sequence	Target NC Strength
UHPCw-NC5	5 textures (3 per texture)	Wet UHPC over cured NC	5 ksi
UHPCw-NC7	5 textures (3 per texture)	Wet UHPC over cured NC	7 ksi
UHPCw-NC10	5 textures (3 per texture)	Wet UHPC over cured NC	10 ksi
UHPCch-NC5	5 textures (3 per texture)	Wet NC on heat-treated UHPC	5 ksi

Two failure modes were noticed: interface failure or NC failure, as shown in Figure 2.23. The authors did FRP retrofitting to NC section of some specimens that did not experience significant sliding due to splitting cracks in NC. The interface shear resistance was calculated by dividing the maximum load along the inclined plane by the interface contact area. Figure 2.24 shows average interface shear resistance

of three specimens for different surface texture depths and concrete compressive strength. The interface shear resistance generally increased with the increase of texture roughness and concrete strength. Average interface shear resistance of textures deeper than 0.08 in. satisfied the ACI 546.3R-06 limits. Also, interface shear capacity calculated based on AASHTO (2010) equations were conservative in predicting NC-UHPC interface shear resistance.

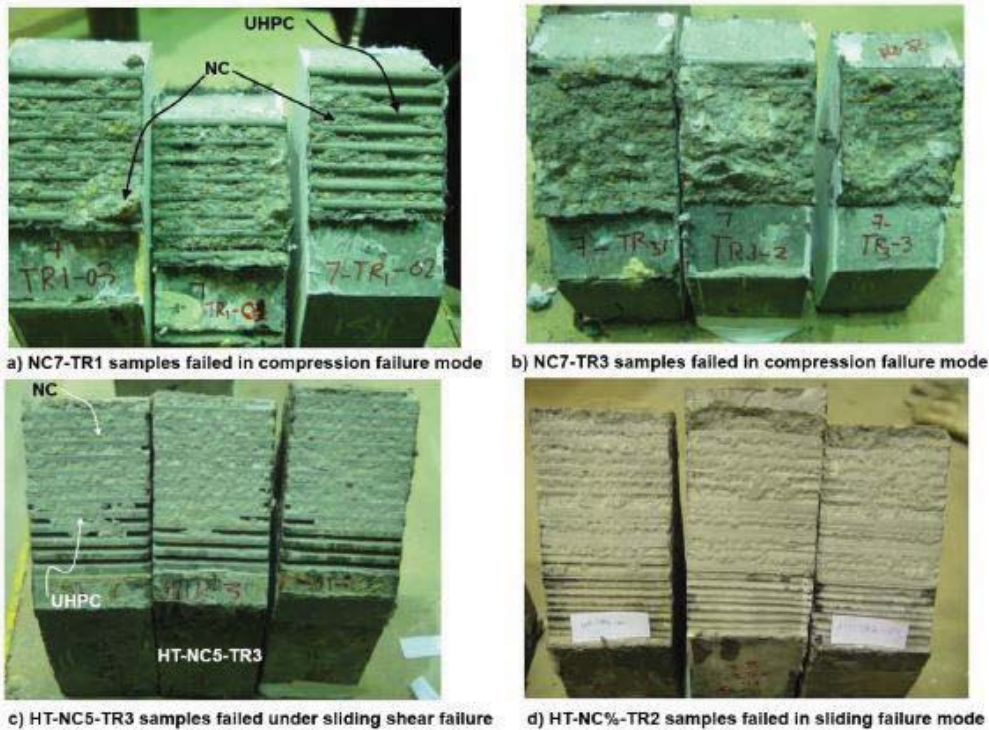


Figure 2.23: Samples of NC-UHPC Interfaces of Specimen with Different Failure Modes (Aaleti and Sritharan 2017)

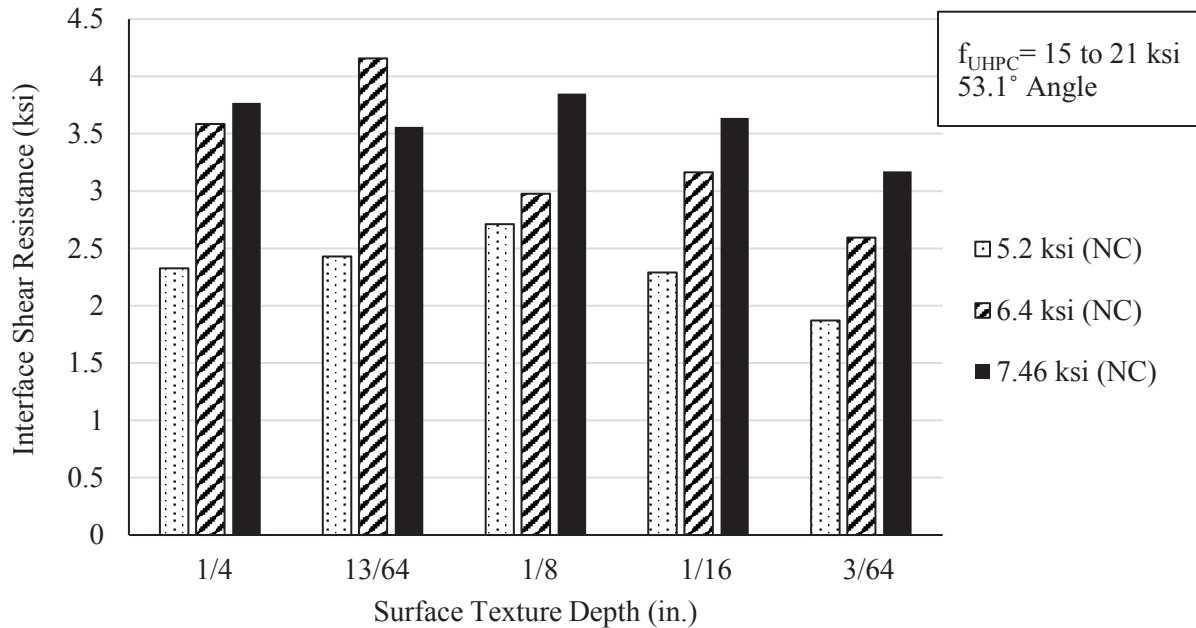


Figure 2.24: Effect of Surface Texture Depth and NC Compressive Strength on Interface Shear Resistance of NC-UHPC (Aaleti and Sritharan 2017)

Jang et al. (2017) conducted vertical shear test on L-shape push-off specimen to evaluate the interface shear resistance between UHPC and normal strength concrete (NSC) without interface reinforcement as shown in Figure 2.25. The L-shape specimen dimensions are 5.9 x 11.8 x 25.2 in. with interface shear area of 5.9 x 7.9 in. Five different surface treatments were applied to the CC sections: smooth, water jet, grooved (0.4 in.), grooved (0.8 in.), and grooved (1.2 in.) as shown in Figure 2.25. The UHPC matrix consists of water-to-binder ratio (w/b) of 0.14, type I/II Portland cement, Australian silica sand, and silica with a fiber content of 1.5% of volume. The CC and UHPC achieved 5.2 and 29.08 ksi respectively. A vertical load was applied to the specimen with a rate of 0.024 in./min. till failure. Four LVDTs were used to measure the horizontal and relative vertical displacement in the L-shape specimen. Figure 2.26 shows the average interface shear resistance of NSC-UHPC with different surface treatments. Based on the results, the interface shear resistance of NSC-UHPC without interface reinforcement increases with the increase of the surface roughening.

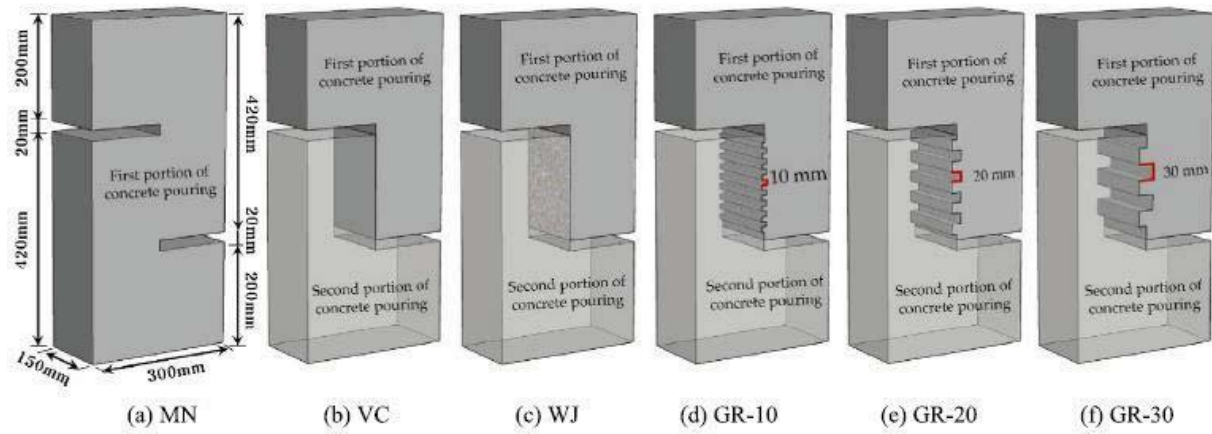


Figure 2.25: L-Shape Specimen Dimensions and Different Surface Treatment of NSC-UHPC (Jang et al. 2017)

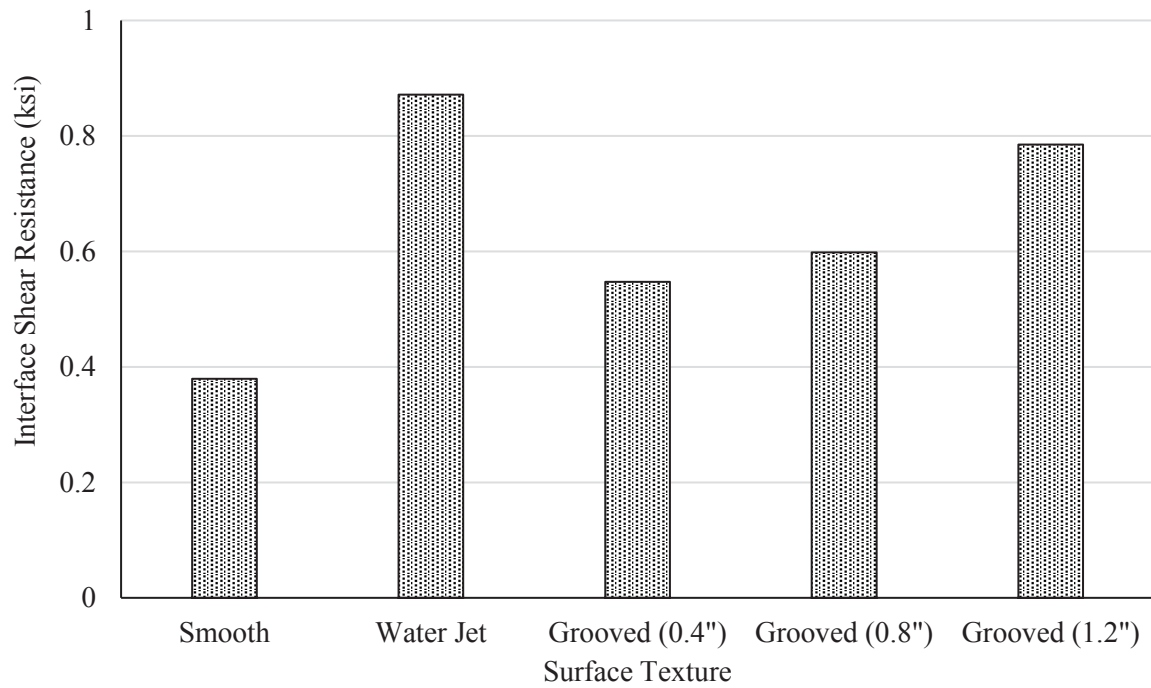


Figure 2.26: L-Shape Test Results of NSC-UHPC Specimens (Jang et al. 2017)

2.4. Existing Provisions for Interface Shear Resistance

According to AASHTO LRFD Bridge Design Specifications (2017) Section 5.7.4, the nominal interface shear resistance between two concrete layers cast monolithically or at different times is calculated using the following equation.

$$V_{ni} = cA_{cv} + \mu(A_{vf}f_y + P_c) \leq K_1f'_cA_{cv} \leq K_2A_{cv}$$

Where:

V_{ni} : nominal interface shear resistance (kips)

c : cohesion factor (ksi)

μ : friction factor

A_{vf} : the cross-sectional area of the interface shear reinforcement crossing the interface area (in.²)

A_{cv} : interface shear area (in.²)

f_y : the reinforcement yield stress which is limited to 60 ksi

K_1, K_2 : factors to limit interface shear resistance

P_c : permanent net compressive force normal to the shear plane; if force is tensile, $P_c = 0.0$ (kips)

The normal weight concrete placed monolithically has cohesion and friction coefficient of 0.40 ksi and 1.4, respectively. For intentionally roughened interface surface to an amplitude of 0.25 in., the cohesion and friction factors are 0.24 ksi and 1.0, respectively. The cohesion and friction factors mentioned in AASHTO LRFD (2017) provisions are developed for conventional concrete. By dividing the previous equation with the interface area, the nominal interface shear resistance can be predicted using the following equation.

$$v_{ni} = c + \mu(\rho f_y + N)$$

Where:

v_{ni} : nominal interface shear resistance (ksi)

ρ : interface shear reinforcement ratio (A_{vf}/A_{cv})

N : normal stress applied to the shear plane (ksi)

The French standard has a specific provision for the interface shear resistance of UHPC in its publication NF-P-18-710-UHPC. The NF-P-18-710-UHPC states that the interface shear resistance equations for CC can be used to predict the interface shear resistance of CC-UHPC. It also states two equations for calculating the nominal interface shear resistance of UHPC cast on hardened UHPC based on the interface surface texture as following:

$$V_{Rdi} = cf_{ctk,el}/\gamma_c + \mu\sigma_n + \rho f_{yd}(\mu \sin\alpha + \cos\alpha) \leq 1.15\alpha_{cc}f_{ck}^{2/3}/\gamma_c$$

$$V_{Rdi} = cf_{ctk,el}/\gamma_c + \mu\sigma_n + \rho f_{yd}(\mu \sin\alpha + \cos\alpha) + (0.35\mu + 0.3) f_{ctfk}/K \cdot \gamma_c \leq 1.15\alpha_{cc} f_{ck}^{2/3} / \gamma_c$$

Where:

V_{Rdi} : nominal shear resistance at interface (MPa)

c and μ : UHPC cohesion and friction factors depend on interface surface roughening

σ_n : the stress caused by the minimum external axial force across the interface that can act simultaneously with the shear force (MPa)

ρ : interface reinforcement ratio across the interface plane (A_s / A_i)

A_s : the area of reinforcement crossing the interlace, including ordinary shear reinforcement (if any), with adequate anchorage at both sides of the interface

A_i : the area of the joint

α : angle of fiber indentation with the interface shear surface of the hardened UHPC as shown in Figure 2.32; $45^\circ < \alpha < 90^\circ$.

$f_{ctk,el}$: characteristic value of the tensile limit of elasticity (MPa)

f_{ctfk} : characteristic value of the post-cracking strength (MPa)

f_{ck} : characteristic value of compressive strength (MPa)

f_{yd} : Design yield strength of reinforcement (MPa)

γ_c : partial factor for compressed UHPC (can be reduced to 1.3)

K : fiber orientation factor

The first equation predicts the nominal interface shear resistance for smooth surface and the second one in case of fluted surface. Figure 2.27 shows the limits that must be satisfied to consider the surface is fluted. Also, the depth of indentation “d” must be larger than twice the length of the longest fibers contributing to ensuring non-brittleness. Table 2.6 shows the UHPC cohesion and friction factors with different surface textures.

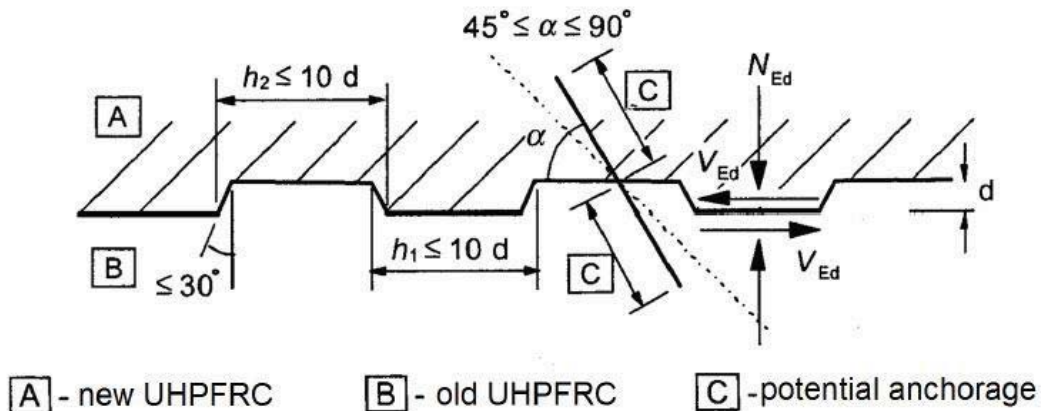


Figure 2.27: Fluted Construction Joint with Indented Fibers (NF-P-18-710-UHPC 2016)

Table 2.6: UHPC Cohesion and Friction Factors of UHPC for Different Surface Textures based on NF-P-18-710-UHPC 2016

UHPC Surface Texture	UHPC Cohesion Factor (c)	UHPC Friction Factor (μ)
Formed Clean Surface	0.025-0.10	0.5
Un-Formed Clean Surface	0.2	0.6
Roughened Clean Surface with Form liner	0.4	0.7
Clean Fluted Surface	0.5	1.4

Chapter 3. Proposed Deck-To-Girder Connection

3.1. Introduction

This chapter presents a new UHPC connection between precast concrete deck panels and precast/prestressed concrete girders that eliminates any changes to girder design/production and any possible conflict between deck and girder reinforcement. Both initial design and final design are presented as well as the construction sequence of the new connection.

3.2. Initial Design

Based on the literature review, the current precast concrete deck-to-girder connections using UHPC consist of open longitudinal joints or covered longitudinal troughs with exposed aggregate finish and grouting holes every 24 in. over each girder line. These two systems consume large quantities of UHPC to fill the joints and haunches that impact significantly the system economics based on the high price of UHPC. Also, using opened/covered longitudinal joints prevent transverse prestressing of concrete deck panels that limits the size of precast panels.

The initial design was forming trough along the width of the panel and casting UHPC through grouting holes to fill the trough and haunch (Abo El-Khier, et al. 2018). Figure 3.1 and Figure 3.2 show two alternatives for forming the haunch: option I requires continuous deck support system and large quantity of UHPC, and option II requires discrete deck support system, compressible material, and smaller quantity of UHPC. Figure 3.3 shows a preliminary design of the panel trough proposed for this application. Figure 3.4 shows two alternatives for panel reinforcement and pre-tensioning strands: Option I with solid concrete zones at the panel ends and middle to provide two layers of pre-tensioning stands at these locations; and Option II with three equal troughs and two layer of pre-tensioning strands at the solid concrete zones. The main advantage of these options over the continuous trough concept presented in the literature is the use of pre-tensioning strands to transversely prestress the precast concrete panels, which minimizes panel cracking during handling and transportation.

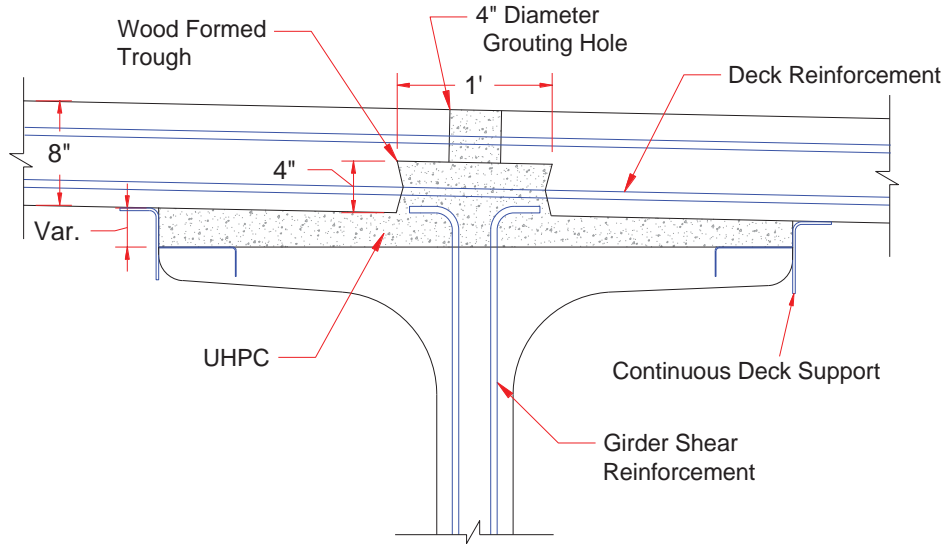


Figure 3.01: Initial Design Connection (Option I)

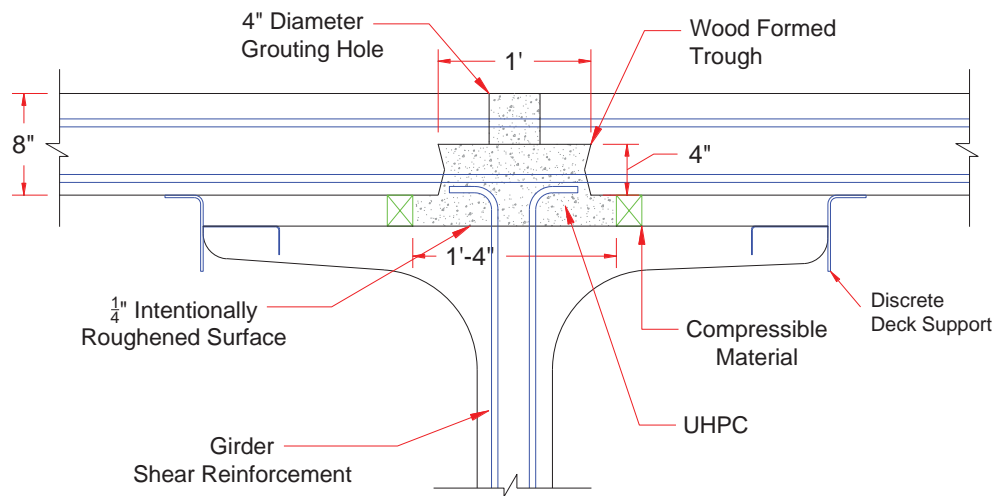


Figure 3.02: Initial Design Connection (Option II)

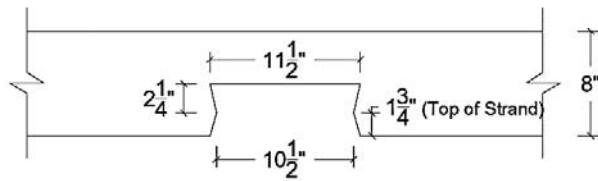


Figure 3.03: Initial Design Proposed Panel Trough.

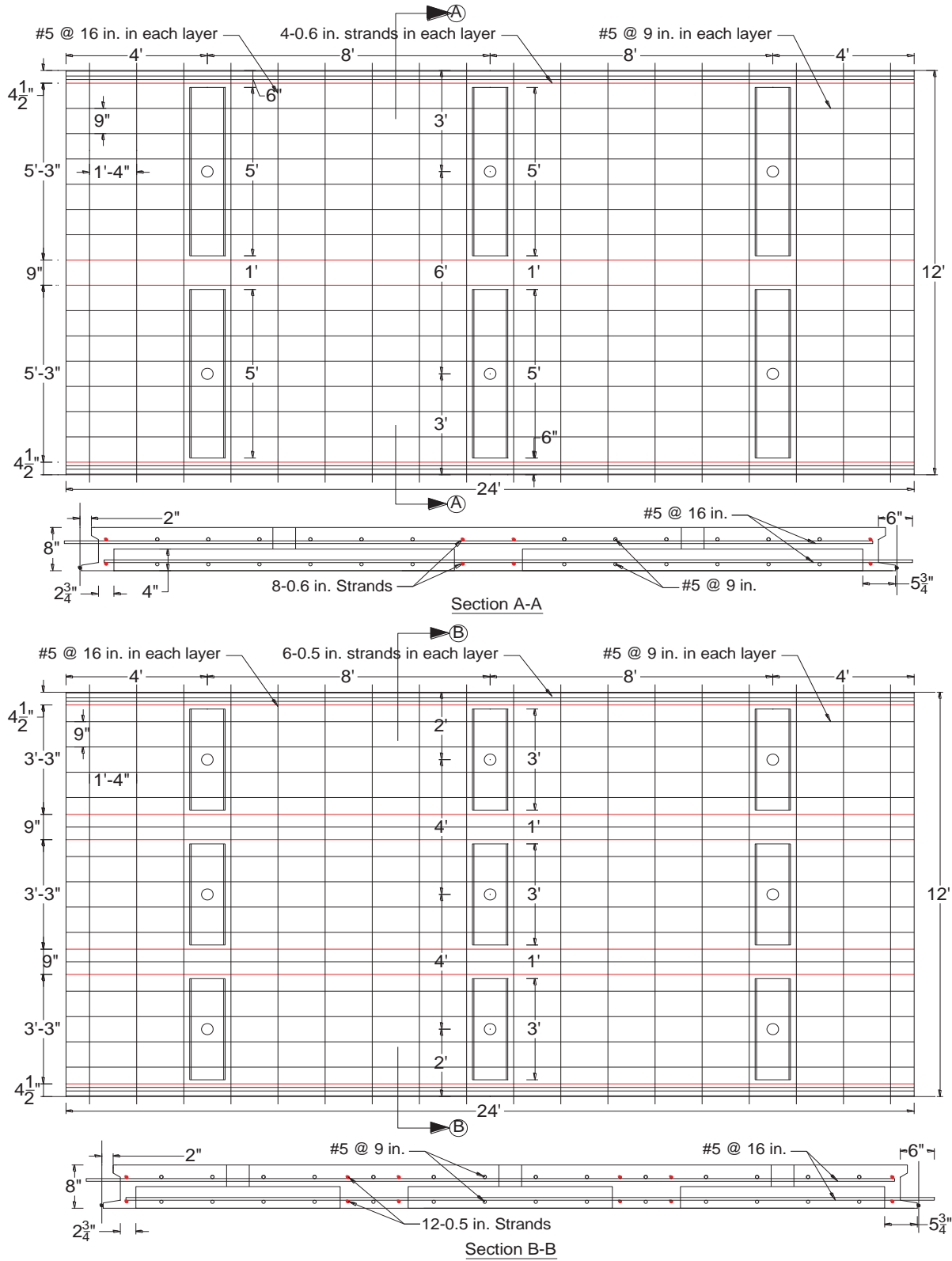


Figure 3.4: Alternatives for Panel Reinforcement and Pre-Tensioning.

3.3. Proposed Deck-to-Girder Connection Using UHPC

The initial design required a huge amount of UHPC to fill the trough and haunch that leads to making the proposed system not economic. Also, the deck panel solid parts would exhibit high stress concentration due to the pre-tensioned strands. To simplify the initial design, the haunch is eliminated and replaced with discrete round shear pockets. Figure 3.5 shows the proposed precast concrete deck-to-girder connection using UHPC supported by precast/prestressed concrete girders. In this connection, discrete round shear pockets 4 – 8 in. in diameter are formed in the deck panels every 2 - 4 ft. over each girder line. The diameter and spacing of these pockets are determined based on the interface shear demand. Girder interface shear reinforcement is the same as it is in case of CIP concrete bridge decks but lowered to remain below the soffit of deck panels. Once all panels are installed at the desired elevation using support angles or leveling bolts, a loop bar is inserted in each shear pocket to cross the interface between the two components. The shear pockets and haunches are, then, filled with UHPC cast from the shear pocket openings to connect the two components and achieve the composite section. The side surface of the shear pockets should be roughened using either form liner or exposed aggregate to provide adequate bond between UHPC and the deck panel concrete. Also, blocks of compressible material are recommended as shown in Fig. 3.5 to form the haunch area and reduce the quantity of field cast UHPC. The same concept can be used to connect precast concrete deck panels to steel girders with conventional shear studs as shown in Figure 3.6, which is not the focus of this study .

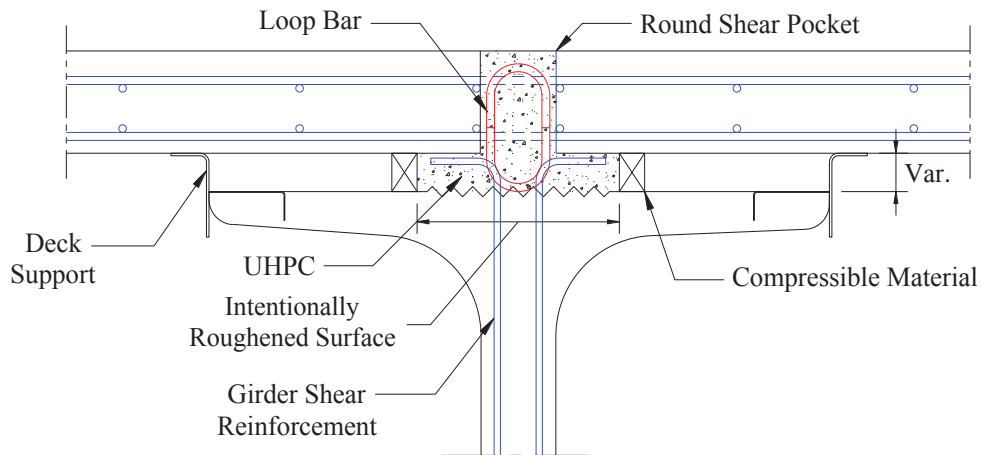


Figure 3.5: Proposed Precast Concrete Deck-To-Concrete Girder Connection

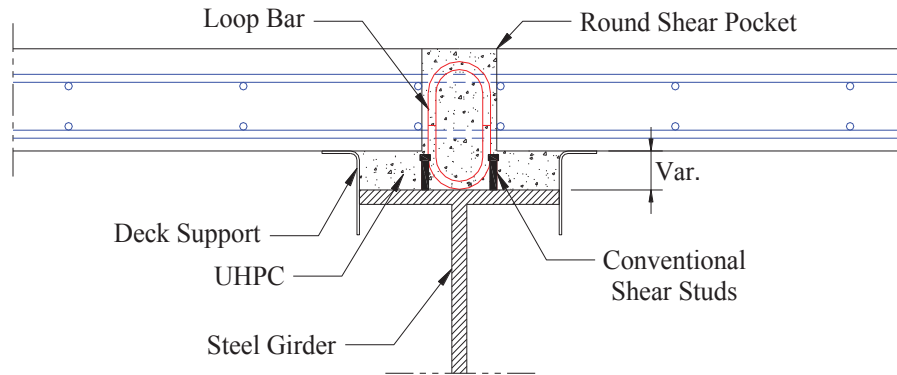


Figure 3.6: Proposed Precast Concrete Deck-To-Steel Girder Connection

The proposed connection allows transverse prestressing of precast deck panels as shown in Figure 3.7. Prestressing the deck panels decreases significantly the deck reinforcement besides eliminating the need for forming the overhangs. Also, prestressing deck panels allow using large panels that reduce the construction time and minimize the number of open joints that need to be ground for leveling the surface. The round shape of proposed shear pocket eliminates any tolerance limits for adding the loop bar and keep it in position as shown in Figure 3.7.

Two critical interface shear planes exist in this connection as shown in Figure 3.8. The first plane is at the girder top surface between fresh UHPC and hardened conventional concrete (CC-UHPC), which is intentionally roughened surface as a common practice. The second plane is at the soffit of the deck panels across the monolithic UHPC. The loop bar placed in each pocket crosses the second plane to enhance its interface shear resistance. Also, the roughened side surface of the shear pocket prevents pocket pull-out from the deck panel concrete. Since current AASHTO LRFD Bridge Design Specifications 2017 does not provide equations for predicting the interface shear resistance of either monolithic UHPC or CC-UHPC, experimental investigations are conducted to understand the new connection behavior and predict the interface shear resistance of connection.

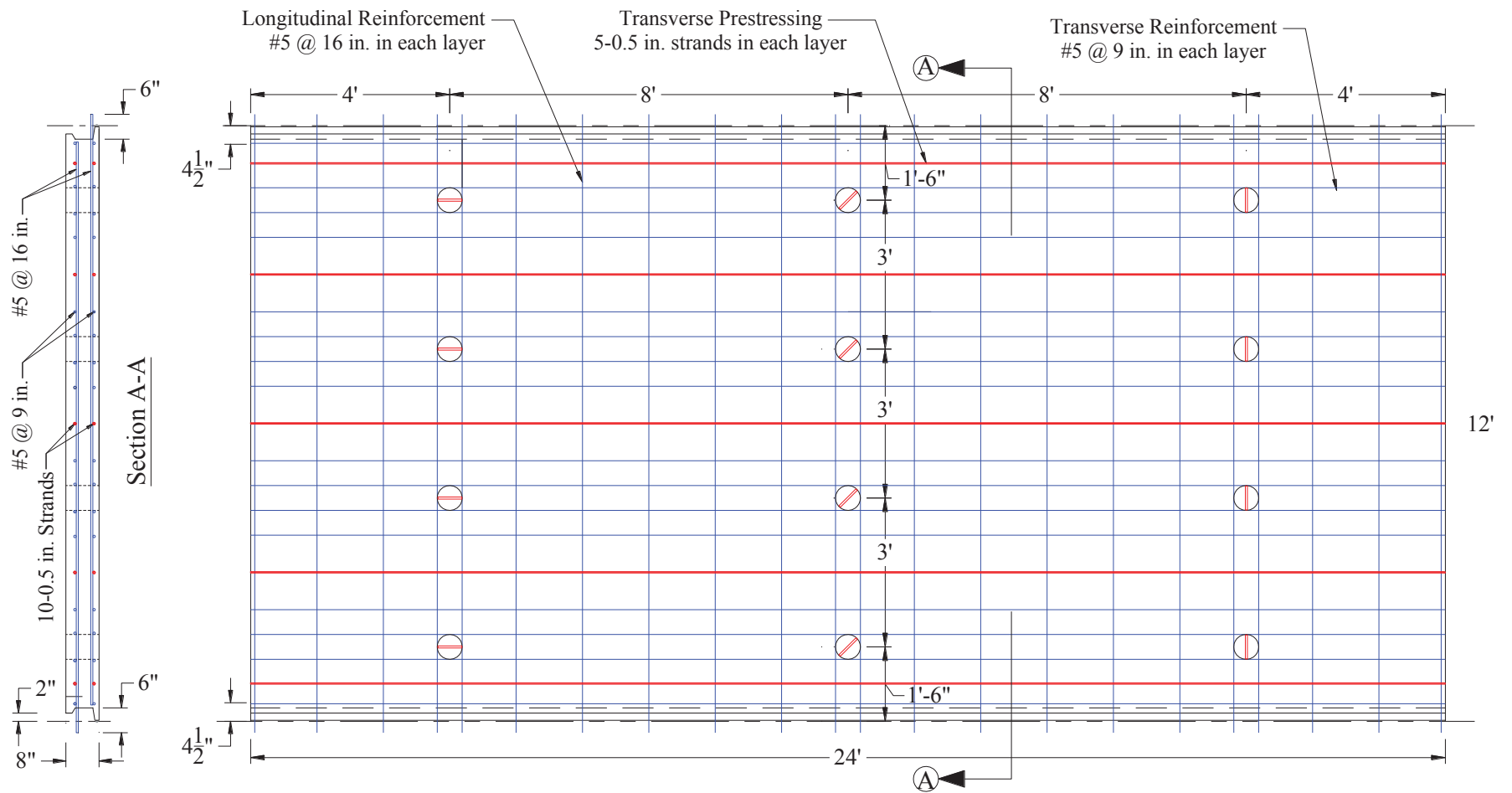


Figure 3.7: Panel Reinforcement and Pre-Tensioning for Proposed Connection.

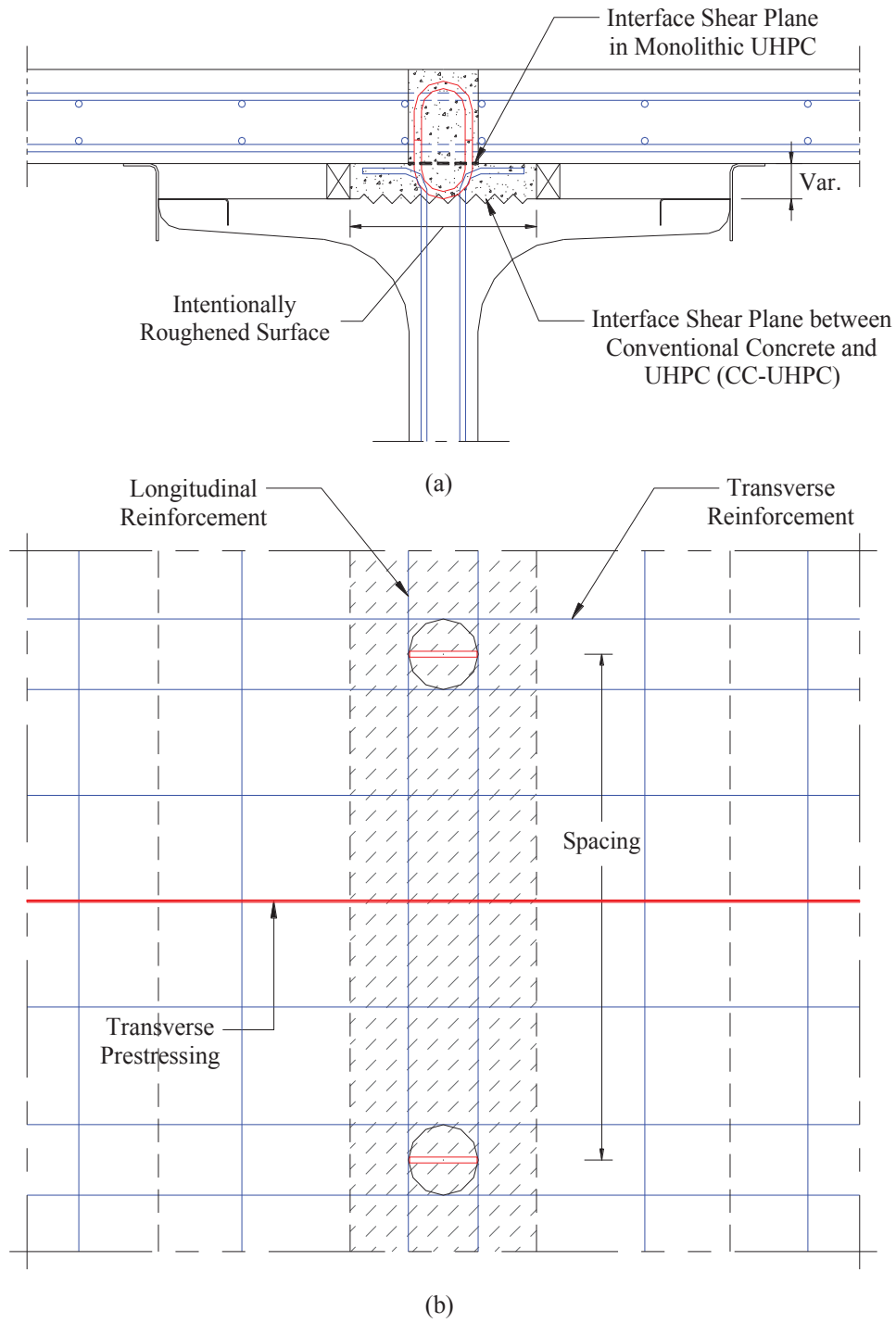


Figure 3.8: Interface Shear Resisting Area; (a) at the Top of the Concrete Girder and (b) at the Soffit of the Deck Panels

3.4. Construction Sequence of New Connection

The construction sequence of the new precast concrete deck-to-concrete girder using UHPC is presented in the following steps as shown in Figure 3.9:

1. Fabricate precast/prestressed concrete girders with conventional shear reinforcement and roughen the girder top flange according to the common practice.
2. Fabricate precast/prestressed concrete deck panels with discrete round shear pockets at designed spacing. Roughen side surface of the shear pockets using either form liner or exposed aggregate.
3. Erect all girders as shown in Figure 3.9.1a
4. Form, reinforce, and pour end diaphragms up to the girder top flange as shown in Figure 3.9.1b.
5. Conduct shim shots on the edges and center of each girder line to determine the actual profile of the cambered girders prior to panel erection.
6. Place blocks of compressible material to form the haunch area and use leveling bolts or shelf angles to achieve the desired deck elevation as shown in Figure 3.9.2a.
7. Attach extruded polystyrene panels to the top of concrete diaphragms between girders to fill the gap underneath the deck panels.
8. Place deck panels on the girders as shown in Figure 3.9.2b.
9. Fill the gaps between adjacent deck panels using backer rod and clean/moist the joint surface prior to casting UHPC as shown in Figure 3.9.3a.
10. Place loop bars in the shear pockets as shown in Figure 3.9.3b.
11. Pour UHPC to fill haunch, round shear pockets, and transverse joints between deck panels as shown in Figure 3.9.4. Pouring should continue until the UHPC overflow from every pocket.
12. Grind the top surface of UHPC to achieved leveled deck top surface.

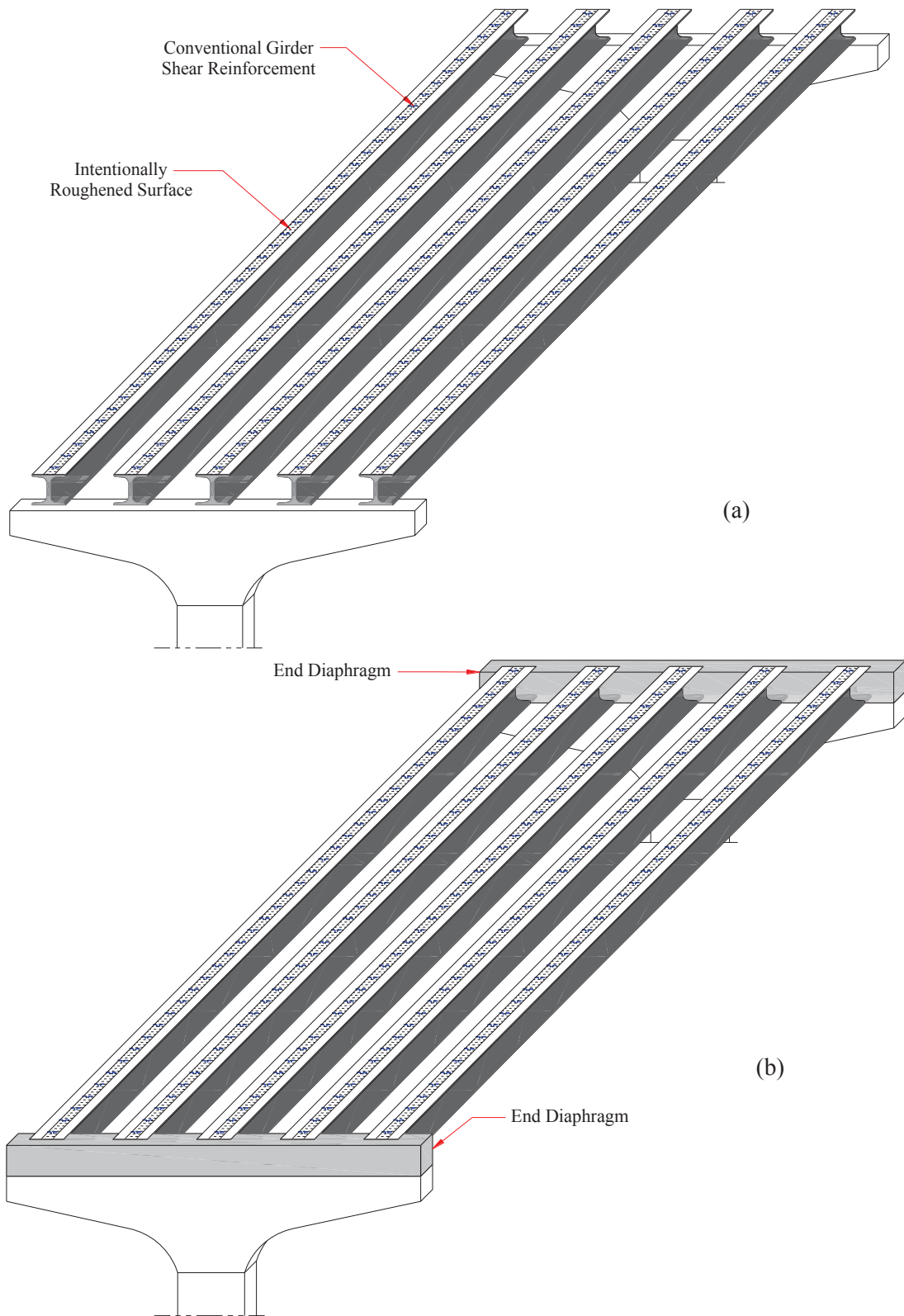


Figure 3.9.1: Construction Sequence of the Proposed Precast Concrete Deck-to-Concrete Girder Connection Using UHPC

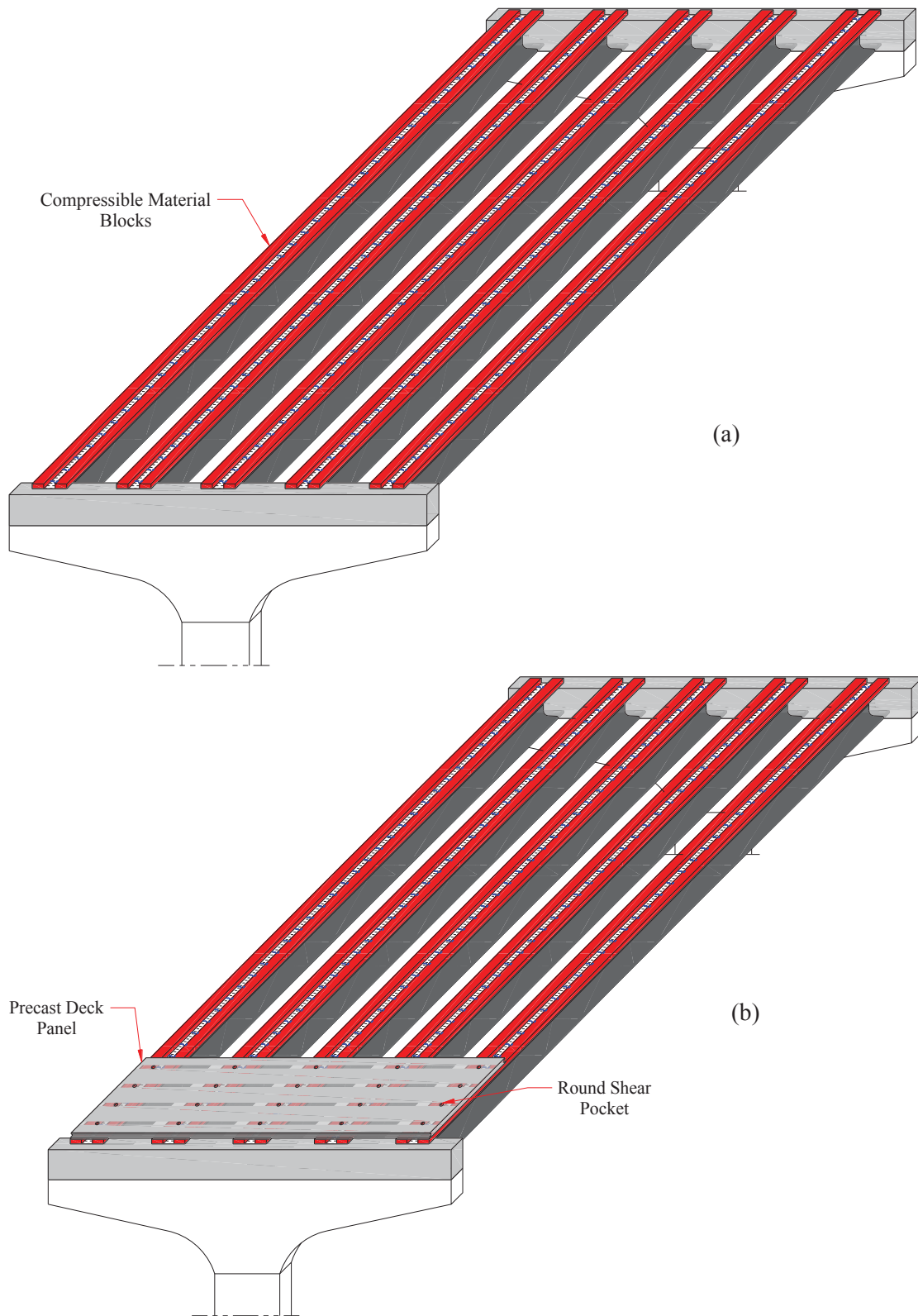


Figure 3.9.2: Construction Sequence of the Proposed Precast Concrete Deck-to-Concrete Girder Connection Using UHPC

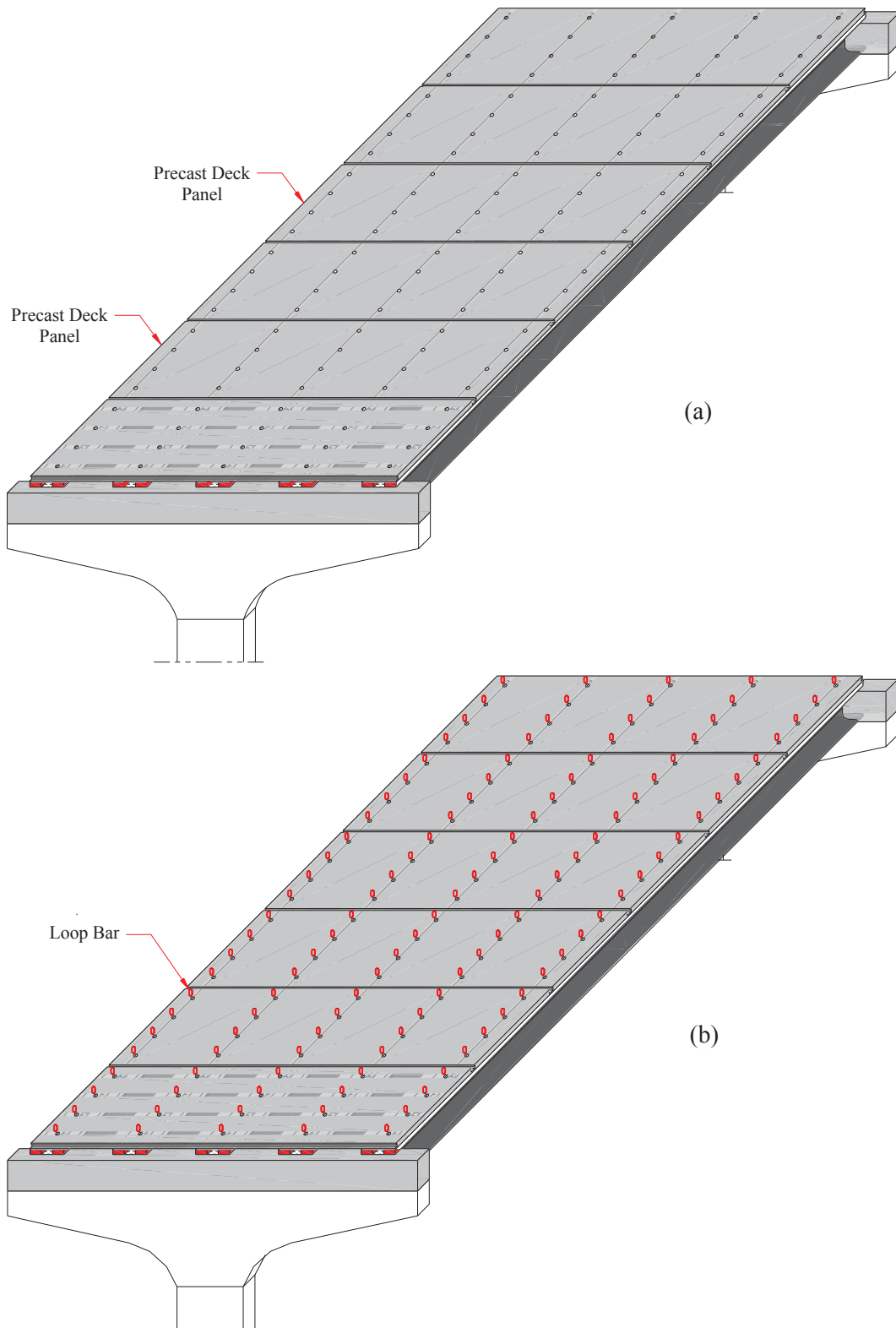


Figure 3.9.3: Construction Sequence of the Proposed Precast Concrete Deck-to-Concrete Girder Connection Using UHPC

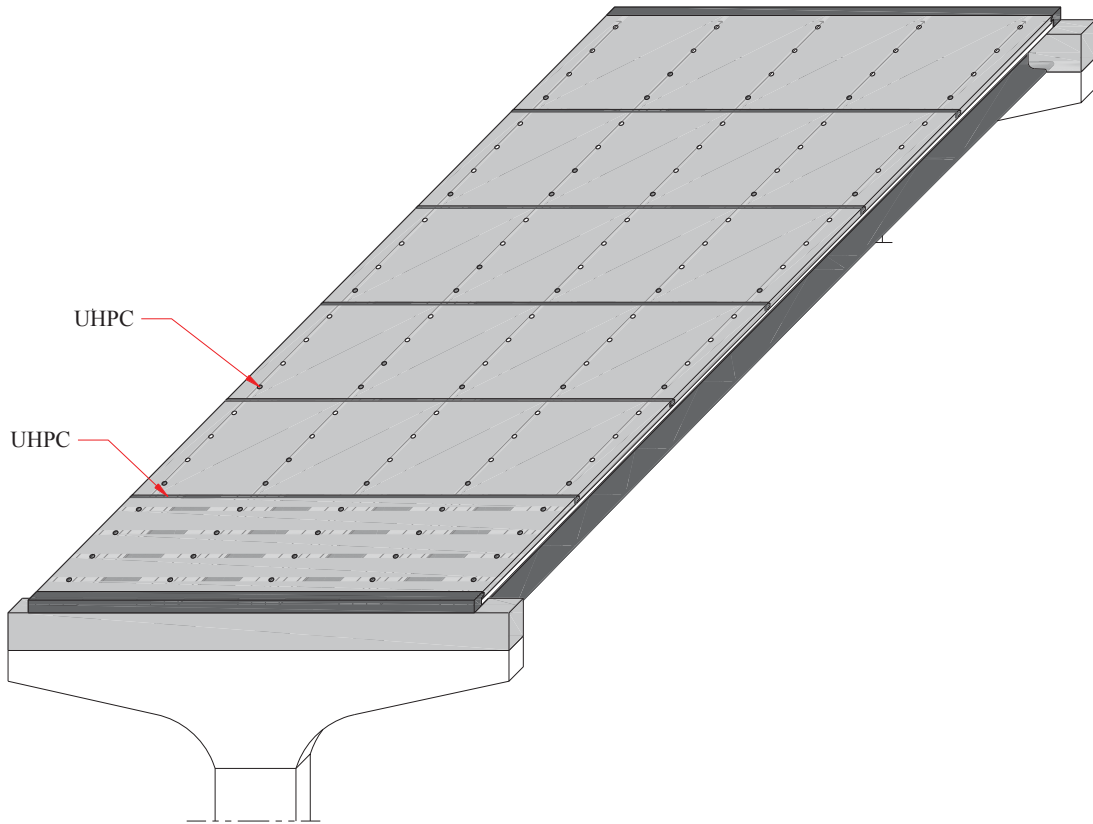


Figure 3.9.4: Construction Sequence of the Proposed Precast Concrete Deck-to-Concrete Girder Connection Using UHPC

3.5. Study Methodology

The study methodology includes two stages: experimental investigation and design procedure. The experimental investigation consists of small-scale testing and full-scale push-off testing. Small-scale testing is conducted to evaluate the interface shear resistance of the connection critical sections using direct shear, L-shape push-off, and double shear tests for monolithic UHPC; and slant shear and L-shape push-off tests for CC-UHPC interface. Full-scale push-off specimens simulating the actual connection are designed and tested to obtain the interface shear resistance and evaluate the constructability of the new connection. Finally, an example bridge is presented to demonstrate connection design using the results of the experimental investigation. Figure 3.10 shows a chart that summarizes the study methodology.

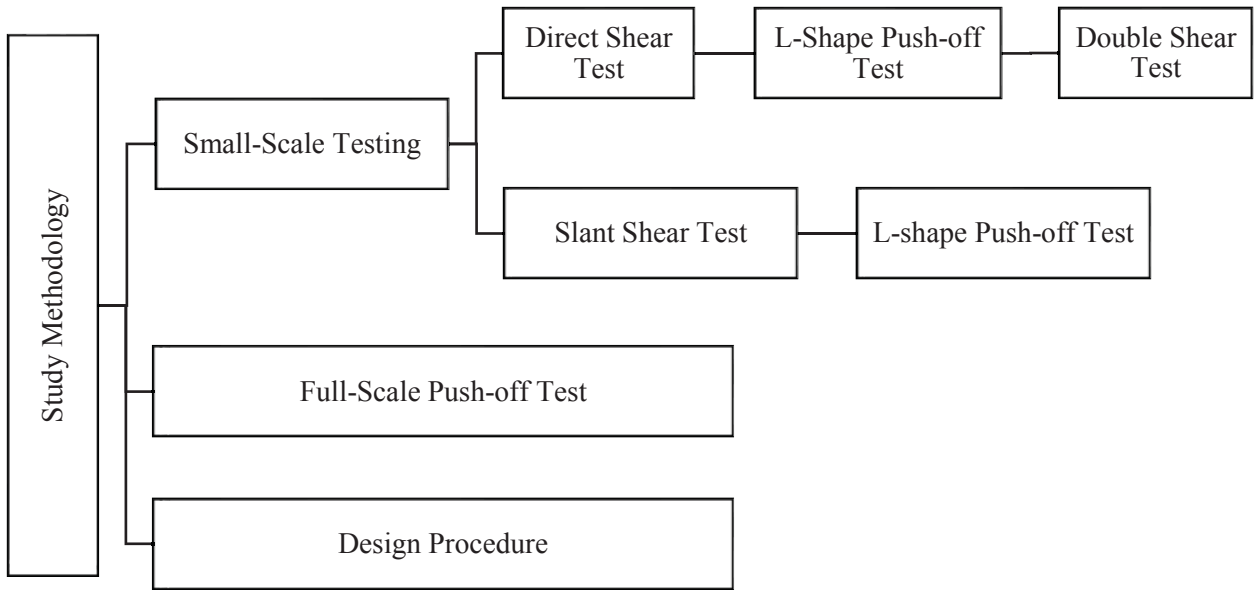


Figure 3.10: Study Methodology for Evaluating Proposed Connection.

Chapter 4. Experimental Investigation

4.1. Introduction

This chapter illustrates the experimental investigation procedure, small-scale and full-scale testing, to evaluate the interface shear resistance of monolithic UHPC and of fresh UHPC cast on hardened conventional concrete (CC-UHPC). Direct shear, L-shape push-off, double shear tests were conducted to evaluate interface shear resistance of monolithic UHPC. The literature review conducted on interface shear resistance of CC-UHPC was summarized and analyzed to propose prediction equations. Then, slant shear test and L-shape push-off test were conducted to evaluate and validate these equations. The constructability and structural performance of the proposed connection was investigated through full-scale push-off tests.

4.2. Material Properties

The experimental program was conducted using a non-proprietary UHPC mix as a primary mix and commercial UHPC mix for some specimens. Table 1 shows the non-proprietary UHPC (UNL UHPC) mix proportions that was designed by University of Nebraska-Lincoln (UNL) research team and sponsored by Nebraska Department of Transportation (NDOT). Straight high strength steel micro-fibers that are 0.50 in. long and 0.078 in. in diameter were used in UNL UHPC at a dosage of 2% by volume. UNL UHPC has 18 ksi compressive strength, 6,377 ksi modulus of elasticity, 4.88 ksi peak flexural strength at 28 days. The UNL UHPC mixing design and mechanical properties can be found in NDOT report No. M072 titled “Feasibility study of development of UHPC for highway bridge applications in Nebraska”. ASTM A615 Grade 60 black rebar was used for specimens and interface reinforcement.

Table 4.1: UNL UHPC Mix Proportions

UHPC mix	Constituent, Ib/yd ³						
	Cement Type I/II	Silica Fume	Slag	#10 Sand	Water/Ice	HRWRA ^a	Steel Fibers
UNL UHPC	1178	152.7	570	1663.7	317	61	263

^aHigh Range Water Reducer Admixture

4.3. Evaluate Interface Shear Resistance of Monolithic UHPC

The following subsections present the interface shear resistance of monolithic UHPC evaluated through direct shear, L-shape push-off, and double shear tests with and without interface reinforcement.

4.3.1. Direct Shear Test

A direct shear test was conducted to evaluate the interface shear resistance of monolithic UHPC without interface reinforcement using 2x2x6 in. prismatic specimens. The specimens were cast from one end in long forms to allow UHPC to flow and align the fiber along the form. The molds were stripped after one day and submerged in lime-saturated water till the day of testing. Then, the specimens were cut using wet saw to the desired length. A steel loading frame was used to apply double shear loading to the specimens as shown in Figure 4.1. A displacement-controlled loading rate of 0.05 in./min. was applied till failure.

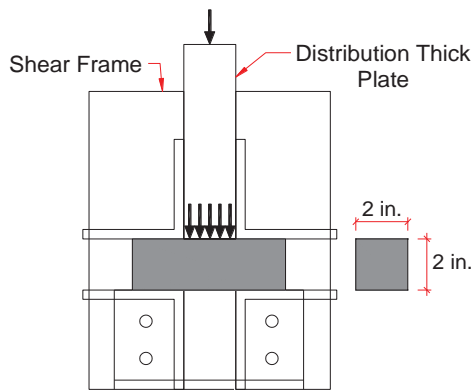


Figure 4.01: Direct Shear Test Setup.

A total of 26 specimens were tested at different compressive strengths of UHPC. All the specimens exhibited double shear failure as shown in Figure 4.2. The obtained direct shear strength was calculated by dividing the applied load by the double shear areas. The average direct shear strength of minimum three specimens ranged from 4.0 to 5.95 ksi as the average compressive strength of UHPC ranged from 11.8 to 23.4 ksi. Figure 4.3 shows the obtained direct shear test results and their comparison to the literature.



Figure 4.02: Double Shear Failure Mode of Direct Shear Test Specimen.

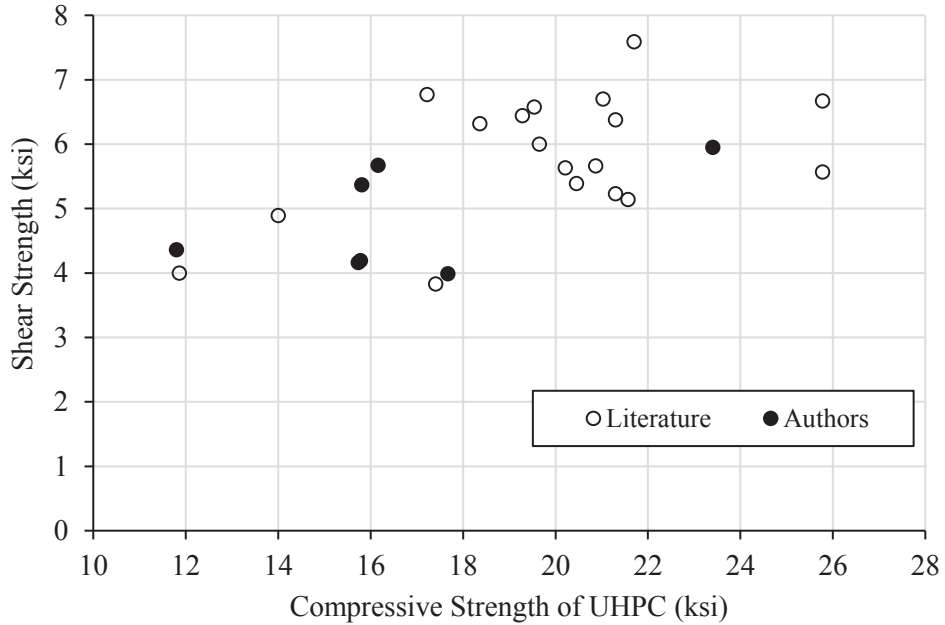


Figure 4.03: The Obtained Direct Shear Test Results and Their Comparison to the Literature.

Figure 4.4 shows the average direct shear strengths of UHPC with different flowability: low (≤ 8 in. spread), medium (8-10 in. spread), and high (>10 in. spread). The flow test was conducted using a standard flow table with diameter of 10 in. according to ASTM C230; specified by ASTM C1856. Specimens with low and medium flowability had almost similar direct shear strength, while specimens with high flowability had 30% less direct shear strength that could be attributed to fiber segregation.

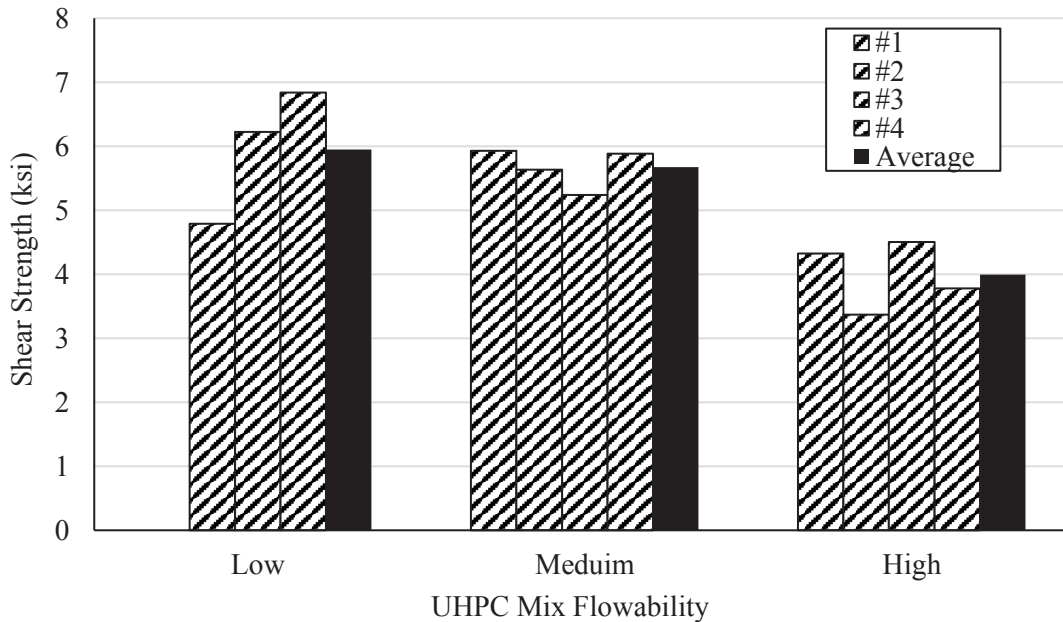


Figure 4.04: Effect of Flowability on Direct Shear Test Results.

It should be noted that direct shear test data shows much higher shear strength than those obtained from L-shape test literature. This difference could be attributed to the small size of the specimens and the presence of a different load path of compression struts from the applied load to the supports, which does not represent the true shear strength of UHPC.

4.3.2. L-Shape Push-off Test

L-shape push-off test was conducted to investigate the interface shear resistance of monolithic UHPC. The L-shape specimens were casted horizontally, stripped out of forms after one day, and covered with plastic till the testing day. Figure 4.6 and Figure 4.7 show the L-shape specimen details and test setup. The relative displacements, parallel (slip) and perpendicular (crack width) to interface plane, between two L-sections were captured using four LVDTs (two LVDTs for each side) as shown in Figure 4.7. A shear load rate of 600 Ib/sec. was applied till failure using a hydraulic ram after being aligned with the interface plane. The applied load was measured using a pressure transducer attached to the ram. The specimens were labeled as UHPC-MON-A%#B where MON means monolithic, A is the interface reinforcement ratio, and B is the specimen number.



Figure 4.05: L-Shape Push-off Specimen Preparation.

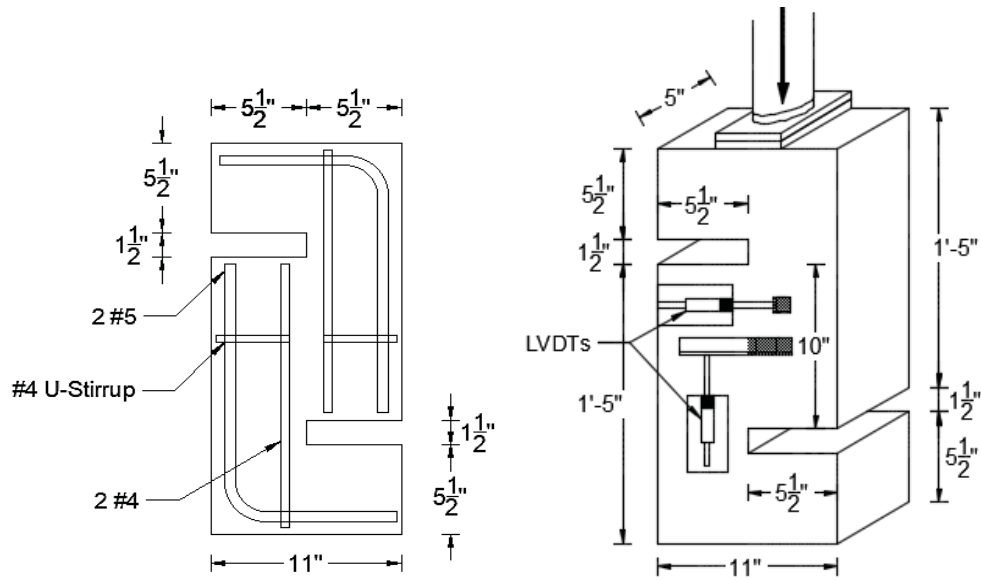


Figure 4.06: L-Shape Push-off Specimen Details

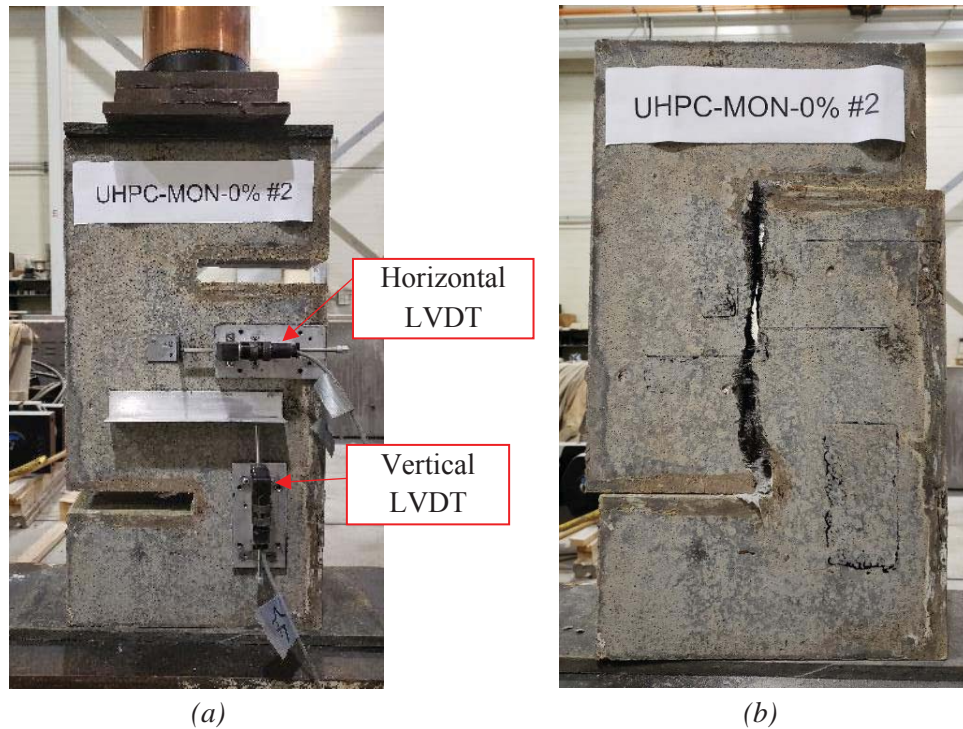
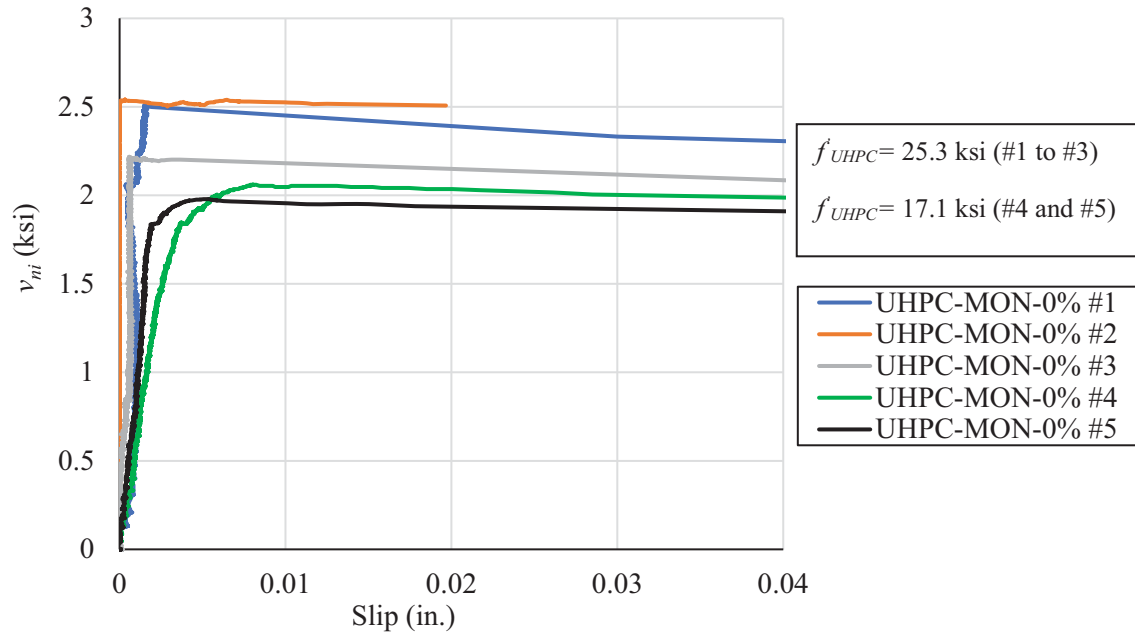


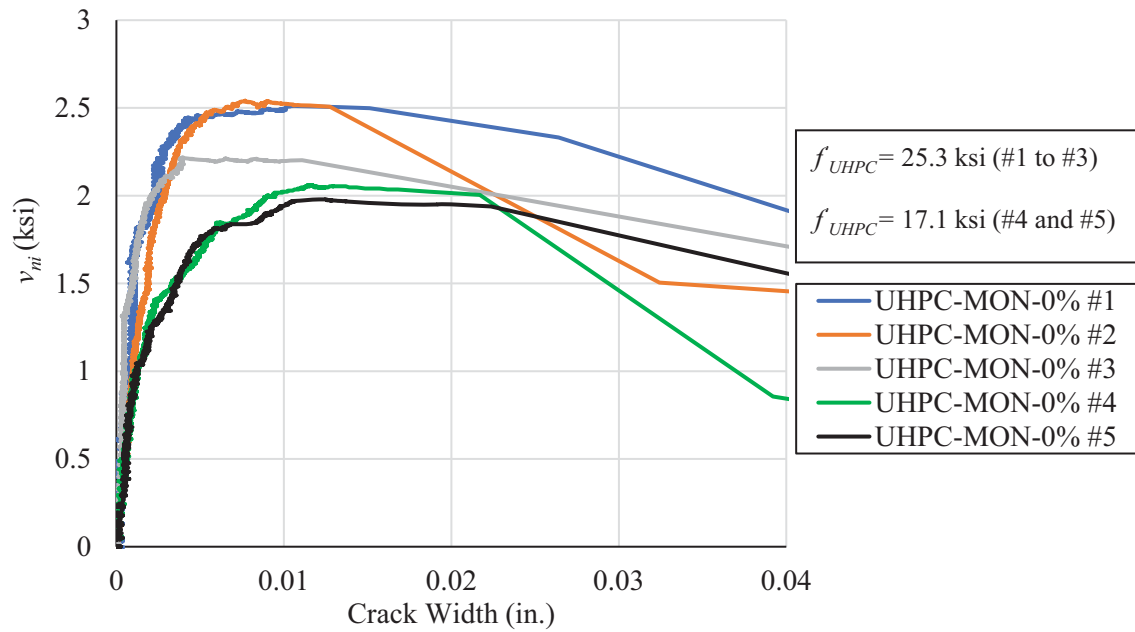
Figure 4.07: L-Shape Push-off Test; (a) Test Setup, and (b) Failure Mode.

All the specimens exhibited interface shear failure as shown in Figure 4.7. The interface shear resistance (v_{ni}) was calculated by dividing the applied load by interface shear area (50 in.^2). The specimens #1 to #3 had a compressive strength of 25.3 ksi and specimens #4 and #5 had a compressive strength of 17.1 ksi. The average interface shear resistance of monolithic UHPC are 2.42 ksi and 2.0 ksi at UHPC compressive strength of 25.3 ksi and 17.1 ksi, respectively. The measured slip did not exceed 0.01 in. at the

peak load as shown in Figure 4.8(a). Figure 4.8(b) shows the effect of fibers crossing the interface that act like stitches and provides ductile behavior at the peak load without interface without reinforcement. This ductile behavior mainly controlled by the fiber content in UHPC mix which might change with different fiber content.



(a)



(b)

Figure 4.8: Interface Shear Resistance versus Relative Displacements of Monolithic L-Shape Push-off Test; (a) Slip, and (b) Crack width

Figure 4.9 shows the results of L-shape push-off tests and their comparison with similar testing in the literature. The L-shape test results had better consistency and less scatter than those of direct shear tests. It also shows that the interface shear resistance of monolithic UHPC depends on the compressive strength of UHPC as the trendline gives high correlation with the square root of UHPC compressive strength. The interface shear resistance of monolithic UHPC can be predicted using the proposed cohesion factor as follows, which is much higher than that of monolithic CC (0.4 ksi):

$$c = 0.49 \sqrt{f'_{UHPC}} \quad (\text{ksi})$$

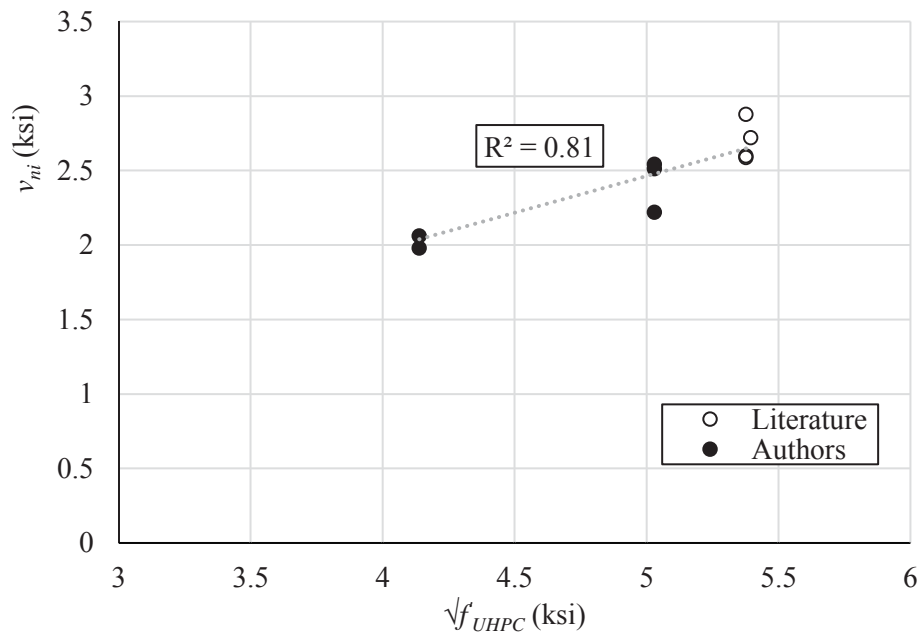


Figure 4.09: L-Shape Push-off Test Results of Monolithic UHPC and their Comparison to the Literature.

4.3.3. Double Shear Test

The interface shear resistance of monolithic UHPC with interface reinforcement was evaluated by performing double shear tests. Double shear specimens were designed to mimic the proposed connection with 6 in. diameter round shear pocket and embedded No. 5 loop bar. Two 20x20x8 in. conventional concrete (CC) slabs, with 6 in. diameter shear pocket in the center, were cast to be used for applying the shear load. Two reinforcement layers (8 #4 each) were used to enhance the capacity of concrete slab. The shear pocket was formed using a corrugated plastic pipe to create 0.25 in. roughened surface between CC and UHPC. Two 16x20x4 in. UHPC slabs were cast on the sides of precast CC slab. Each UHPC slab had two U-shape #4 bars to enhance the slab capacity. A #5 loop bar was added to the shear pocket as shown in Figure 4.10 before casting UHPC. The specimens were labeled similar to the L-shaped push-off specimens.

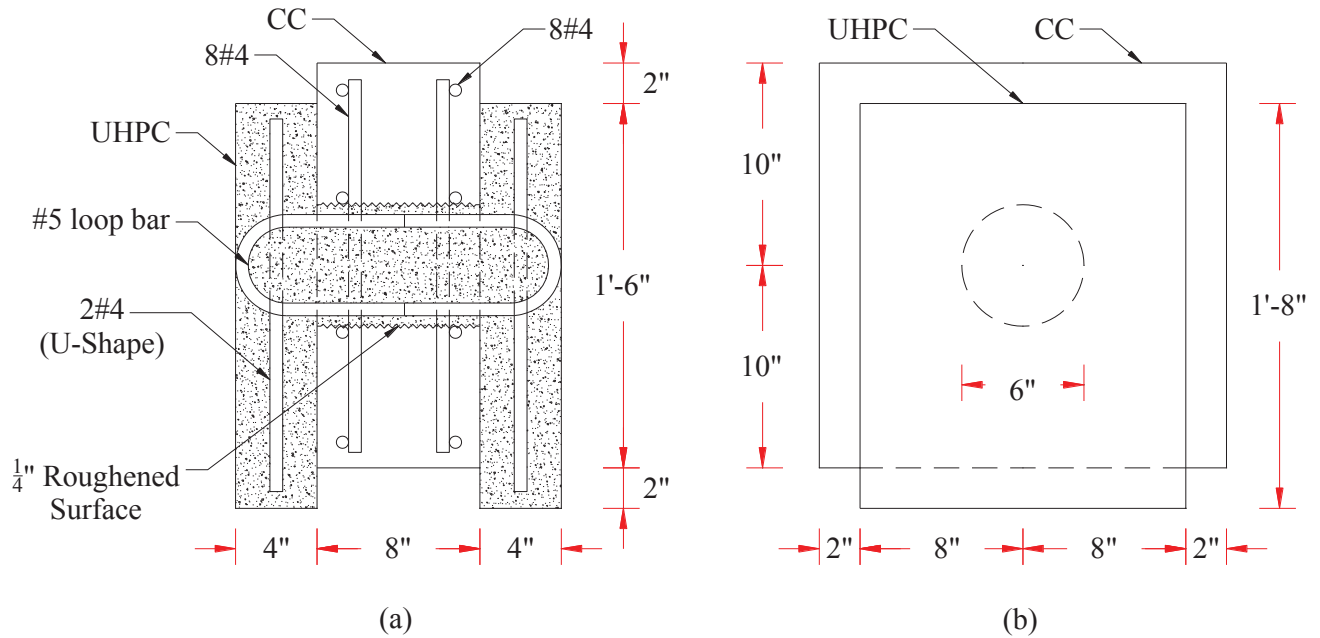


Figure 4.010: Double Shear Test Specimen Details; (a) Section Elevation, and (b) Side View.

- **Specimen Fabrication**

Figure 4.11 shows the fabrication of the CC slab with 6 in. corrugated plastic pipe. The CC slab was cast using self-consolidating concrete and then, was covered with plastic for 28 days to cure. The plastic pipe was removed easily from the shear pocket without damaging the roughening as shown in Figure 4.12(a). In order to eliminate the contact between UHPC and CC, the top and bottom surfaces of CC slabs were covered with wax as shown in Figure 4.12(b). A 2 in. rigid structural foam was used to form the 4 in. UHPC slabs thickness and the No. 5 loop bar was added through the shear pocket as shown in Figure 4.13. The UHPC was cast vertically to fill the slabs and shear pocket. Finally, the top surface of specimens was covered with rigid foam and plastic sheet till the day of testing.



Figure 4.011: Concrete Section of Double Shear Test Specimen



(a)



(b)

Figure 4.012: Concrete Section Preparation of Double Shear Test Specimen; (a) Removed Plastic Pipe, and (b) Applying Wax on Concrete Surfaces.

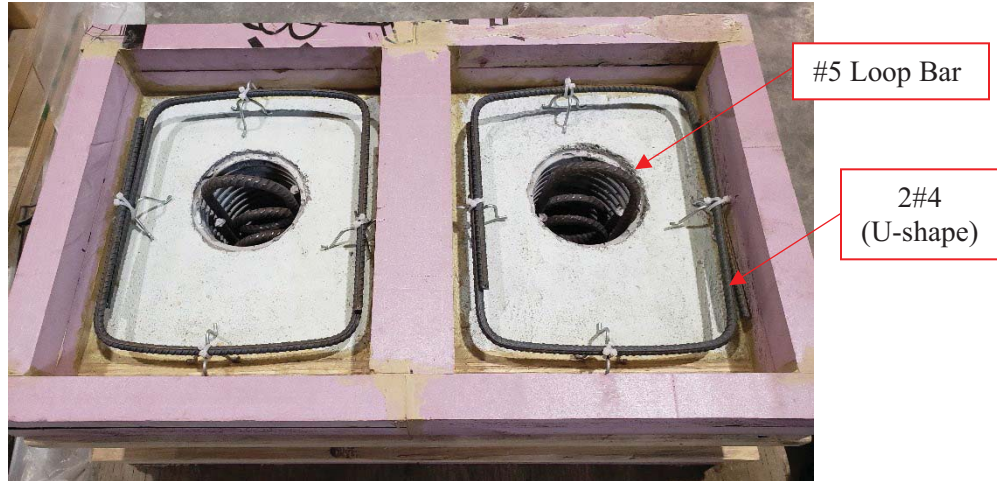


Figure 4.13: Double Shear Specimen Forming

- **Test Setup and Results**

At time of testing, the compressive strength of CC slab was 6.9 ksi, while the compressive strength of UHPC slabs was 17.7 ksi. The specimen base was ground and placed on structural bearing pads to avoid uneven loading. The shear load was applied using a hydraulic ram and steel plates to distribute the load over an area of 8 in. x 14 in. Four LVDTs were attached vertically to the specimen (two for each side) to capture the relative vertical displacement (slip) between the CC slab and UHPC at the two interface shear planes. Figure 4.13 shows the double shear test setup and instrumentation.

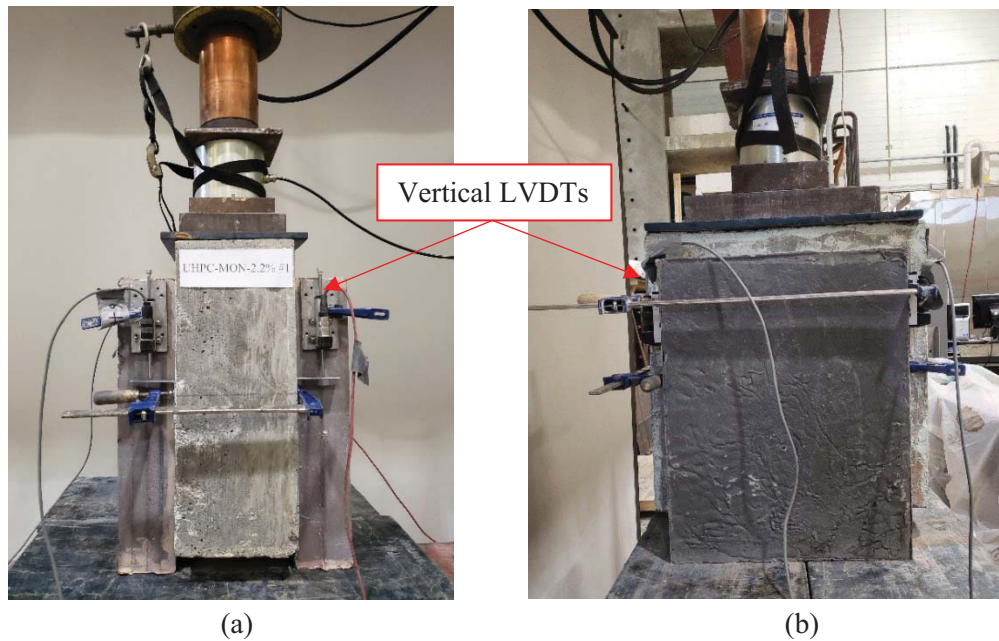


Figure 4.14: Double Shear Specimen Test Setup; (a) Front View, and (b) Side View.

The two specimens exhibited similar double shear failure at the UHPC shear pocket between CC and UHPC slabs as shown in Figure 4.15(a). Figure 4.15(b) shows the rupture of #5 loop bar at the interface

plane. Figure 4.16 shows the average measured slip at the top and bottom interface plane, as the specimens were cast. The average interface shear resistance was 6.77 ksi for monolithic UHPC with 2.2% interface reinforcement as shown in Figure 4.16. The clamping force produced by interface reinforcement provides more ductility to the interface behavior compared to L-shape specimens without interface reinforcement. The average slip recorded by the four LVDTs reached 0.1 in. at the peak load which reflects the effect of clamping forces.

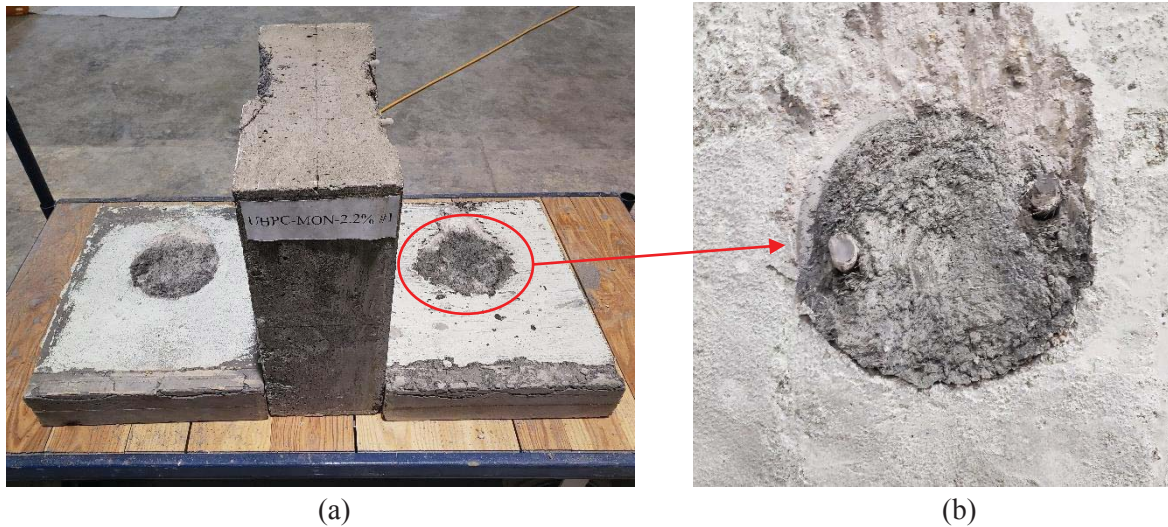


Figure 4.015: Double Shear Specimen Failure Mode; (a) Double Shear Failure, (b) No. 5 Bar Rupture

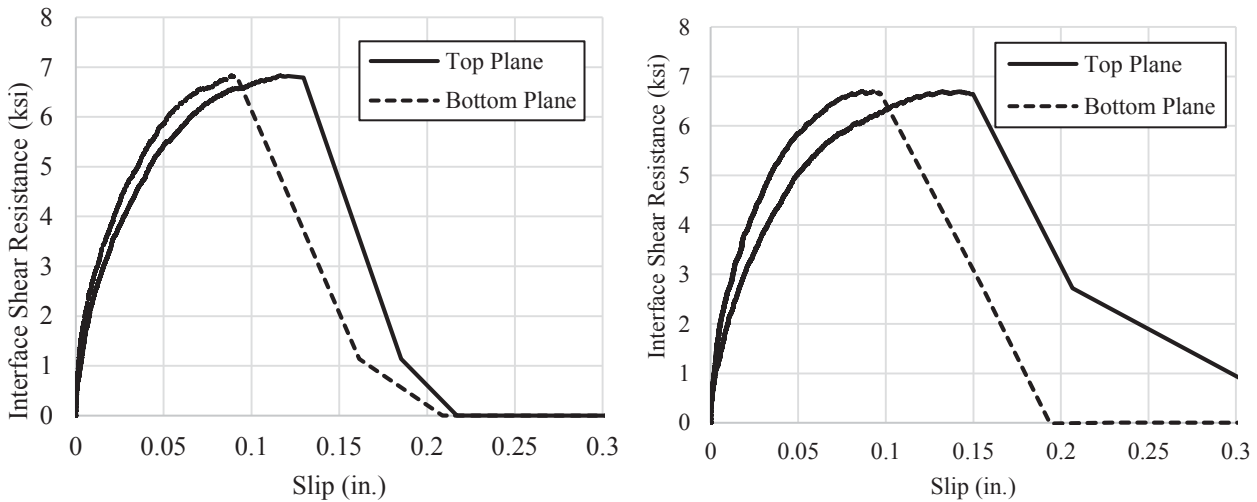


Figure 4.016: Interface Shear Resistance versus Measured Slip at Top and Bottom Interface Planes for Double Shear Specimen #1 (left) and #2 (right)

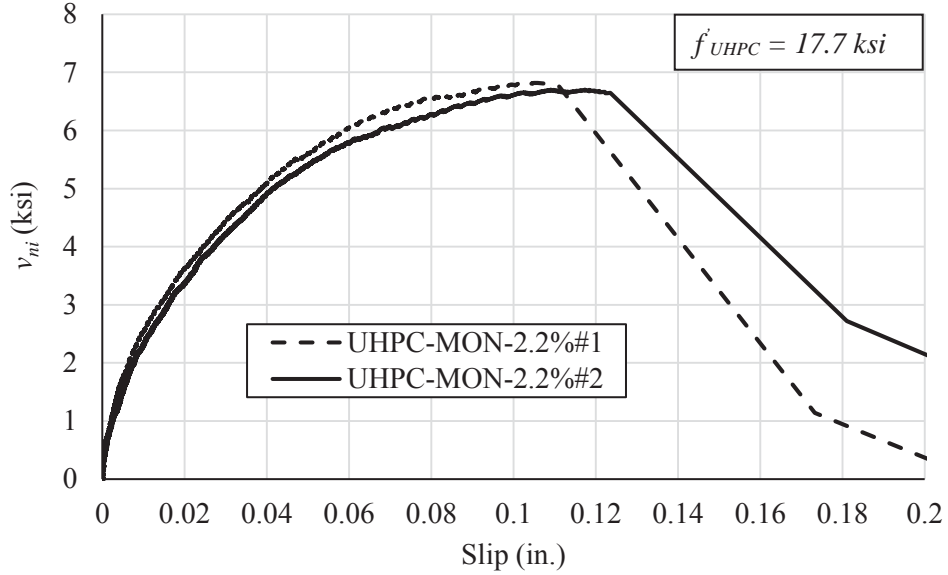


Figure 4.017: Interface Shear Resistance versus Average Measured Slip of Double Shear Test

To develop an equation for predicting the effect of reinforcement clamping force on the interface shear resistance of monolithic UHPC, data obtained from the double shear tests and from the literature (Crane, 2010) were summarized as shown in Table 4.2. The shear friction model of AASHTO LRFD (2017) was used but with considered the effect of UHPC compressive strength on both cohesion and friction factors. Below is the proposed shear friction equation for predicting the interface shear resistance of monolithic UHPC with 2% fiber content:

$$v_{ni} = 0.49\sqrt{f'_{UHPC}} + 0.85\sqrt{f'_{UHPC} * \rho * f_y}$$

Table 4.2: Interface Shear Resistance Analysis of Monolithic UHPC with Interface Reinforcement.

Specimen ID		ρ (%)	v_{ni} (ksi)		f'_{UHPC} (ksi)	$c = 0.49\sqrt{f'_{UHPC}}$ (ksi)	$\mu * \rho * f_y$ (ksi)	μ	$\mu / \sqrt{f'_{UHPC}}$		COV %
Authors	#1	2.2	6.83	6.77	17.7	2.06	4.70	3.56	0.85	0.85	1.01
	#2		6.70								
Literature	#1	0.5	3.79	4.02	28.9	2.63	1.39	4.62	0.86	0.85	1.01
	#2		4.03								
	#3		4.24								

4.4. Evaluate Interface Shear Resistance of CC-UHPC

The following subsections present the interface shear resistance of CC-UHPC evaluated using slant shear and L-shape push-off tests with and without interface reinforcement.

4.4.1. Slant Shear Test

A slant shear test based on ASTM C882/C882M was performed to evaluate the interface shear resistance of CC-UHPC. A 4 in. by 8 in. cylinder specimen was used instead of 3 in. by 6 in. to allow the use of conventional concrete as a substrate (Abo El-Khier et al. 2019). Hardened CC cylinders were saw cut diagonally at 60° angle with the horizontal axis. The compressive strength of hardened concrete at 28 days was 8 ksi, which represents the common compressive strength of precast concrete girders. Figure 4.18 shows three different textures applied to interface shear surface using wet saw; as-cut (as cut with the wet saw and without additional treatment), shallow grooved (average 1/8 in. depth), and deep grooved (average 1/4 in. depth).

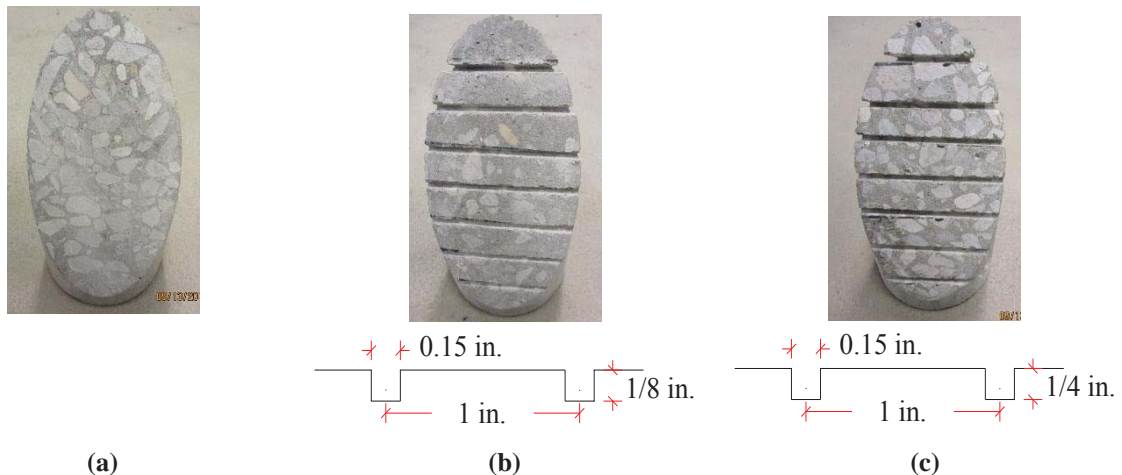


Figure 4.018: Interface Textures of Hardened Concrete Section; (a) Smooth, (b) Shallow Grooved, and (c) Deep Grooved.

The concrete sections were placed back in the molds after applying surface textures and the interface surface was pre-wetted directly before casting UHPC. The composite specimens were stripped out of the molds after one day and submerged in lime-saturated water in a room temperature of 73°F (23°C) temperature till the day of testing. Both ends of composite section specimen were ground prior to being tested under a compression load rate of 300-400 lb/sec. till failure according to ASTM C39 for CC as shown in Figure 4.19.

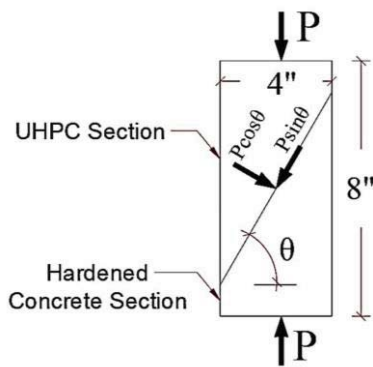


Figure 4.019: Slant Shear Test Specimen Dimensions and Test Setup.

A total of 24 slant shear specimens were tested at different UHPC compressive strengths. The CC had an average compressive strength of 8 ksi and UHPC had a compressive strength ranging from 17.67 to 27.2 ksi. Different failure modes were observed for different surface textures as shown in Figure 4.20. All specimens with as-cut surface had interface failure as shown in Figure 4.20(a). All specimens with shallow grooved surface had interface failure with fractured CC as shown in Figure 4.20(b). All specimens with deep grooved surface had failure in the CC portion as shown in Figure 4.20(c). The interface shear resistance and normal stress were calculated by dividing the applied load components, based on the interface angle as shown in Figure 4.19, by the interface surface area (25.1 in.^2). Figure 4.21 shows the average interface shear resistance of three identical specimens at different UHPC compressive strengths for each surface texture. This figure indicates that there is no significant difference in the interface shear resistance of CC-UHPC with shallow and deep grooved surface textures. However, different mode failures were exhibited for each surface texture. Also, the interface shear resistance increases with the increase of UHPC compressive strength for as-cut surface texture.

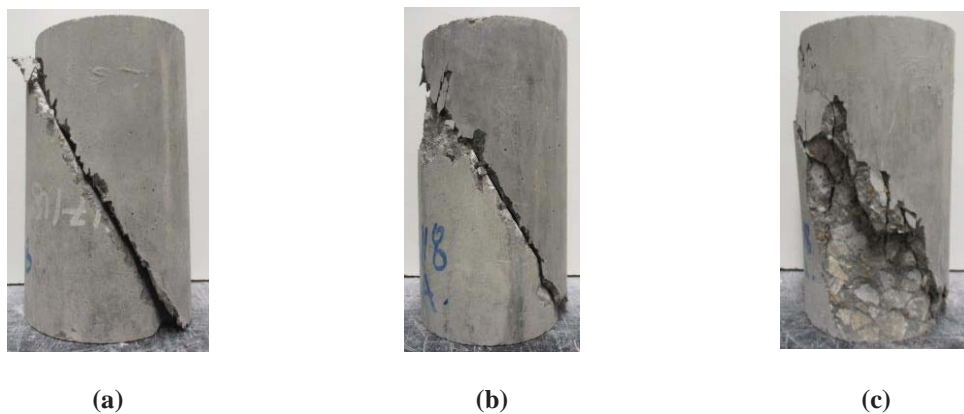


Figure 4.020: Slant Shear Specimen Failure Modes; a) Interface Failure, b) Interface Failure and CC Fracture, and c) CC Failure.

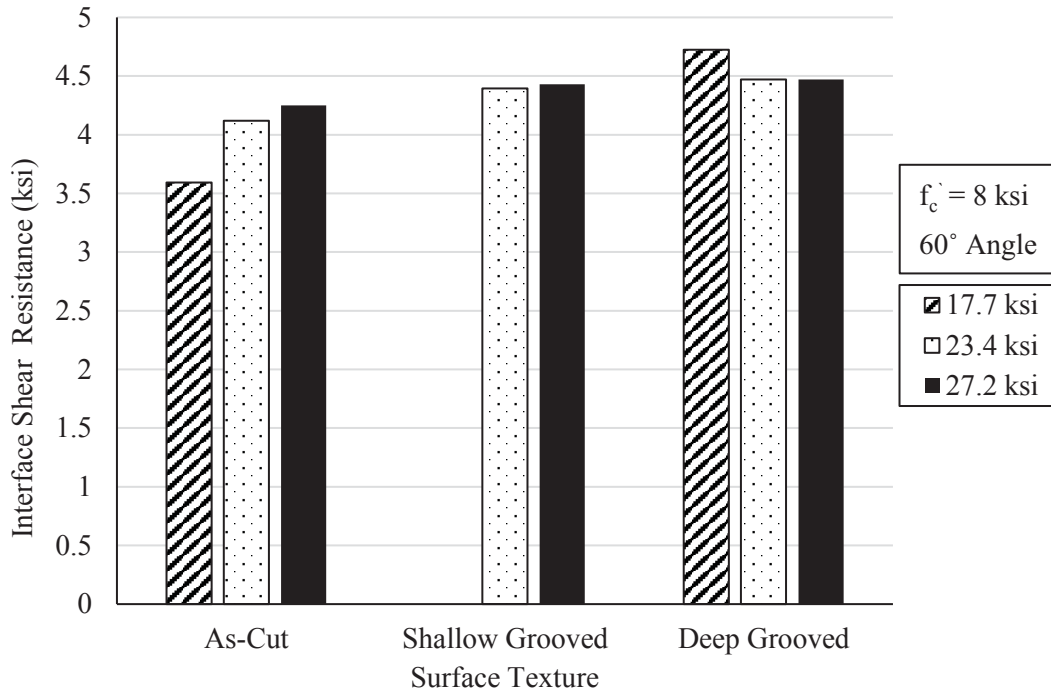


Figure 4.021: Interface Shear Resistance of CC-UHPC at Different UHPC Compressive Strength for Different Surface Textures.

Slant shear test data collected from the literature are listed in Table 4.3 and classified into three categories according to the surface texture: sandblasted, low roughening, and high roughening. The sandblasted category includes only the specimens with sandblasted interface. Low-roughening category represents the brushed and form liner textures with roughening amplitude less than ¼ in.. Grooved, aggregate exposed, and form liners with flutes deeper than ¼ in. are considered in the high-roughening category. Different specimen shapes, dimensions and interface angles are used to calculate shear and normal stresses at the interface plane of these specimens. The AASHTO LRFD (2017) shear friction model was used to obtain cohesion (c) and friction (μ) factors for each category. Figure 4.22 shows the plots of interface shear resistance (v_{ni}) and normal stress (N) at the interface plane for all specimens as well as the trendline fitting for each category. Based on the analysis results, the effect of UHPC and CC compressive strengths was not significant in predicting the interface shear resistance in all categories. Tables 4.4 summarizes the obtained cohesion and friction factors for each surface texture category and compares them against those of AASHTO LRFD for CC with intentionally roughened surface. The comparison indicate that UHPC cohesion factor is significantly higher than that for CC, while UHPC friction factor for low and high roughening surfaces are very close to that of CC. The high coefficients of determination (R^2) of the developed models indicate strong correlations between interface shear resistance and normal stress of CC-UHPC for all surface textures.

Table 4.03: Interface Surface Texture Categories Based on the Literature of CC-UHPC Interface Resistance

Surface Texture Category	Reference	Surface Preparation	Average f'_c (ksi)	Average f'_{UHPC} (ksi)	Interface Shear Resistance (v_{ni}) (ksi)	Normal Stress (N) (ksi)	Failure Location
Sandblasted (7)	Muñoz 2012	Sandblasted	8.11	18.35	3.14	1.79	CC
			8.11	18.35	2.12	0.72	CC
	Tayeh et al. 2012		6.50	24.7	2.23	1.29	CC
	Rangaraju et al. 2013		6.77	18.52	3.96	2.28	IP & CC
			6.77	17.92	3.84	2.22	CC
			6.77	22.93	3.58	2.07	CC
			6.77	23	4.10	2.37	CC
Low Roughening (17)	Harris et al 2011	Wire Brushed	5.00	15	1.82	1.05	IP & Mortar
	Muñoz 2012	Brushed	6.46	15.29	2.34	1.36	CC
			6.46	15.29	1.76	0.61	IP
			8.24	12.30	2.59	1.86	CC
			8.11	11.69	2.22	1.22	CC
			8.11	11.69	0.83	0.62	UHPC
			6.67	11.69	0.75	0.54	UHPC
	Tayeh et al. 2012	Wire Brushed	6.50	24.7	1.60	0.93	IP & CC
	Aaleti and Sritharan 2017	Form Liner (Panara)	5.20	18.00	2.29	1.72	BF
			7.46	18.00	3.64	2.73	CC
			6.40	18.00	3.16	2.37	IP
		Form Liner (2/61 Thame)	5.20	18.00	1.87	1.40	IP
			7.46	18.00	3.17	2.38	IP
			6.40	18.00	2.59	1.95	IP
		Form Liner (2/98 Vltava)	5.2	18	2.71	2.03	CC
			7.46	18	3.85	2.89	CC
			6.403	18	2.98	2.23	IP
High Roughening (16)	Harris et al. 2011	Grooved	5.00	15.00	2.17	1.25	Mortar
	Muñoz 2012	Grooved	6.46	15.29	2.55	1.45	CC
			6.46	15.29	1.63	0.63	CC
			8.11	11.36	1.38	0.45	IP & CC
		Roughened (Aggregate Exposed)	6.61	17.89	2.47	1.36	CC
			6.61	17.89	1.77	0.62	CC
			7.28	12.30	2.43	1.74	CC
			7.28	12.30	1.40	0.56	CC
		7.28	11.69	0.49	0.17	IP & UHPC	
		Tayeh et al. 2012	Grooved	6.50	24.70	1.75	1.01
	Aaleti and Sritharan 2017	Form Liner (Fluted Rib)	5.20	18.00	2.33	1.75	CC
			7.46	18.00	3.77	2.83	CC
			6.40	18.00	3.58	2.69	CC
		Form Liner (2/63 Wisla)	5.20	18.00	2.43	1.82	CC
			7.46	18.00	3.56	2.67	CC
			6.40	18.00	4.16	3.12	CC

* IP: Interface Plane.

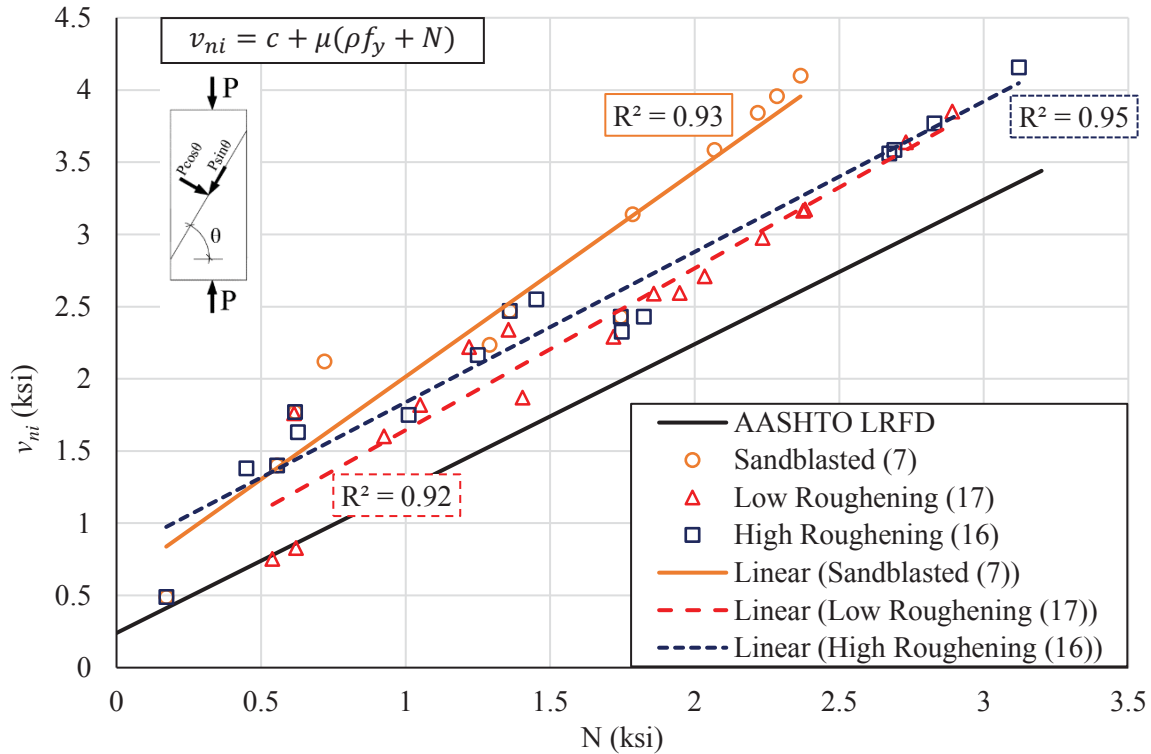


Figure 4.022: Average Interface Shear Resistance of CC-UHPC with Different Surface Textures.

Table 4.4: CC-UHPC Cohesion and Friction Coefficients of Different Interface Surface Textures

Surface Texture	UHPC Cohesion Coefficient (c), ksi	UHPC Friction Coefficients (μ)	R ²
Sandblasted	0.59	1.42	0.93
Low Roughening	0.52	1.12	0.92
High Roughening	0.80	1.0	0.95
AASHTO LRFD	0.24	1.0	NA

Figure 4.23 plots the authors slant shear test results against the relations developed based on the data obtained from the literature. The plot shows that interface shear resistance of as-cut texture, which have a little roughening due to using wet saw, is very close to predicted values of sandblasted surface texture. The shallow and deep grooved are higher than those of low and high roughening interface due to high compressive of CC. However, the deep grooved surface texture specimens' results validate the proposed equations for high roughening surface texture.

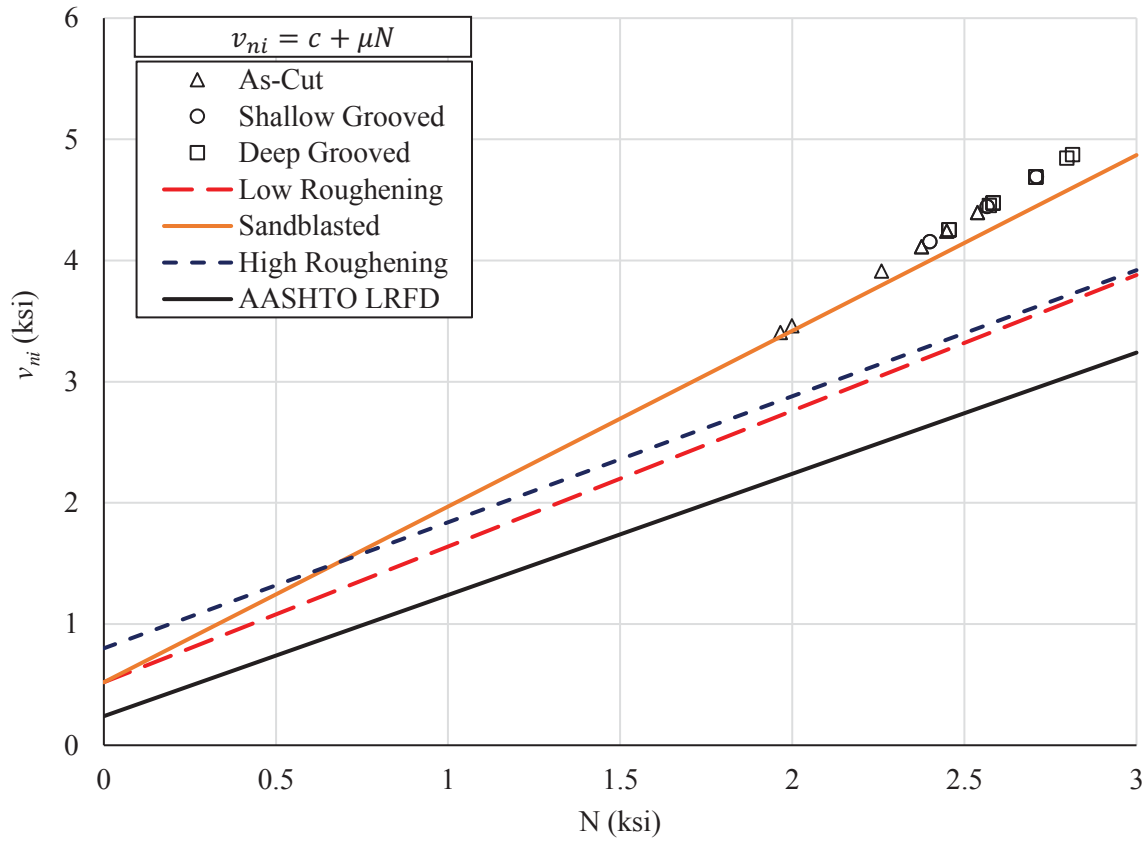


Figure 4.023: Results of Slant Shear Test and their Comparison to the Literature.

4.4.2. L-Shape Push-off Test

L-shape push-off test was conducted to investigate the effect of clamping force produced by interface reinforcement on the interface shear resistance of CC-UHPC. L-shape specimen dimensions and reinforcement details are shown in 4.24. Three different interface reinforcement were investigated: no reinforcement, two #3 Grade 60 bars, and two #4 Grade 60 bars, which represent reinforcement ratios of 0%, 0.44%, and 0.8% respectively. The CC section was cast first vertically using a low-slump mix to allow for applying $\frac{1}{4}$ in. deep roughening as shown in Figure 4.25. The CC section forms were stripped after 24 hours and covered with plastic sheets for curing in room temperature. The average compressive strength of CC at 28 days was 6.6 ksi. The UHPC section was cast vertically on top of the CC section to simulate the in-situ casting of connections. The UHPC forms were stripped after four days and the specimens were covered with plastic sheets for curing in room temperature till the day of testing. The average compressive strength of UHPC at time of testing was 20.84 ksi.

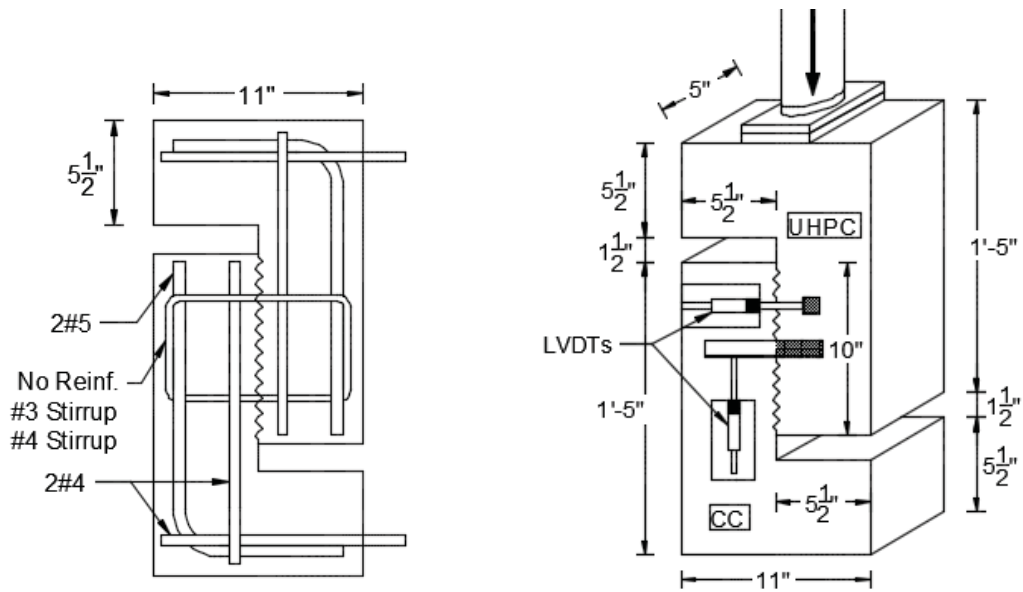


Figure 4.024: L-Shape Push-off Specimen Details and Test Setup.



Figure 4.025: Interface Surface Roughening and Different Reinforcement across Interface; No Reinforcement (Left), 2#3 (Middle), and 2#4 (Right).

Four LVDTs (two each side) were used to measure the relative displacements parallel (slip) and perpendicular (crack width) to the interface plane as shown in Figure 4.26. A load rate of 600 lb/sec. was applied till failure using a hydraulic ram and measured using a pressure transducer. The specimens were labeled using the form A-B-C%#D, where A is the section cast first, B is the section cast second, C is the interface reinforcement ratio, and D is the specimen number as shown in Table 4.5.

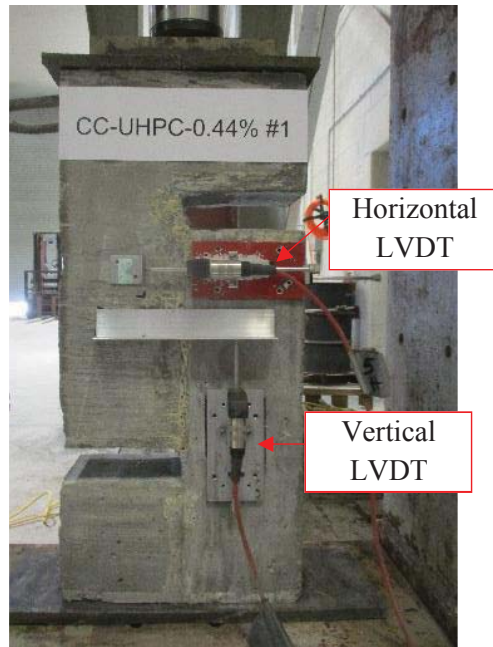


Figure 4.026: L-Shape Push-off Test Setup

Table 4.005: L-Shape Push-off Specimens Details and Labels

Surface Texture	A_{cv} (in. ²)	Interface Reinforcement	A_{vf} (in. ²)	Interface Reinforcement Ratio, $\rho = A_{vf} / A_{cv}$ (%)	Label
Roughened (> 1/4 in. depth)	50.0	None	0.0	0.0	CC-UHPC-0%
		2 #3	0.22	0.44	CC-UHPC-0.44%
		2 #4	0.4	0.80	CC-UHPC-0.8%

A total of nine L-shape specimens were tested and the maximum applied load was measured as shown in Table 4.6. All the specimens exhibited failure in the CC section parallel to the interface plane as a vertical crack at the reinforcement location as shown in Figure 4.27. Figure 4.28 and Figure 4.29 show the interface shear resistance versus slip and crack width, respectively, at the interface plane of the tested specimens. All the specimens had slip and crack width less than 0.01 in. at the peak shear load. The unreinforced specimens exhibited brittle failure at the peak load, however, the reinforced specimens exhibited ductile failure as the interface shear reinforcement provided a clamping force across the interface that enhanced the post-cracking interface shear resistance. The L-shape push-off test results show good agreement with the predicted resistance using proposed c and μ factors for high roughening surface texture with depth greater than 0.25 in as shown in Figure 4.30.

Table 4.06: L-Shape Push-off Test Results and Compared to Proposed Equation.

Specimen Label	f'_{cc} (ksi)	f'_{UHPC} (ksi)	Maximum Applied Load (kips)	Average Applied Load (kips)	Predicated Load, (kips)	Failure Location
CC-UHPC-0% #1	6.6	20.84	41.07	42.05	40.0	CC
CC-UHPC-0% #2			49.21			CC
CC-UHPC-0% #3			35.86			CC
CC-UHPC-0.44% #1			67.13	59.88	53.2	CC
CC-UHPC-0.44% #2			52.13			CC
CC-UHPC-0.44% #3			60.39			CC
CC-UHPC-0.8% #1			66.17	63.68	64.0	CC
CC-UHPC-0.8% #2			62.95			CC
CC-UHPC-0.8% #3			61.94			CC

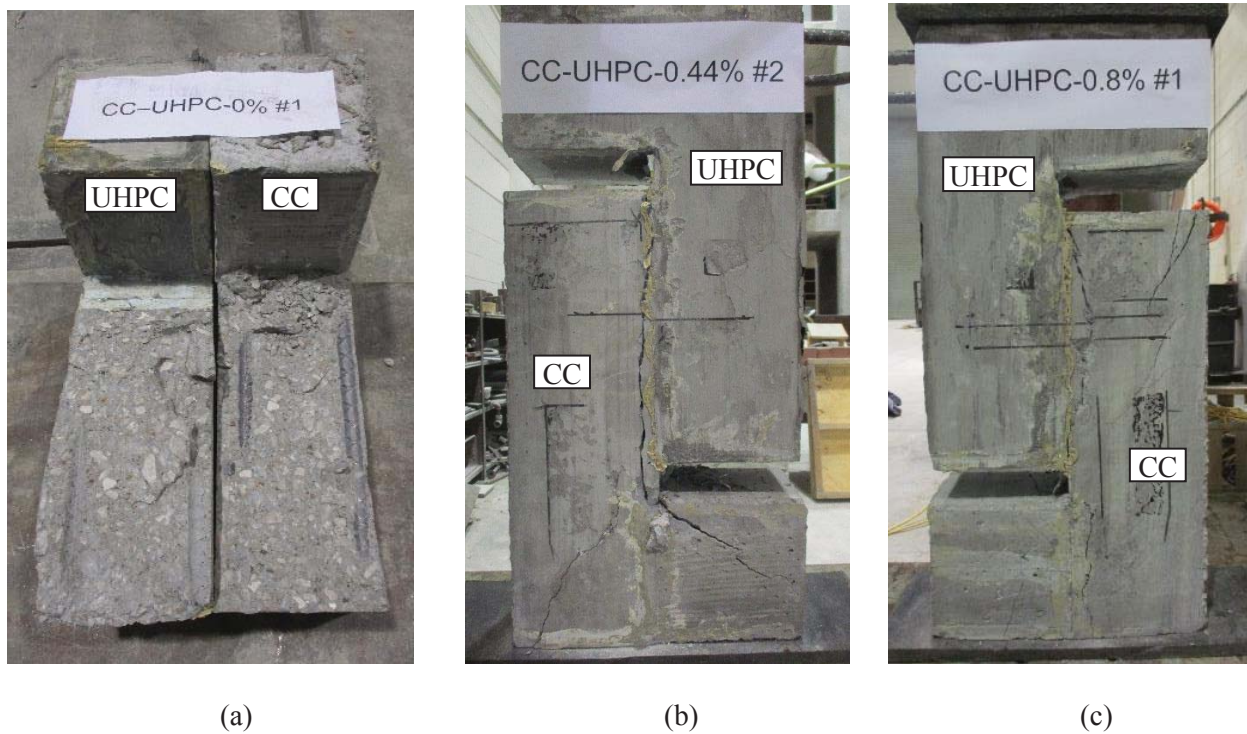
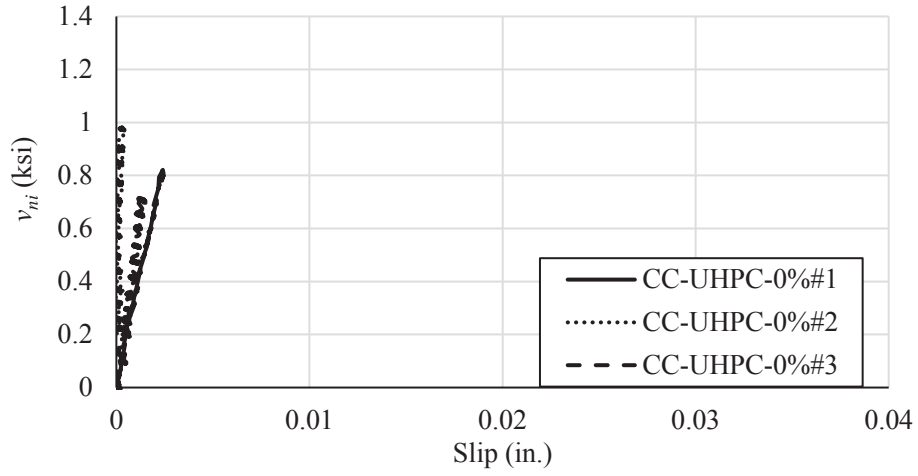
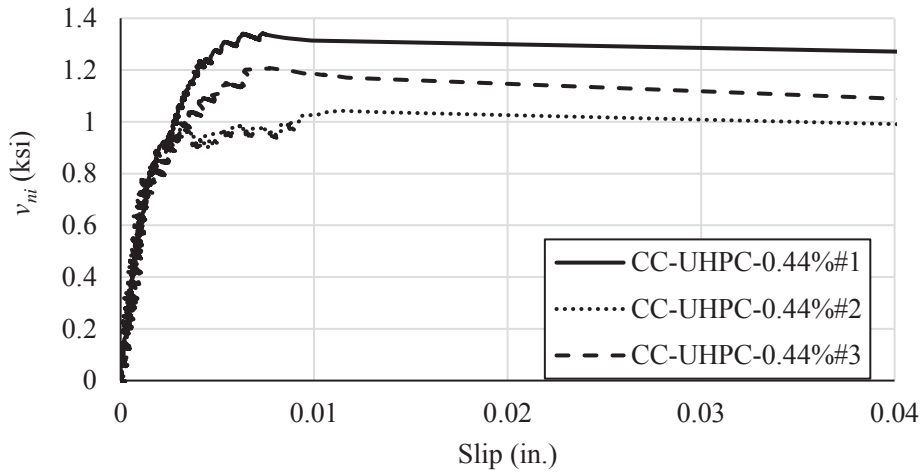


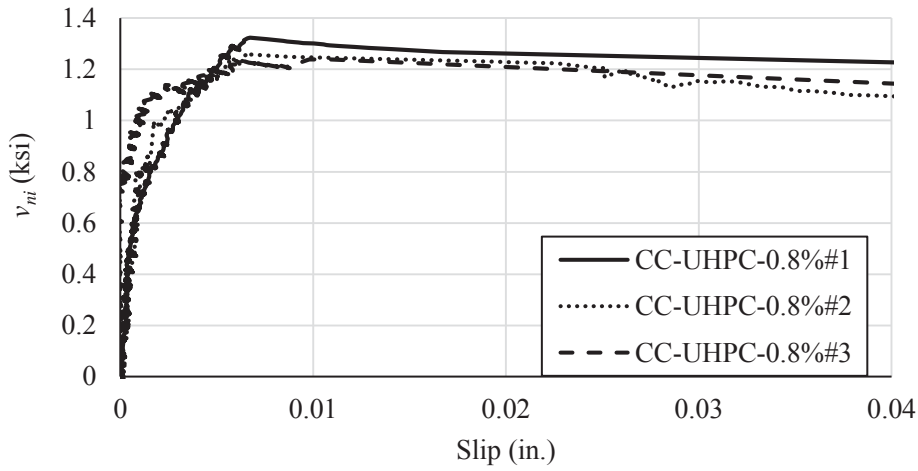
Figure 4.27: CC Failure Modes of L-Shape Specimens with different interface reinforcement ratios; (a) No Reinforcement, (b) 0.44%, and (c) 0.8%.



(a)

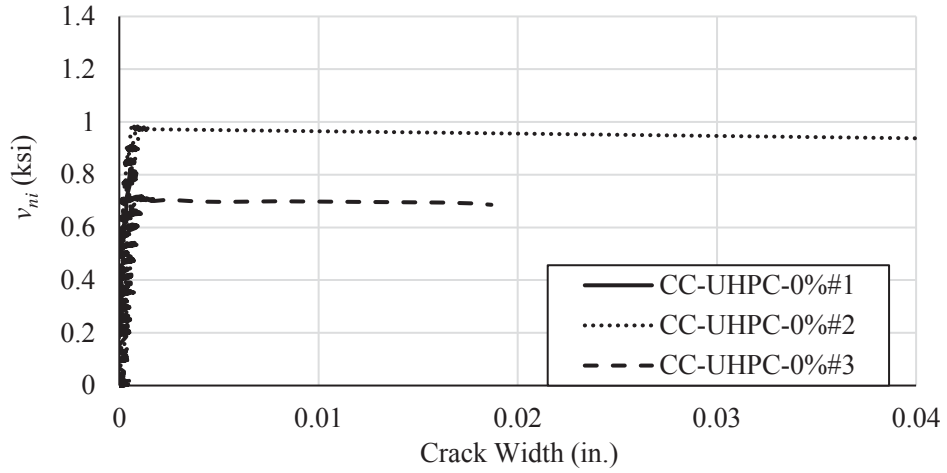


(b)

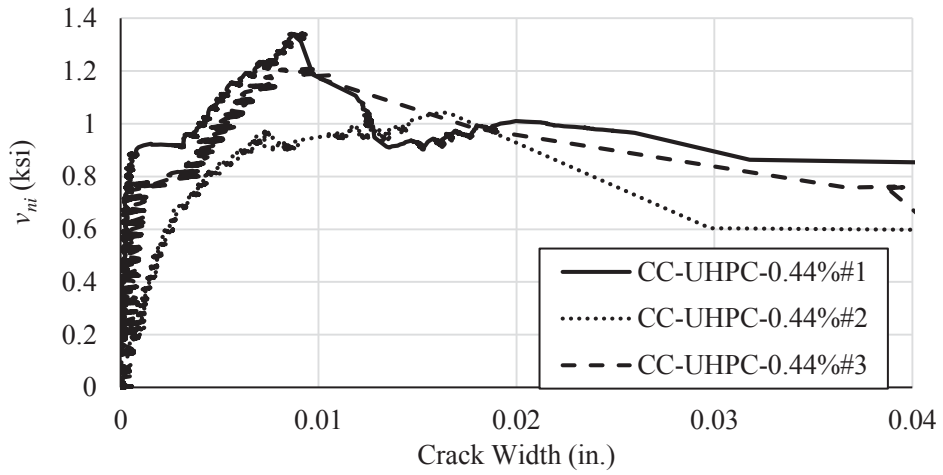


(c)

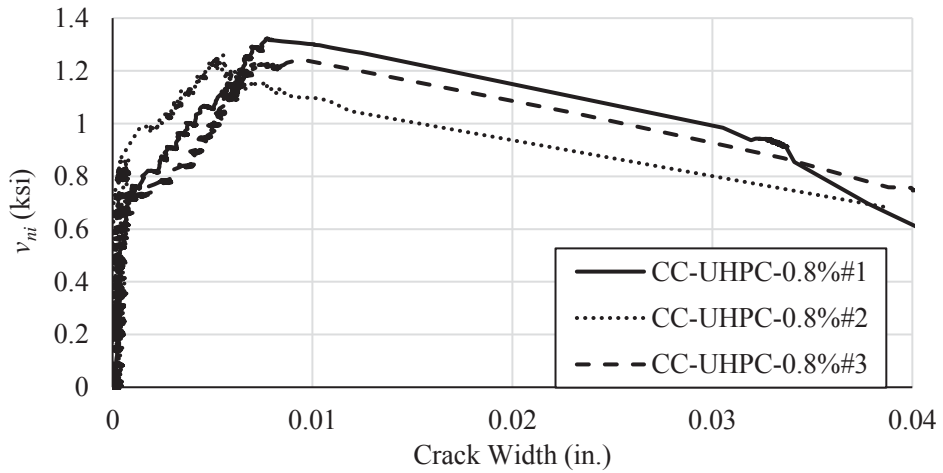
Figure 4.028: Effect of Different Interface Reinforcement on Measured Slip between the Two L-Shape Sections; (a) No Reinforcement, (b) 0.44%, and (c) 0.8%.



(a)



(b)



(c)

Figure 4.029: Effect of Different Interface Reinforcement on Crack Width; (a) No Reinforcement, (b) 0.44%, and (c) 0.8%.

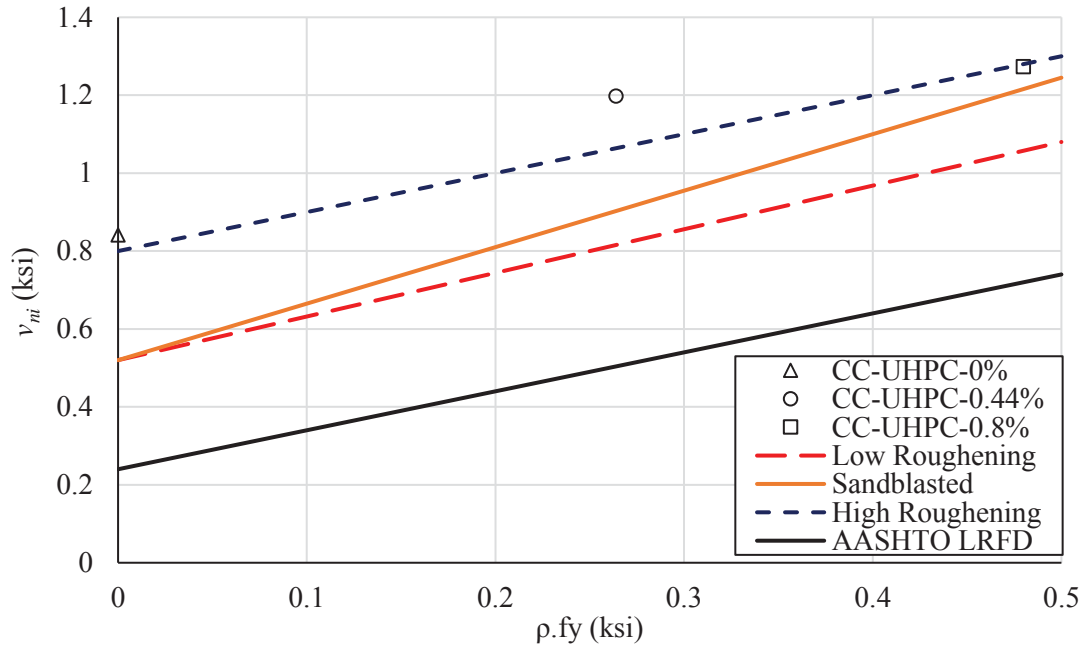


Figure 4.030: Average Interface Resistance of CC-UHPC Obtained from L-Shape Push-off Test and Their Comparison with Proposed Equations.

4.5. Full-Scale Push-off Test

The purpose of full-scale testing is twofold: 1) evaluate the constructability of the new connection especially with the blind casting of a highly viscous material, such as UHPC; and 2) verify the structural performance. Three full-scale push-off specimens were designed and tested using concrete blocks to simulate precast/prestressed concrete girders with 16 in. wide roughened surface. Two #4 bars at 2 ft spacing were used to represent the girder interface shear reinforcement. Two 6 in. diameter shear pockets at 3 ft. spacing were formed using corrugated plastic pipes that provide roughened surface at the sides of the pockets. One #5 loop bar that is 10 in. long was used to reinforce the monolithic UHPC connection and enhance its capacity. Table 4.7 shows the description of the three full-scale push-off specimens, while Figure 4.31 shows their dimensions and reinforcement details.

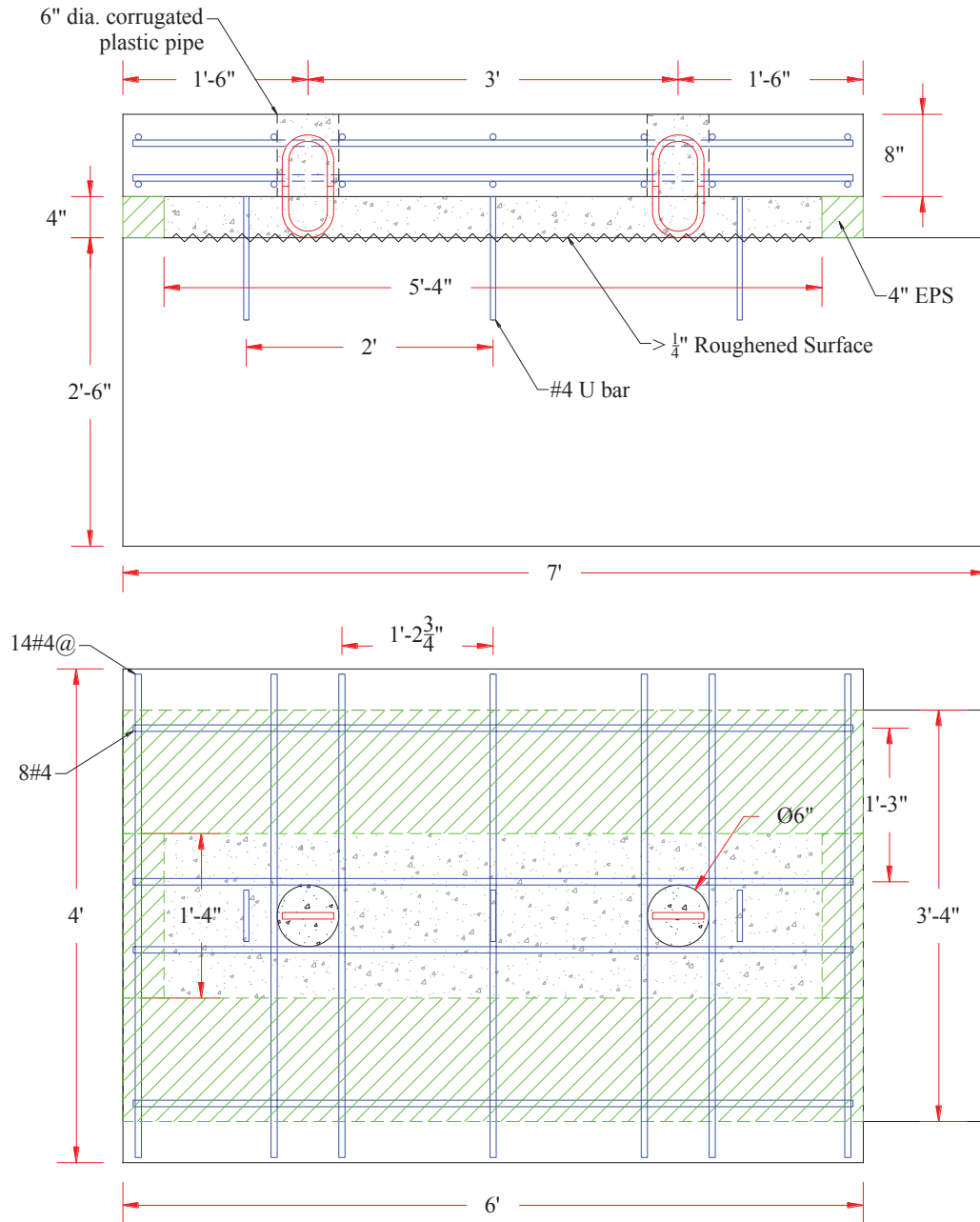


Figure 4.031: Full-Scale Push-Off Specimen Details.

Table 4.7: Full-Scale Push-off Specimens Configuration

Specimen ID	Girder Type	Deck Panel	Shear Pocket
UHPC#1	Concrete Block 3'4" x 7' x 2'6"	Precast Concrete 4' x 6' x 8"	Two 6 in. diameter @ 3 ft. spacing
UHPC#2			
UHPC#3			

- **Specimen Fabrication**

Each shear pocket was formed using a 6 in. diameter corrugated plastic pipe (known by drain pipe) to provide a roughened surface for the inside surface of the shear pocket. The bottom and top of the pipe were sealed with liquid nails and plastic sheet, respectively, to prevent the leakage of concrete while casting the deck panel. Eight #4 bars (four in each layer) were used to hold the plastic pipe in place and strengthen the area around the shear pockets. Figure 4.32 shows the shear pocket forming and deck panel reinforcement details. The deck panel was cast using self-consolidated concrete (SCC) and then cured for seven days using wet burlap and stored in the room temperature.



Figure 4.032: Shear Pockets Forming and Slab Reinforcement Details.

Figure 4.33 shows the interface surface at the top of the concrete block and haunch forming with 2 in. rigid foam boards. The deck slab was placed on the foam boards and was sealed using liquid nail to prevent any leakage of UHPC. The #5 loop bar was bent according to the standard hook specifications, as shown in Figure 4.34, and installed either before or after casting UHPC in the shear pocket. Finally, UHPC was cast to fill the shear pockets and haunch area as shown in Figure 4.35, then, the top of the pocket with covered plywood for curing. It worth mentioning that the research team kept adding UHPC to ensure having a leveled top surface of the deck as shown in Figure 4.36.

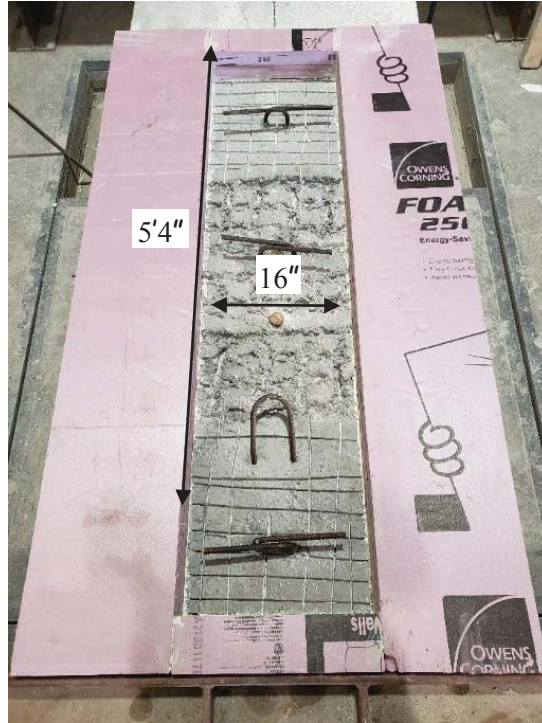


Figure 4.033: CC Interface Shear Area Preparation



Figure 4.034: #5 Loop Bar Details and Installation.



Figure 4.035: UHPC Casting for UHPC#2 Specimen.

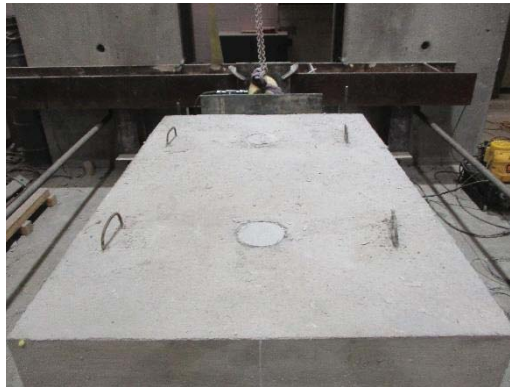


Figure 4.036: UHPC Filled Shear Pockets to Top Surface.

- **Material Properties**

The precast concrete deck panels were made using normal weight self-consolidated concrete (SCC) that has a 28-day compressive strength of 6.6 ksi in the first specimen and 7.34 ksi in the other two specimens. The push-off girder concrete was cast using a ready-mixed SCC with an average slump flow of 22 in and average 28-day compressive strength of 6.8 ksi. For each connection, a total of 3.2 cubic feet of UHPC was grouted to fill the two shear pockets and haunch area. The flowability of UHPC batches were measured, at a temperature of 80° F and relative humidity of 50%, using 10 in. diameter flow table according to ASTM C230 as specified by ASTM C1856. The three UHPC batches had three different levels of flowability: low (< 9 in.), medium (~ 10 in.), and high (>> 10 in.) for UHPC#1, UHPC#2, and UHPC#3

specimens, respectively. Figure 4.37 shows cross-sections of hardened 3"x6" cylinders, cut in half longitudinally using a wet saw, for each of UHPC mixes. The UHPC#1 cylinder had a good distribution of fiber along the height of the section. UHPC#2 cylinder had good fiber distribution with a minor segregation that can be noticed at the top part of the section. However, the UHPC#3 had a severe fiber segregation that barely had fibers at the top half of the cylinder. These three conditions were used to study the effect of flowability on the performance of proposed connection. The three full-scale push-off specimens were tested at an average UHPC compressive strength of 18 ksi.

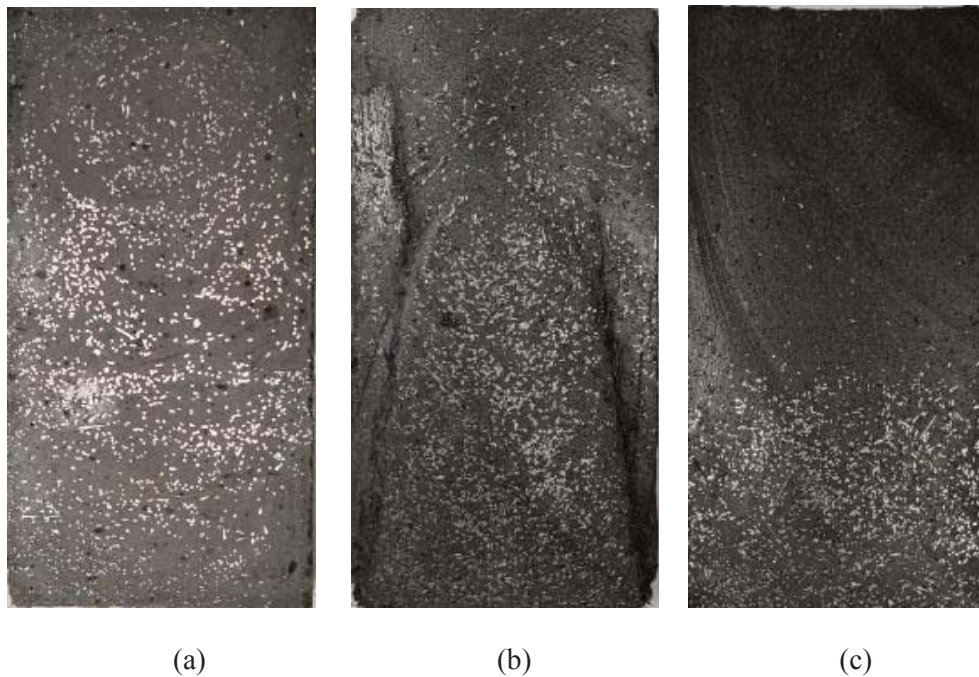


Figure 4.037: Cross-Section of UHPC Cylinders Obtained from Each Full-Scale Push-Off Specimen; (a) UHPC#1, (b) UHPC#2. And (c) UHPC#3

- **Test Setup and Results**

After UHPC achieved a compressive strength of 18 ksi, the full-scale push-off specimens were tested by applying a horizontal load to the deck slab using a hydraulic ram as shown in Figure 4.38. A set of steel plates was used to distribute the applied load over a larger area. The concrete blocks were anchored to the floor by a set of two beams and two threaded rods to prevent their rotation while loading. Also, the concrete blocks were restrained from horizontal movement by a steel beam at the end of the blocks that is tied to a reaction wall by two threaded rods. Four LVDTs (two LVDTs for each side) were used to measure the relative displacements between the deck panel and concrete block, parallel (slip) and perpendicular (crack width) to interface plane. The load was measured using a pressure transducer attached to the ram till failure.

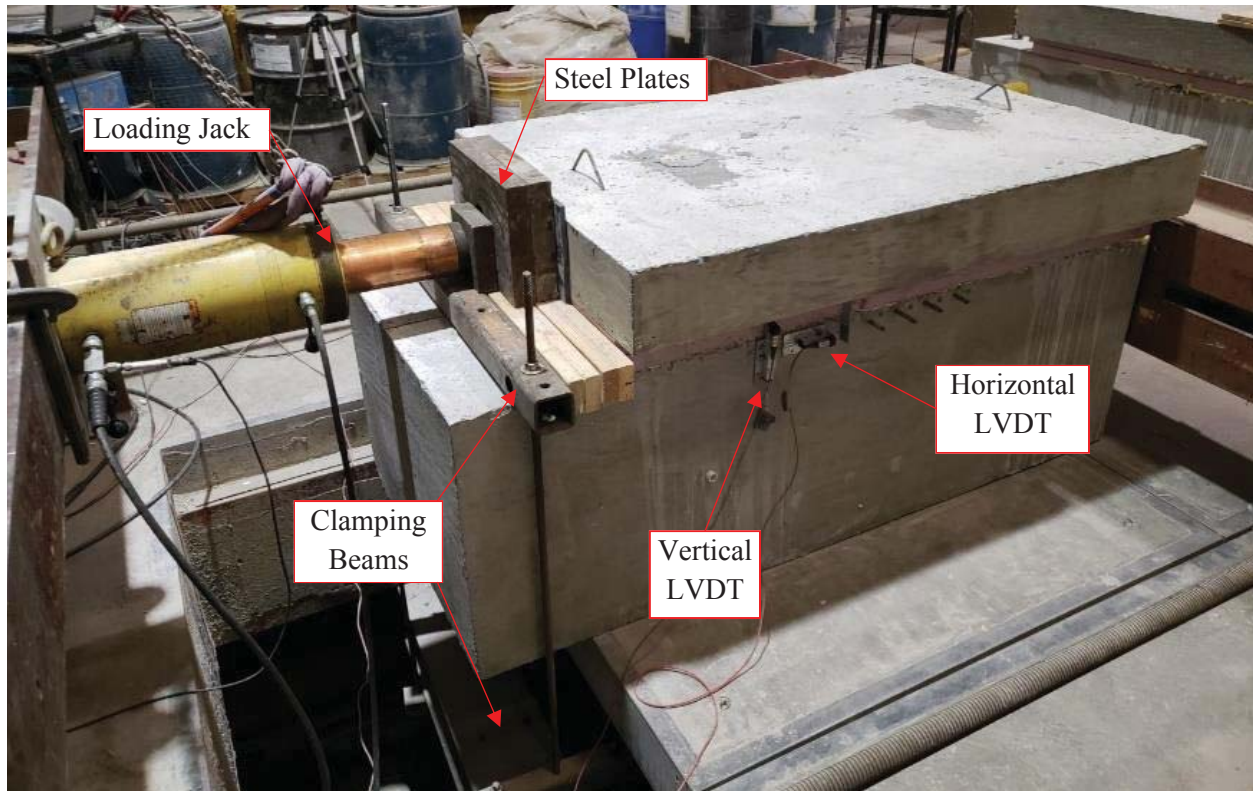


Figure 4.038: Full-Scale Push-Off Specimen Test Setup.

Table 4.9 shows the maximum applied load and the corresponding interface shear force per unit length. Figure 4.39 and Figure 4.40 show the applied load versus measured relative displacements in both parallel (slip) and perpendicular (crack width) directions respectively, for the three full-scale specimens. UHPC#1 specimen exhibited interface shear failure at the first pocket and CC-UHPC at the end of the block as shown in Figure 4.41(a). This CC-UHPC failure can be attributed to the lack of interface reinforcement at the specimen end which is the same case as real girder; more shear reinforcement at the end. The other two specimens had no interface failure and the loop bar were pulled out from the UHPC haunch as shown in Figure 4.41(b) and (c). The fiber segregation in these two specimens affected the bond strength between the UHPC and embedded loop bar, which did not happen in UHPC#1 specimen. The three tests showed that the provided side surface roughening of shear pocket was adequate to prevent pull-out of UHPC from the pocket. The effect of UHPC mix stability can be observed in UHPC#3 results as its UHPC mix had the highest flowability that causes fiber segregation despite its high compressive strength. The stability of UHPC mix is a key parameter that highly impact the capacity of the proposed connection. Therefore, it is recommended that field-cast UHPC have a flowability less than 10 in. to ensure adequate UHPC stability and achieve the full capacity of the proposed connection.

Table 4.08: Full-Scale Push-off Test Results.

Specimen ID	f'_{UHPC} (ksi)	Maximum Load (kips)	V_{ni} (kips/in.)
UHPC#1	18.40	305	4.24
UHPC#2	17.36	240	3.33
UHPC#3	18.40	192	2.67

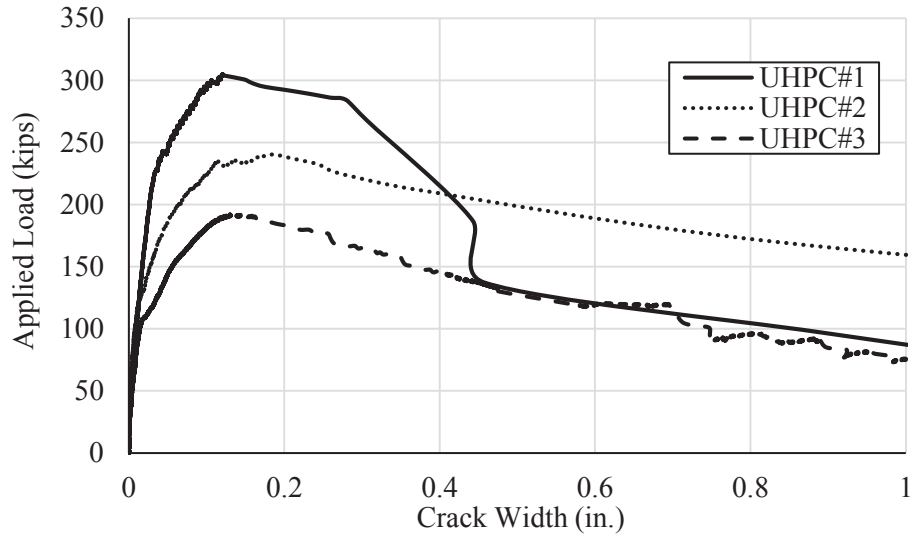


Figure 4.39: Load versus Relative Vertical Displacement of Full-Scale Push-off Specimens.

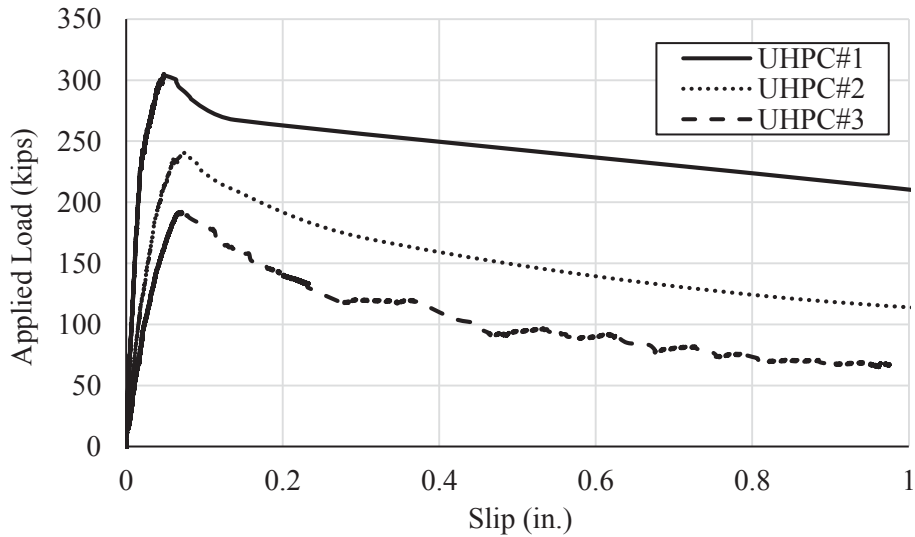
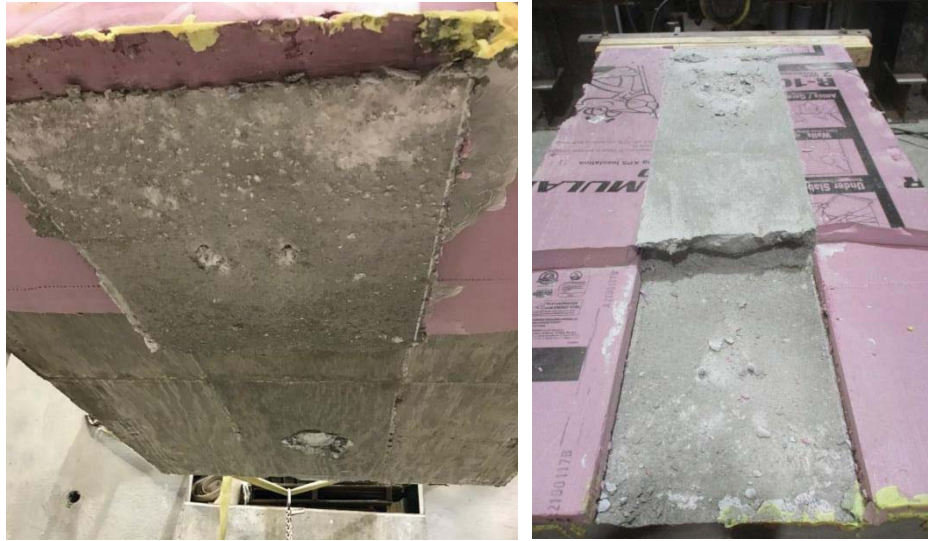


Figure 4.040: Load versus Measured Slip of Full-Scale Push-off Specimens.



(a)



(b)



(c)

Figure 4.041: Full-Scale Specimen Failure Modes; (a)UHPC#1, (b)UHPC#2, and (c)UHPC#3.

Chapter 5. Design Procedures and Design Aids

5.1. Introduction

This chapter provides a design methodology for the proposed connection based on the prediction equations obtained from the experimental investigation. An example bridge from PCI Bridge Design Manual 2014 (PCI BDM Ex. 9.1a) is used to present the design procedure of the proposed connection. Design aid charts were also developed to assist in connection design.

5.2. Design Procedure

The advantage of utilizing the new deck-to-girder connection in precast concrete deck systems are twofold: First, the exceptional mechanical properties of UHPC simplify the design and production of bridge girders and deck panels as they eliminate the need for HSS-formed shear pockets and special connectors; Second, the excellent durability of UHPC eliminates the need for an overlay or other protection systems. However, the design codes do not provide provisions for designing the new connection. So, the cohesion and friction factors obtained from the experimental investigation are used to develop the design procedure shown in Figure 4.25.

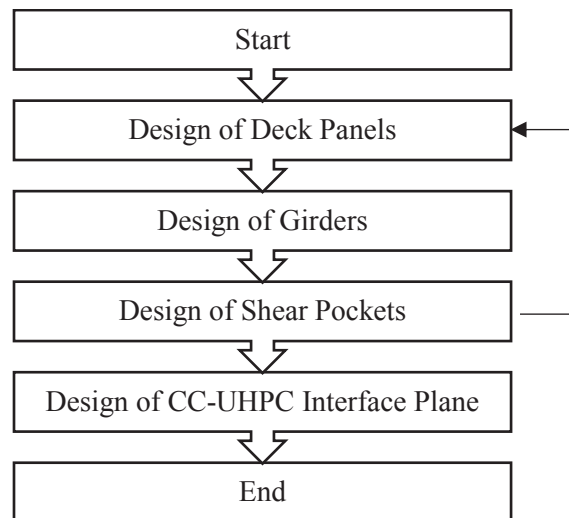


Figure 5.1: Flowchart of General Design Procedures for Proposed System.

The design procedure starts with obtaining the nominal interface shear resistant demand from the different load cases. Then, the spacing between shear pockets is calculated based on preliminary pocket diameter and loop bar size. The spacing between shear pockets is recommended to be from 2 to 4 ft. The obtained spacing is used to predict the minimum UHPC haunch width using the girder shear reinforcement;

obtained from the girder shear design. If the minimum UHPC haunch width is greater than the girder top flange width, the interface shear reinforcement needs to be designed based on considering the top flange width as UHPC haunch width. The design procedure is shown in Figure 5.2 and provided in a Mathcad file in Appendix A to obtain the following outcomes:

- Shear pocket diameter and spacing
- Loop bar embedded in the shear pocket
- Girder shear reinforcement
- Haunch width

Where:

A_{cv-MN} : monolithic UHPC interface shear area (in.²)

A_{cv-CC} : CC-UHPC interface shear area (in.²)

A_{vf-MN} : interface shear reinforcement Area across monolithic UHPC plane (in.²)

A_{vf-CC} : interface shear reinforcement Area across CC-UHPC plane (in.²)

A_{s1} : loop bar area (in.²)

A_{s2} : girder shear reinforcement bar area (in.²)

b : girder top flange width (in.)

b_w : UHPC haunch width (in.)

c_{MN} : monolithic UHPC cohesion coefficient (ksi)

c_{cc} : CC-UHPC cohesion coefficient (ksi)

D_p : shear pocket diameter (in.)

f'_c : compressive strength of precast deck slab panel (ksi)

f'_{UHPC} : compressive strength of field cast UHPC (ksi)

f_{yh} : bar yield strength (ksi)

N : Number of interface reinforcement bar legs crossing interface plane

V_{ni} : nominal interface shear resistance per unit length (kips/in.)

V_{ni-MN} : nominal interface shear resistance of monolithic UHPC plane (kips)

V_{ni-CC} : nominal interface shear resistance of CC-UHPC plane (kips)

S : girder shear reinforcement spacing (in.)

S_p : spacing between shear pockets (in.)

μ_{MN} : monolithic UHPC friction coefficient

μ_{cc} : CC-UHPC friction coefficient

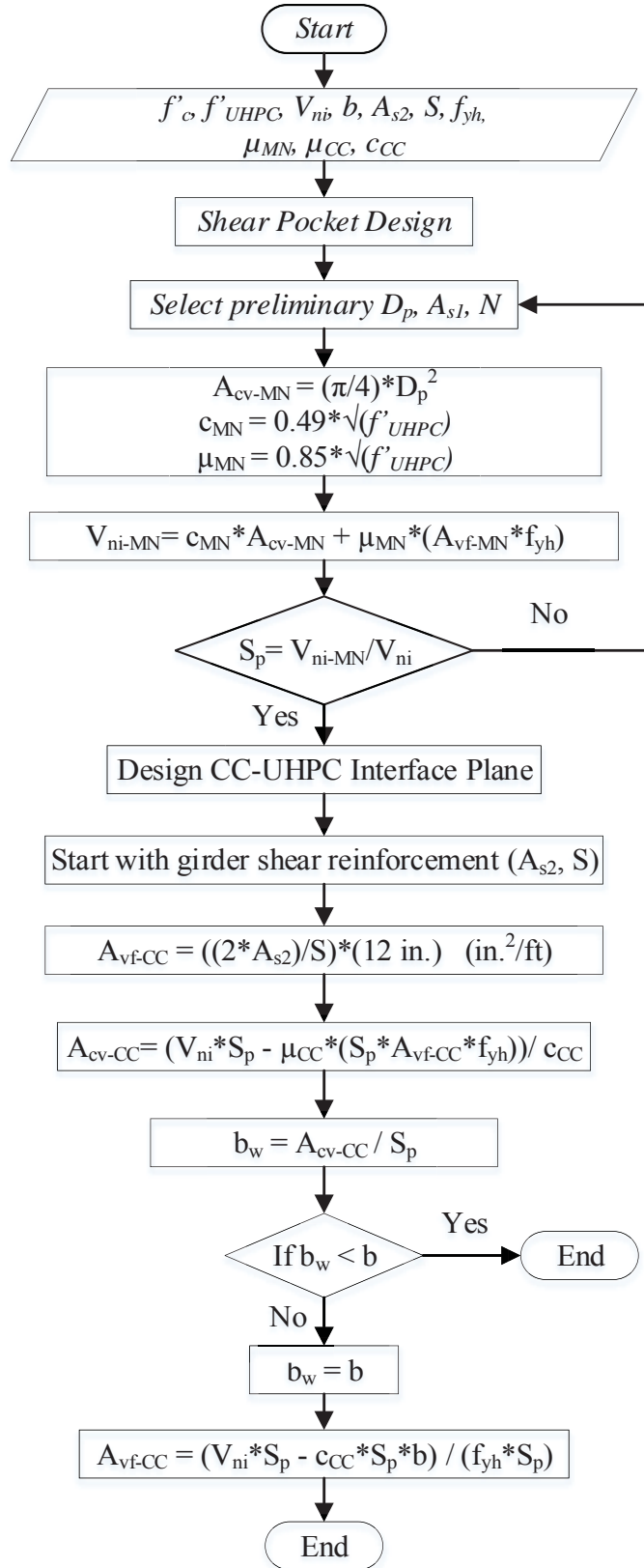


Figure 5.2: Design Procedure flowchart of new connection.

5.3. Design Aids

Design aids were generated using the proposed equations for predicting the interface shear resistance of monolithic UHPC, which controls the connection design. The interface shear resistance was calculated for shear pocket spacing ranging from 2 – 4 ft. with using different loop bar sizes. Figure 5.3 and Figure 5.4 show the generated design charts presenting 17 ksi and 21.7 ksi compressive strength of UHPC, respectively. The design chart legend is labeled using the form DA#B where D is diameter, A is the shear pocket diameter (in.), and B is the embedded loop bar size.

To demonstrate the use of the design charts, the interface shear demand of 3.07 kips/in. of the example bridge is used as shown in Figure 5.5 to determine the different alternatives in terms of shear pocket spacing, diameter, and reinforcement. Example of these design alternatives is using 4in. diameter shear pockets at 3 ft spacing and #4 loop bar to satisfy interface shear demand at girder ends. The interface shear demand is significantly reduced towards the middle of the girder and, therefore, pocket spacing could be increased or pocket size and/or loop bar size could be reduced.

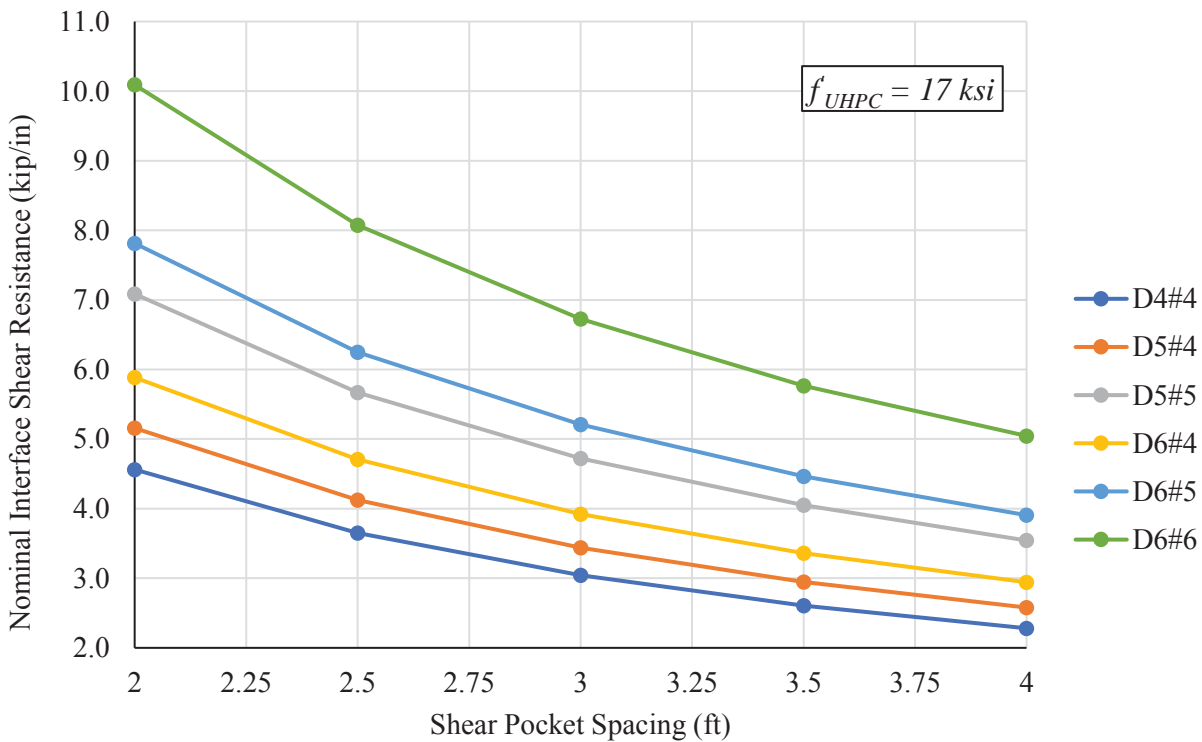


Figure 5.3: Design Chart for UHPC with Compressive Strength of 17 ksi.

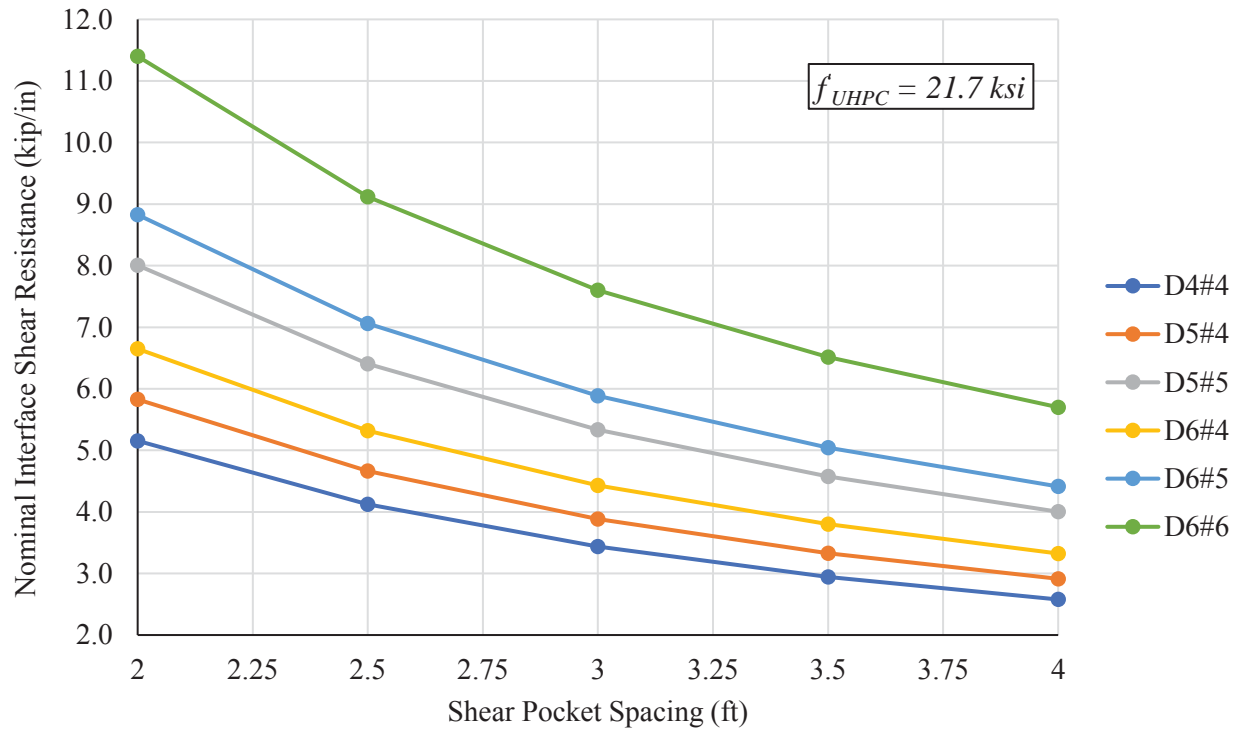


Figure 5.4: Design Chart for UHPC with Compressive Strength of 21.7 ksi.

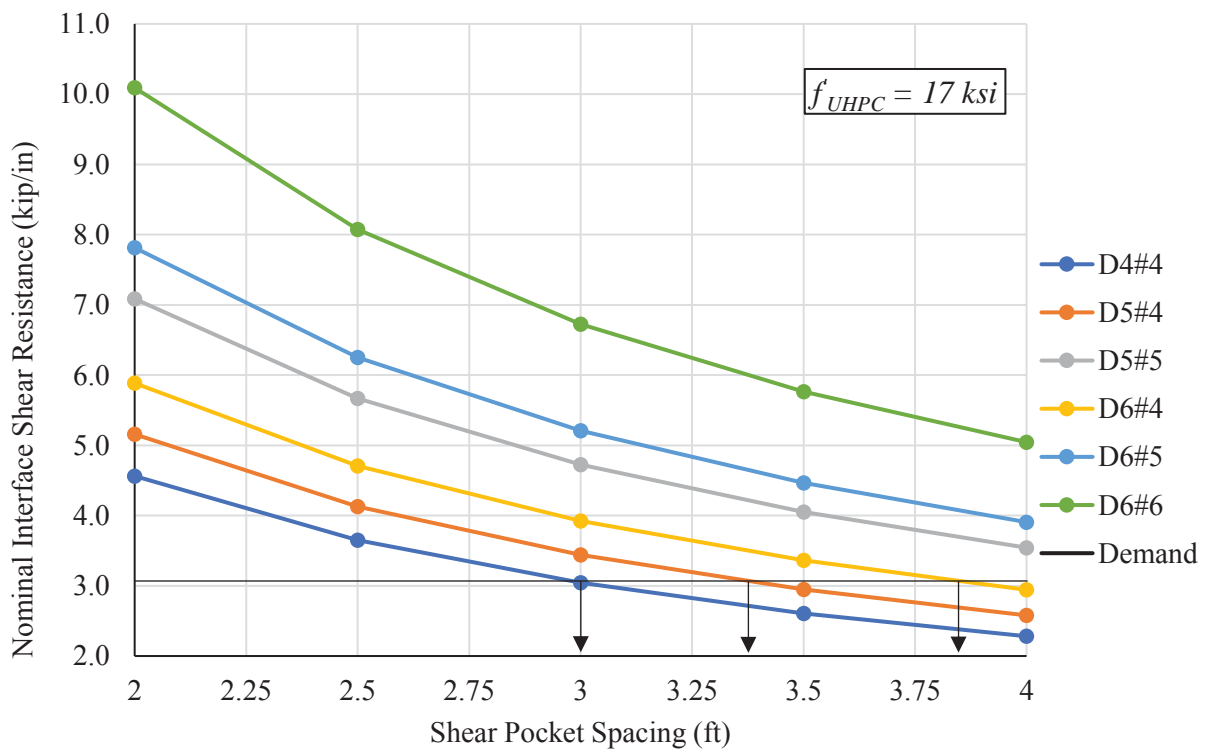


Figure 5.5: Demonstration of Using the Design Aid Chart.

Chapter 6. Summary and Conclusions

6.1. Summary

This report presents a new precast concrete deck-to-concrete girder connection using UHPC. This connection makes advantage of exceptional mechanical properties, workability and durability to eliminate any change to the design and production of typical precast/prestressed concrete girders (no special shear connectors are needed). The new connection also simplifies deck panels by using discrete round shear pockets, 4 – 8 in. in diameter, every 2 - 4 ft over each girder line. This panel design allows transverse prestressing that significantly reduces the amount of reinforcement and reduces the cracks caused by handling and transportation. The composite action between precast deck panels and girders is achieved through filling the shear pockets and the haunch areas with UHPC instead of extending girder shear connectors into the shear pockets of the deck panels. This connection provides adequate production and erection tolerances of precast concrete components and improves the economics of the precast systems.

Two critical interface shear planes control the design of the new connection. The first plane is at the girder top surface between fresh UHPC and hardened conventional concrete (CC-UHPC), which is usually an intentionally roughened surface. The second plane is at the soffit of the deck panels across the monolithic UHPC. A loop bar is placed in each pocket to cross the second plane and enhance its interface shear resistance. Also, corrugated plastic pipe is used to form the shear pocket and provide a roughened side surface to bond UHPC with the deck panel concrete. Since current AASHTO LRFD Bridge Design Specifications 2017 does not provide equations for predicting the interface shear resistance of either monolithic UHPC or CC-UHPC, experimental investigation was conducted to understand the behavior of the new connection and predict its interface shear resistance.

The study methodology includes two stages: experimental investigation, and design procedure. A non-proprietary UHPC mix developed at UNL was used as a primary mix for conducting the experimental investigation. Straight steel micro-fibers, 0.50 in. long and 0.078 in. in diameter, were used in UHPC mixes at 2% dosage by volume. The experimental investigation consists of small-scale and full-scale push-off testing. Small-scale testing is conducted to evaluate the interface shear resistance at the connection critical sections: direct shear, L-shape push-off, and double shear tests for monolithic UHPC; and slant shear and L-shape push-off tests for CC-UHPC. Full-scale push-off testing was conducted to evaluate its structural performance and constructability of the new connection. Prediction equations obtained from the experimental investigation results were used to develop design procedures and design aids for the new connection. Finally, an example bridge is presented to demonstrate the design of the new connection.

6.2. Conclusions

Below are the main conclusions made based on the results of the experimental investigation:

1. Interface shear resistance of monolithic UHPC and UHPC cast on hardened conventional concrete (CC-UHPC) can be predicted using AASHTO LRFD shear friction model, but with different cohesion and friction factors for different surface textures.
2. Interface shear resistance of UHPC cast on conventional concrete with at least 1/4 in. amplitude roughened surface can be predicted using a cohesion factor of 0.8 ksi and a friction factor of 1.0. The cohesion factor is much higher than that of conventional concrete (0.24 ksi), while the friction factor is the same as that of conventional concrete (1.0).
3. The intentionally roughened CC interface surface results in CC failure rather than bond failure. Therefore, the compressive strength of CC is a key parameter in predicting the interface shear resistance of CC-UHPC with roughened interface surface.
4. Interface shear resistance of monolithic UHPC obtained from direct shear test ranges from 4 ksi to 8 ksi. The small size of the test specimens and the possibility of having a load path other than shear could be the reason of this inconsistency and high values.
5. The L-shape push-off test shows more consistent results compared to the direct shear test and in good agreement with the literature.
6. Interface shear resistance of monolithic UHPC can be predicted using a cohesion and friction factors that are dependent on UHPC compressive strength as follows: $c = 0.49\sqrt{f'_{UHPC}}$ (ksi) and $\mu = 0.85\sqrt{f'_{UHPC}}$, which provide a cohesion factor of 2.1 ksi and friction factor of 3.6 for 18 ksi UHPC.
7. The proposed connection is easy to fabricate, simple to erect, and economical when non-proprietary UHPC is used. It can be designed to satisfy interface shear demands in most bridges while using practical pocket size and spacing as shown in the design aids.
8. The flowability of UHPC should be between 8 in. and 10 in. using a flow table test according to ASTM C230, specified by ASTM C1856, to ensure adequate UHPC workability and fiber stability.
9. The loop bars can be either placed before or after casting UHPC. It is preferred to be placed before to ensure adequate embedment and prevent fiber disturbance caused by inserting the loop bar.
10. The shear pockets shall have a roughening surface for its sides with either a minimum amplitude of 1/4 in. or exposed aggregate to bond with UHPC. Corrugated plastic pipe has shown to be an excellent and economical solution to form the shear pocket.

REFERENCES

- Aaleti, S., and Sritharan, S. 2017. "Investigation of a suitable shear friction interface between UHPC and normal strength concrete for bridge deck applications." *The Bridge*, 515, 294-8103.
- AASHTO (American Association of State Highway and Transportation Officials). 2017. *AASHTO LRFD Bridge Design Specifications*, 8th Edition, Washington, D.C.
- Abo El-Khier, M., Morcou, G., and Hu, J. (2019). "Interface Shear Resistance of Ultra-High Performance Concrete (UHPC)." *Proc., 2nd International Interactive Symposium on UHPC*, Albany, NY, USA.
- Abo El-Khier, M., Kodsy, A., and Morcou, G. (2018) "Precast Concrete Deck-to-Girder Connection Using UHPC." *10th International Conference on Short and Medium Span Bridges Proceedings*, Quebec City, Quebec, Canada.
- AFNOR (Association française de normalization). 2016. NF-P-18-710-UHPC, "P18-710: National addition to Eurocode 2—Design of concrete structures: Specific rules for ultra-high performance fiber-reinforced concrete (UHPFRC)." France.
- ASTM (American Society for Testing and Materials). 2013. Standard test method for bond strength of epoxy-resin systems used with concrete by slant shear. *ASTM C882/C882M-13a*, West Conshohocken, PA.
- ASTM (American Society for Testing and Materials). 2013. Standard test method for compressive strength of cylindrical concrete specimens. *ASTM C39*, West Conshohocken, PA.
- ASTM (American Society for Testing and Materials). 2014. Standard specification for flow table for use in test of hydraulic cement. *ASTM C230/C230M*, West Conshohocken, PA.
- ASTM (American Society for Testing and Materials). 2017. Standard practice for fabricating and testing specimens of ultra-high performance concrete. *ASTM C1856/C1856M*, West Conshohocken, PA.
- Birkeland, P. W., and Birkeland, H. W. 1966. "Connections in precast concrete construction." *Journal Proceedings*, 63(3), 345-368.
- Crane, C. K. 2010. "Shear and shear friction of ultra-high performance concrete bridge girders." *Doctoral Thesis*, Georgia Institute of Technology, Georgia, USA.
- Graybeal, B. 2014. "Design and Construction of Field-Cast UHPC Connections." FHWA-HRT-14-084, U.S. Department of Transportation, Federal Highway Administration, Washington, D.C.
- Haber, Z. B., Graybeal, B. A., Nakashoji, B., and Fay, A. 2017. "NEW, simplified deck-to-girder composite connections using UHPC." *2017 National ABC Conference Proceedings*, 1–10.

- Harris, D., Sarkar, J., and Ahlborn, T. 2011. "Characterization of interface bond of ultra-high-performance concrete bridge deck overlays." *Transportation Research Record: Journal of The Transportation Research Board*, 2240, 40-49.
- Jang, HO., Lee, H.S., Cho, K., and Kim, J. 2017. "Experimental study on shear performance of plain construction joints integrated with ultra-high performance concrete (UHPC)," *Construction and Building Materials*, 152, 2017, 16–23.
- Maroliya, M. K. 2012. "Behaviour of reactive powder concrete in direct shear." *IOSR Journal of Engineering (IOSRJEN)*, 2(9), 76–79.
- Muñoz, M. Á. C. 2012. "Compatibility of ultra high performance concrete as repair material: bond characterization with concrete under different loading scenarios." Michigan Technological University, MI.
- PCI (Precast/Prestressed Concrete Institute). 2014. *Bridge design manual. 3rd Edition, 2nd Release*, Chicago, IL.
- Rangaraju, P. R., Kizhakommudom, H., Li, Z., and Schiff, S. D. 2013. "Development of high-strength/high performance concrete/grout mixtures for application in shear keys in precast bridges." FHWA-SC-13-04a. US Department of Transportation.
- Tayeh, B. A., Bakar, B. A., Johari, M. M., and Voo, Y. L. 2012. "Mechanical and permeability properties of the interface between normal concrete substrate and ultra high performance fiber concrete overlay." *Construction and building materials*, 36, 538-548

APPENDIX A
Design of the Proposed UHPC Deck-to-Girder Connection
PCI BDM Example. 9.1a

Deck Panel Concrete Compressive Strength $f'_c := 6 \text{ ksi}$

UHPC Haunch Compressive Strength $f'_{UHPC} := 18 \text{ ksi}$

According to PCI Bridge Design Manual Example 9.1a Section 9.1a.12:

Factored Interface Shear due to DW and LL at h/2 (DC does not apply to the composite section) $V_u := 1.5 \cdot 10.8 \text{ kip} + 1.75 \cdot 104.4 \text{ kip} = 198.9 \text{ kip}$

Shear Depth $d_v := 75.78 \text{ in} - \frac{7.5 \text{ in}}{2} = 72.03 \text{ in}$

Ultimate Interface Shear at Critical Section $V_{ui} := \frac{V_u}{d_v} = 2.76 \frac{\text{kip}}{\text{in}}$

Strength Reduction Factor $\phi := 0.9$

Nominal Interface Shear Resistance per unit length $V_{ni} := \frac{V_{ui}}{\phi} = 3.07 \frac{\text{kip}}{\text{in}}$

UHPC Monolithic Interface Shear Resistance

Pocket Diameter $D_p := 6 \text{ in}$ (4 to 8 in.)

Interface Shear Area Per Pocket $A_{cv_MN} := \frac{\pi}{4} \cdot D_p^2 = 28.27 \text{ in}^2$

Monolithic Cohesion Coefficient $c_{MN} := 0.49 \cdot \sqrt{f'_{UHPC} \cdot \text{ksi}} = 2.08 \text{ ksi}$

Monolithic Friction Coefficient $\mu_{MN} := 2.5$ Based on UHPC#1 test result

Embedded Loop Bar Area (Single Leg) $A_{s1} := 0.31 \text{ in}^2$

Number of Loop Bar Legs crossing Interface $N := 2$

Monolithic Interface Shear Reinforcement $A_{vf_MN} := N \cdot A_{s1} = 0.62 \text{ in}^2$

Yield Strength $f_{yh} := 60 \text{ ksi}$

Nominal Interface Shear Resistance Per Pocket $V_{ni_MN} := c_{MN} \cdot A_{cv_MN} + \mu_{MN} \cdot (A_{vf_MN} \cdot f_{yh}) = 151.8 \text{ kip}$

Spacing Between Pockets $S_p := \frac{V_{ni_MN}}{V_{ni}} = 4.122 \text{ ft}$

Use $S_p := 4 \text{ ft}$ (2 to 4 ft.)

Conventional Concrete (CC)-UHPC Interface Shear Resistance

Width of Roughened Girder Top Flange

$$b := 16 \text{ in}$$

Area of Roughened Girder Top Flange per ft

$$A_{cv_CC} := b = 1.333 \frac{\text{ft}^2}{\text{ft}}$$

Girder Shear Reinforcement Bar

$$A_{s2} := 0.2 \text{ in}^2$$

Use the same shear reinforcement obtained from girder shear design

Girder Shear Reinforcement Spacing

$$S := 12 \text{ in}$$

CC-UHPC Interface Shear Reinforcement

$$A_{vf_CC} := \frac{2 \cdot A_{s2}}{S} \frac{12 \text{ in}}{1 \text{ ft}} = 0.4 \frac{\text{in}^2}{\text{ft}}$$

CC-UHPC Cohesion Coefficient

$$c_{CC} := 0.8 \text{ ksi}$$

CC-UHPC Friction Coefficient

$$\mu_{CC} := 1.0$$

Yield Strength

$$f_{yh} := 60 \text{ ksi}$$

CC-UHPC interface shear resistance

$$V_{ni_CC} := c_{CC} \cdot A_{cv_CC} + \mu_{CC} \cdot (A_{vf_CC} \cdot f_{yh}) = 14.8 \frac{\text{kip}}{\text{in}}$$

$$check := \text{if}(V_{ni} \leq V_{ni_CC}, \text{"OK"}, \text{"NG"}) = \text{"OK"}$$